VOLUME 39 [J. CELL. AND COMP. PHYSIOL.] NUMBER 2

JOURNAL OF CELLULAR AND COMPARATIVE PHYSIOLOGY

APRIL 1952

PUBLISHED BIMONTHLY BY

THE WISTAR INSTITUTE OF ANATOMY AND BIOLOGY

WOODLAND AVENUE AND THIRTY-SIXTH STREET, PHILADELPHIA 4, PA.

Entered as second-class matter February 19, 1932, at the post office at Philadelphia, Pa., under Act of March 3, 1879. Acceptance for mailing at special rate of postage provided for in section 1103, Act of October 3, 1917, authorized on July 2, 1918

Price, $7.50 per volume, Domestic; $8.00 per volume, Foreign

Publications of The Wistar Institute

JOURNAL OF MORPHOLOGY

Devoted to the publication of original research on animal morphology, including cytology, protozoology, and the embryology of vertebrates and invertebrates. Articles do not usually exceed 50 pages in length.

Issued bimonthly, 2 vols. annually: $20.00 Domestic, $21.00 Foreign, per year.

THE JOURNAL OF COMPARATIVE NEUROLOGY

Publishes the result of original investigations on the comparative anatomy and physiology of the nervous system.

Issued bimonthly, 2 vols. annually: $15.00 Domestic, $16.00 Foreign, per year.

THE AMERICAN JOURNAL OF ANATOMY

Publishes the results of comprehensive investigations in vertebrate anatomy — descriptive, analytical, experimental.

Issued bimonthly, 2 vols. annually: $15.00 Domestic, $16.00 Foreign, per year.

THE ANATOMICAL RECORD

Organ of the American Association of Anatomists and the American Society of Zoologists

For the prompt publication of concise original articles on vertebrate anatomy, preliminary reports; technical notes; critical notes of interest to anatomists and short reviews of noteworthy publications.

Issued monthly, 3 vols. annually: $22.50 Domestic, $24.00 Foreign, per year.

THE JOURNAL OF EXPERIMENTAL ZOOLOGY

Publishes papers embodying the results of original researches of an experimental or analytical nature in the field of zoology.

Issued 9 times a year, 3 vols. annually: $22.50 Domestic, $24.00 Foreign, per year.

AMERICAN JOURNAL OF PHYSICAL ANTHROPOLOGY

Organ of the American Association of Physical Anthropologists

Publishes original articles on comparative human morphology and physiology as well as on the history of this branch of science and the techniques used therein. In addition it gives comprehensive reviews of books and papers, an annual bibliography, and informal communications.

Issued quarterly, 1 vol. annually: $7.50 Domestic, $8.00 Foreign, per year.

JOURNAL OF CELLULAR AND COMPARATIVE PHYSIOLOGY

Publishes papers which embody the results of original research of a quantitative or analytical nature in general and comparative physiology, including both their physical and chemical aspects.

Issued bimonthly, 2 vols. annually: $15.00 Domestic, $16.00 Foreign, per year.

THE JOURNAL OF NUTRITION

Organ of the American Institute of Nutrition

Publishes original researches in the field of nutrition and occasional reviews of literature on topics with which the journal is concerned.

Issued monthly, 3 vols. annually: $22.50 Domestic, $24.00 Foreign, per year.

THE AMERICAN ANATOMICAL MEMOIRS

Publishes original monographs based on experimental or descriptive investigations in the field of anatomy which are too extensive to appear in the current periodicals. Each number contains only one monograph. List of monographs already published, with prices, sent on application.

ADVANCE ABSTRACT CARD SERVICE

Every paper accepted for publication in one of the above periodicals is accompanied by the author's abstract. The abstract and the complete bibliography reference to the paper as it will eventually appear is printed on the face of a standard library catalogue card. This Advance Abstract Card Service is issued promptly, in advance of the journal containing the paper, and is offered in three styles.

Prices per year $2.00, $2.50 and $3.00, postpaid.

These publications enjoy the largest circulation of any similar journals published.

THE WISTAR INSTITUTE OF ANATOMY AND BIOLOGY

WOODLAND AVENUE AND THIRTY-SIXTH STREET, PHILADELPHIA 4, PA.

CELLULAR FRAGILITIES AND RESONANCES OBSERVED BY MEANS OF SONIC VIBRATIONS[1]

EUGENE ACKERMAN[2]

Johnson Research Foundation, University of Pennsylvania, Philadelphia

TEN FIGURES

I. INTRODUCTION

Sonic vibration is becoming an ever more useful tool for breaking up cells and extracting their contents. It is well known that this type of cellular disruption occurs only under conditions which produce cavitation in the suspending liquid. However, the mechanism of sonic disruption is poorly understood (Gregg, '50). Since cavitation is necessary for cellular breakdown, it is desirable to know the physical behavior of a liquid containing acoustically generated cavities. This has been discussed recently by Noltingk and Neppiras ('50); but there are no empirical checks on their theory except for the results reported in this paper.

We have been attempting to learn more of the mode of action of intense sonic fields on biological cells. For this purpose we have developed acoustic generators whose frequencies can be varied continuously over considerable ranges and whose sonic outputs can be measured quantitatively. This apparatus is described briefly in section II of this paper. With this equip-

[1] Initial phases of this work were supported by a grant from the Wisconsin Alumni Research Foundation to Professor H. B. Wahlin and were included in the author's thesis submitted to the Graduate School of the University of Wisconsin in partial fulfillment of the requirements for the degree of Doctor of Philosophy, August, 1949. The remainder was supported by a grant from the Raytheon Manufacturing Company to the Johnson Foundation.

[2] Present address, Physics Department, Pennsylvania State College, State College, Pennsylvania.

ment, we can study the frequency and sonic output dependence of cellular breakdown, and look for "resonant" frequencies, at which particular types of cells would be selectively destroyed.

The results of such studies are reported in sections III and IV. It is found that the rate at which smaller cells like Trichomonus foetus break down in an acoustic field of fixed frequency is proportional to the maximum velocity attained by the vibrating diaphragm in the acoustic generator. On the other hand, if this velocity is held constant and the frequency varied, the rate of breakdown is found to be independent of the frequency. The relative rates at which different cells break down under the same mechanical forces (such as those produced by cavitation in a liquid) is considered to be a measure of their mechanical fragility. Thus we can measure such fragilities for a wide variety of cell types.

Larger cells like Paramecia show constant mechanical fragilities over most of the frequency spectrum, but have anomalously high breakdown rates in certain narrow frequency bands. The frequency band in which this anomalously high breakdown rate occurs varies with the species. By using differential counts on mixtures of two species, we have established that the characteristic frequencies are actually properties of the biological cells. These selective effects occur only in the presence of the mechanical agitation due to cavitation; this indicates that the results are due to mechanical resonances of the cellular architecture. Reasonable theories can be constructed which describe these results in terms of structural resonances.

II. APPARATUS AND PROCEDURES

A brief discussion of our apparatus is included here; it is discussed in detail in another journal (Ackerman, '51a). Our apparatus consists of an electrical power supply, a sound generator, and a phonograph cartridge for measuring the sonic output.

Electrical power supply

The electrical power supply consists of a commercially built beat frequency oscillator, a buffer amplifier, and a push-pull class B amplifier. Electrical outputs of from 1 to 8 amperes of audio frequency current are available at impedance levels of 1 to 10 ohms. The frequency of this current

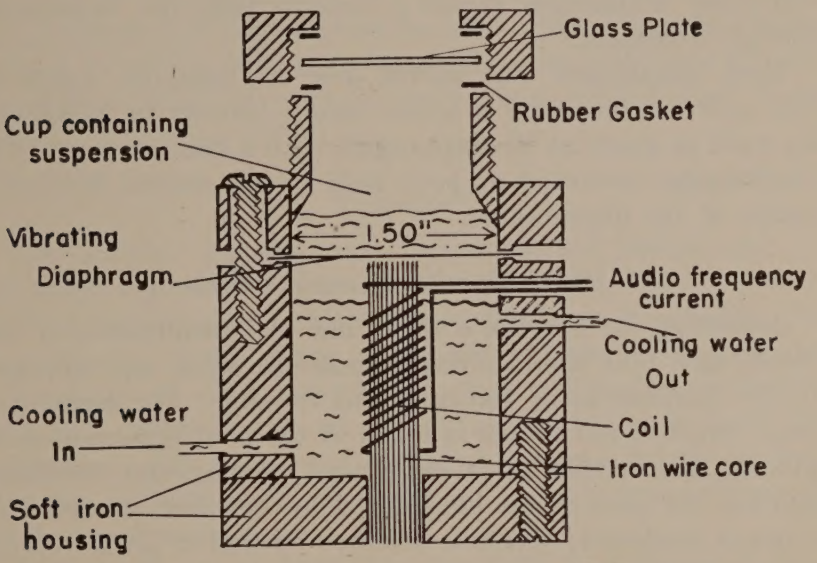

Fig. 1 One of the transducers constructed to convert electrical energy to acoustical energy. A definite volume of suspension, usually 5 ml with this transducer, is pipetted into the cup. Water cooling is necessary to remove heat generated by eddy currents in the iron and by viscous losses, and cavitation in the biological suspension.

is read directly on the oscillator dial which has been calibrated to better than $\pm 2\%$, which is entirely adequate for our purposes.

Transducers

The transducers constructed to convert electric power to acoustic power are similar to standard earphones. One of these transducers is illustrated in figure 1. An audio frequency current flows through the coil of insulated wire

wrapped about a core of soft iron wire. This generates an audio frequency magnetic field in the core above which is a diaphragm of suitable magnetic material. Since it is pulled down every time the magnetic field increases, the diaphragm vibrates at twice the frequency of the electric current flowing through the coil. The vibrating diaphragm is clamped at its rim; the upper half of the clamp together with the vibrating diaphragm forms a cup to hold the suspension during treatment.

Each diaphragm was useful over a frequency range of two octaves. To cover a wider range, 200 cps to 20,000 cps, we used as many as 10 diaphragms with 4 transducers. Thus overlapping occurred at both ends of the useful frequency range of the diaphragms.

Measurements of sonic output

According to Newton's third law the momentum of the diaphragm plus liquid above it must be equal and opposite to the momentum of the core and housing. For measuring sonic outputs, advantage is taken of the housing's motion by placing the needle of a calibrated phonograph cartridge against any part of the housing. The cartridge, mounted on a heavy stationary mass, is oriented so that it gives a maximum response to vertical motions of the needle. The amplified electric output of the phonograph cartridge is observed on the screen of a cathode ray oscilloscope. Besides giving peak voltage readings, the oscilloscope displays wave shape and aids in distinguishing the signal from noise.

For a given diaphragm and a given volume of suspension, the oscillograph reading, corrected for the frequency response of phonocartridge and amplifier, is proportional to the space average of the peak velocity of the diaphragm. The proportionality factor was not determined accurately; instead an arbitrary constant, α, times the corrected oscilloscope readings, C, was used as a measure of the peak velocity for a given diaphragm. A constant, α, was chosen for each diaphragm so that biological results at overlapping frequencies

were the same for the same value of C. The ratios of the value of α for different diaphragms could be estimated from Newton's third law knowing the housing and core masses on the one hand, and the vibrating diaphragm and liquid masses on the other. An accurate determination would involve a knowledge of the effective mass of the diaphragm and liquid; this we had no way of determining directly. In spite of this, the ratios of α for different combinations of diaphragms and transducers based on mass measurements agreed to within 40% with those based on biological effects. Since the biological methods were more precise, they were used to determine values of α.

Procedure

The cellular concentration was measured before and after timed exposures to measured sonic fields. The concentration of an untreated control was also measured after the experiment. From these measurements we computed the percentage of cells remaining whole after the treatment. For each determination of cellular concentration at least 250 individual cells were counted. Control experiments showed that the cellular destruction was not due to toxic substances in the transducer cup.

Periods of exposure to the sonic field were timed so that 20 to 80% of the cells were destroyed. The lower limit of 20% was chosen to restrict errors in the estimate of the fraction of cells destroyed. The upper limit of 80% destruction was chosen so that enough cells remained to be counted and so that the cells in a population which are either more resistant to sonic disruption, or else remained unmixed and in the less intense parts of the sonic field, would not contribute too heavily to the count.

With all protozoan cultures we attempted to have the cell population as homogeneous as possible. Cells were used which were growing no faster than one fission per day and which were well fed. This was especially important for the Paramecium experiments.

Different counting techniques were used with different cell types. Doctor J. R. Preer suggested a convenient method for counting Paramecia. A sample of standard volume (0.4 ml) is pipetted rapidly into a depression slide; the animals in the depression are then counted as they are drawn into a suitable micropipette under a wide field dissecting microscope. The concentrations used varied from 100 to 800 animals per milliliter.

Trichomonad cultures were diluted with isotonic saline to about 500 animals per cubic centimeter. Since the dilutions were done before the cultures were used, errors of dilution were avoided. An aliquot of the diluted suspension was placed in a standard hemocytometer. This was observed with a travelling stage microscope using the low power (16 mm) objective. The trichomonads swam freely in the hemocytometer. Animals were counted as being in a square, if they were there when the eye first focussed on that square. Many animals were stunned after exposure to a sonic field; all which retained the general shape of a trichomonad were counted as whole.

III. THE FRAGILITY OF TRICHOMONUS FOETUS IN SONIC FIELDS

The fraction of cells remaining whole after exposure to an intense sound field might depend on a number of different independent variables. These include the frequency, the sonic output, the length of exposure, and the cell type. We varied these one at a time to determine how they affected the fraction of cells remaining whole. Similar results were obtained by using a variety of small cells. The results of experiments on Trichomonus foetus are typical and are discussed in detail in this section.

Effect of length of sonic exposure

Suspensions of T. foetus were exposed for various lengths of time to a sonic field of fixed frequency while the oscilloscope reading was held constant. Figure 2 shows the results of

two such series of experiments, one at 0.6 kc. and the other at 10 kc. The fraction of cells remaining whole, N/N_o, is plotted on a logarithmic scale against the length of exposure. The linear relationship confirms the earlier work (e.g. Chambers, '36) which showed that for fixed sonic output and fixed frequency there exists a breakdown rate, R, defined by $\log N/N_o = -Rt$. N_o is the concentration of cells in the con-

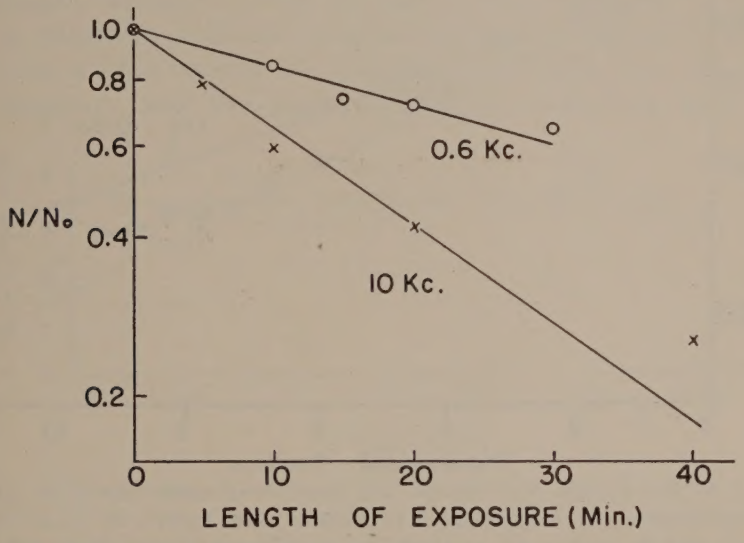

Fig. 2 The survival of T. foetus in sonic fields. N/N_o, the fraction of cells remaining whole, is plotted on a logarithmic scale against the length of exposure, t, to constant sonic fields at 600 cps and at 10,000 cps. We note that $\log N/N_o$ is proportional to t.

trol, while N is the concentration of cells in the suspension treated for the time, t.

Effect of sonic output

We then investigated how this breakdown rate depended on the diaphragm velocity at fixed frequencies. Sets of experiments were performed in which the time of exposure and the frequency were held constant, but the oscilloscope reading was varied from one experiment to the next. The results of one set of experiments at 1 kc. and another at 10 kc. are

shown in figure 3. Here the fraction remaining whole has been plotted on a logarithmic coordinate against the oscilloscope readings. The linear relationship was a pleasant surprise; it justified using oscilloscope readings as a measure of sonic output.

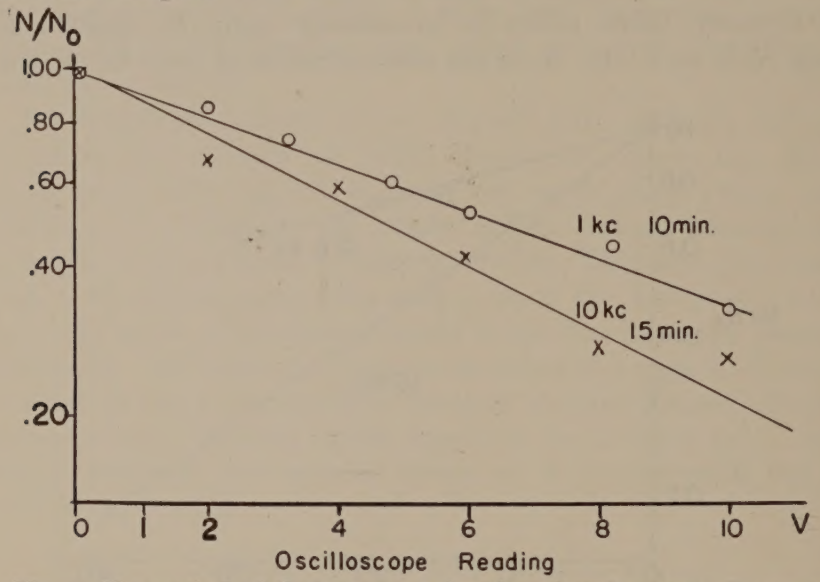

Fig. 3 The survival of T. foetus as a function of sonic output. In one set of experiments cells were exposed to various sonic outputs at 1 kc. for 10 minutes and in another set at 10 kc. for 15 minutes. N/N_o, the fraction of cells remaining whole, is plotted on a logarithmic scale against the oscilloscope reading, V, which is proportional to the peak velocity of the vibrating diaphragm. We note that log N/N_o is proportional to V for fixed frequency and length of exposure.

The results of these experiments at fixed frequencies can be expressed mathematically as:

$$\log N/N_o = -KVt$$

where N_o, N, t, are defined above; and

$$V = \alpha C$$

In this C is the corrected oscilloscope reading, and α is a constant for a given diaphragm in a given transducer.[3] The

[3] Therefore V is proportional to the space average of the peak diaphragm velocity.

quantity K is a constant whose value depends on the organism treated and the choice of α. We call K the breakdown constant.

Effect of sonic frequency

Since the above simple relationship held at widely different frequencies, we could now study the effect of varying the frequency without having to restrict the values of v and t to be constant. Cellular suspensions were exposed to sonic fields at a wide variety of frequencies. In each case, the time of exposure and the peak oscilloscope deflection were re-

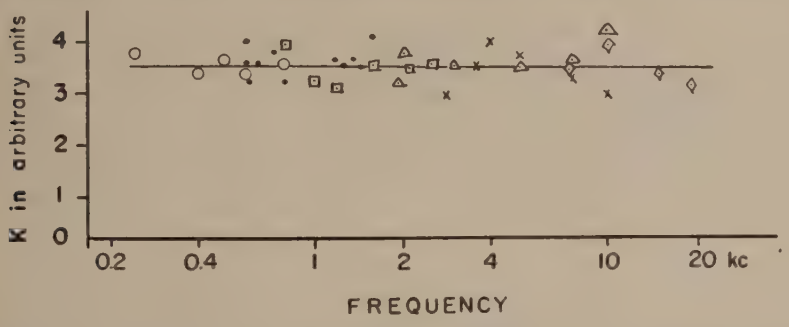

Fig. 4 Relationship of the breakdown constant, K, for T. foetus to the frequency of the sonic field. The frequency is plotted on a logarithmic scale. Different symbols indicate different diaphragms. K is independent of frequency from 0.2 to 20 kc. for T. foetus.

corded. The corrected oscilloscope readings were used to compute a value of the breakdown constant K for each experiment. For a given diaphragm and a given α, K was found to be a constant over the two octaves available, to within a probable error of not more than $\pm 10\%$. As noted earlier, the values of α were chosen so that different diaphragms operating at the same frequency gave the same breakdown constant.

The graph in figure 4 shows values for the breakdown constant K, observed by this method, plotted against the frequency. The probable error in K for two octaves covered with a given diaphragm is, at most, $\pm 10\%$. If we assume

that errors add as random errors, the probable error in K through the 6 octaves studied should be $\pm 20\%$, i.e. K is independent of frequency from 0.2 kc. to 20 kc. to within a probable error of $\pm 20\%$. Even a change in K of 5 times this probable error (e.g. K at 200 cps would be double K at 20,000 cps), would represent an extremely slow variation of K with frequency. This result is in direct contradiction to the theoretical predictions of Noltingk and Neppiras (op. cit.) which indicated that K should decrease rapidly as the frequency increased. Their theory is at best an incomplete approximation at audible frequencies.

Discussion of results

Since K does not vary appreciably with the frequency, the logarithmic breakdown rate depends only on the peak velocity of the diaphragm (rather than the amplitude or peak acceleration). For any simple harmonic oscillator, we can write:

$$v = 2\pi\nu A$$

where v = peak velocity; ν = frequency; and A = amplitude. A simplified expression of our results is that the logarithmic breakdown rate is proportional to "how hard" the diaphragm hits, A, and how often it hits, ν.

The breakdown constant, K, is a property of the particular organism treated. The larger K is, the more rapidly the organism breaks down under the mechanical agitation produced by the sonic field. Therefore we interpret K as a measure of the mechanical fragility of the cell.

We have measured the value of K for diverse cell types, arbitrarily choosing $K = 1$ for human red blood cells. (In absolute units K for human r.b.c. is about 10^{-1} $\frac{\log \text{ units}}{\text{min}} / \frac{\text{m}}{\text{sec}}$). The results of studies on the relative mechanical fragility of various cells are shown in table 1, together with their approximate sizes. Although one might expect the smaller cells to be much tougher, the size differences are only one consideration. Thus the largest cells listed in the table, Amoeba

proteus, are among the least fragile, whereas the smallest object, T2 phage, has far from the lowest K value.

The choice of the human red blood cell as a standard is one of convenience. These are always available to all experimenters and lie in the middle of the fragility range studied here. The comparison with a standard cell makes

TABLE 1

Approximate cell sizes and mechanical fragilities for various cultures. T. foetus cultures were obtained from Dr. Banner Bill Morgan, Veterinary Science Department, University of Wisconsin; E. coli and Staph. albus from Dr. C. V. Seastone, Med. Bact., University of Wisconsin. Paramecium cultures were obtained from Dr. J. R. Preer, Zoology Department, University of Pennsylvania; E. coli B and T-2 phage from Dr. T. F. Anderson, Johnson Foundation, University of Pennsylvania.

CELL	MECHANICAL FRAGILITY	APPROXIMATE AVERAGE
	K/K Human R.B.C.	Diameter (microns)
P. aurelia G's	16	80
P. caudatum	4	150
Amphiuma tridactyla R.B.C.	3	50
T. foetus	2	12
Human R.B.C. (E.A.)	1	6
Rabbit sperm	0.7	5
Amoeba proteus	0.4	200
T-2 bacteriophage	0.2 [2]	0.01
E. coli	0.15 [1]	1
Staph. albus	0.07 [1]	1
E. coli B	0.01 [2]	1
Baker's yeast	< 0.0003	5

[1] Values based on measurements of soluble nitrogen/total nitrogen.

[2] Values based on optical density measurements.

it possible to describe quantitatively the cellular fragility, rather than merely stating that a particular cell is "resistant" or "sensitive" to intense acoustic fields. Since the fragilities vary over such a wide range it seems desirable to report them on a quantitative basis.

These mechnical fragilities increase markedly when red blood cells are aged, just as the osmotic fragility does. However, our measurements on human, beef, sheep and rabbit

erythrocytes show that the mechanical fragilities are nearly the same although the osmotic fragilities are very different. Thus taking the mechanical fragility of human red blood cells, as 1, we found that the fragility of beef r.b.c. is 1.15 ± 0.05,[4] and that of sheep r.b.c. is 1.18 ± 0.05.[4]

This method of measuring mechanical fragility can be used for a variety of cells. The method fails for baker's yeast cells (Sacchromyces cereviseae), which are not broken by exposure to sonic fields (although yeast cells lose their ability to reproduce after exposure to intense acoustic fields). Nor can the mechanical fragility of excessively sticky cells be measured; thus ascarid eggs clumped in our sonic fields, protecting the eggs in the middle of the clump.

The data presented in the next section show that the fragilities of different strains of a single species, Paramecium aurelia, differ appreciably. Thus we suspect that the fragility in general is a property of the particular strain studied. The results of experiments on Paramecia also indicate that, at certain frequencies, the association of the mechanical fragility and the breakdown constant is unwarranted.

IV. RESONANT PHENOMENA IN CILIATES

At most frequencies the ciliates broke down in a manner similar to that of T. foetus, but in narrow frequency bands (a different band for each strain tested) the breakdown rate increases anomalously. Also in these frequency bands the logarithm of the fraction of cells remaining whole is no longer proportional either to the peak diaphragm velocity or to the length of sonic exposure. It was therefore necessary to hold both V and t constant to compare experiments in the anomalous frequency bands.

Paramecium caudatum

Figure 5 shows the values of K computed from several series of experiments in which Paramecium caudatum cul-

[4] Probable errors.

tures were exposed to sonic fields of different frequencies. The breakdown constant, K, is independent of frequency except from 0.8 to 1.7 kc. The increase of K at 1.2 kc. is over 30 times the probable error. For the frequencies in the anomalous region, both the time of exposure and the peak plate velocity were held constant and only the frequency varied. Experiments were repeated using vibrating diaphragms resonant at 0.8 kc., 1.2 kc., and 2 kc.; in every case the striking increase in K was observed at 1.2 kc. Thus the

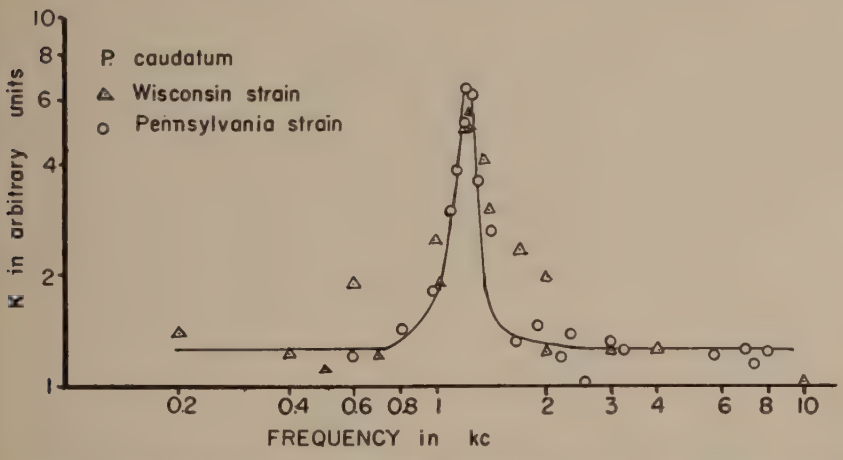

Fig. 5 Relationship of the breakdown constant, K, for P. caudatum to the frequency of the sonic field. Both K and frequency are plotted on logarithmic scales. K has a sharp peak at 1.2 kc. for P. caudatum.

peak of the curve in figure 5 is not due to a resonance of the diaphragm.

As noted above, K depended on both t and V as well as on frequency in the anomalous region. When long exposures or large diaphragm velocities were used the computed value of K did not increase above the base line, as much as when short exposures, or low diaphragm velocities were used. (The values plotted in fig. 5 are not at either extreme.) To study this further, several series of experiments were performed in which only the time of exposure or only the peak

diaphragm velocity was varied. The results of these experiments are shown in figures 6 and 7. The data make it clear that K, as defined earlier, is not a constant for P. caudatum at 1.2 kc., but is a constant outside of the anomalous frequency region.

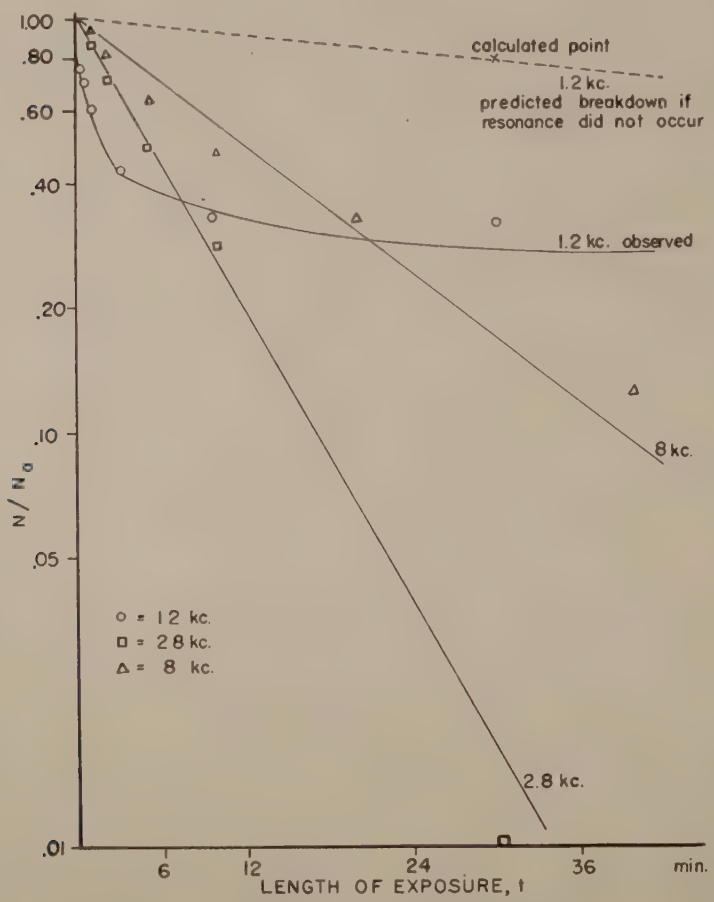

Fig. 6 The survival of P. caudatum in sonic fields. N/N_o, the fraction of cells remaining whole, is plotted on a logarithmic scale against the length of exposure, t, to sonic fields at 1.2, 2.8, and 8 kc. Log N/N_o is proportional to t at 2.8 and 8 kc. but not at 1.2 kc. From the sonic output used at 1.2 kc. we would have expected N/N_o to have followed the dotted line, if the breakdown constant, K, had been independent of frequency.

It is interesting to note in figure 7 that a certain minimum velocity is needed for cellular breakdown. This minimum is the same for P. caudatum, P. aurelia, and mammalian red

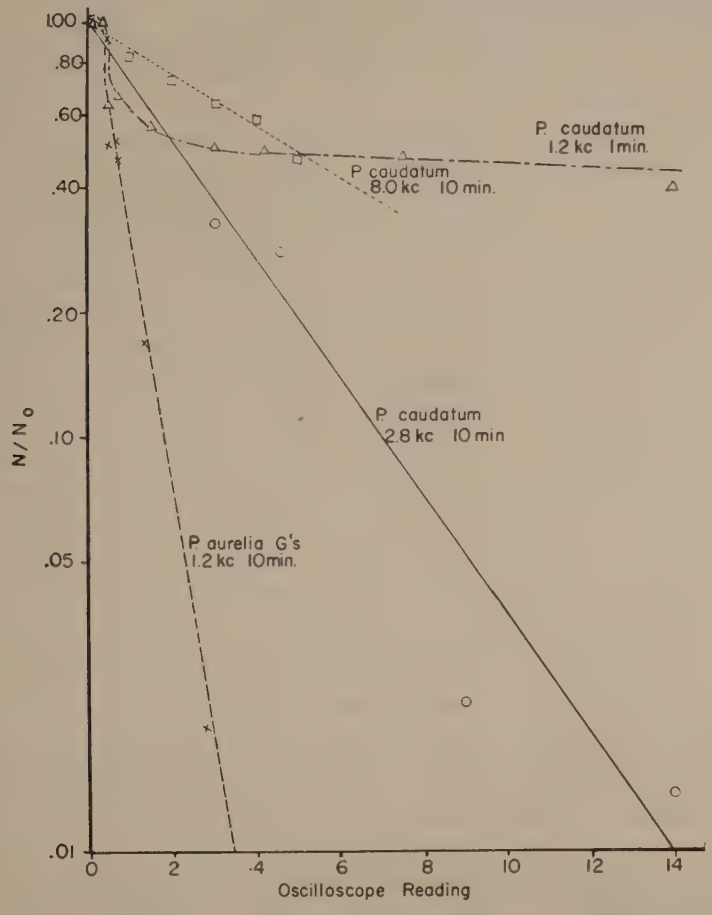

Fig. 7 The survival of Paramecia as a function of the sonic output. P. caudatum cells were exposed to various sonic outputs at 1.2 kc. for 1 minute and at 2.8 and 8 kc. for 10 minutes. P. aurelia G's was exposed at 1.2 kc. for 10 minutes. N/N_o, the fraction remaining whole, is plotted on a logarithmic scale against the oscilloscope reading. The oscilloscope readings at 8 kc. correspond to sonic outputs half those at 1.2 and 2.8 kc. At both 2.8 and 8 kc. log N/N_o is proportional to V for P. caudatum, but at 1.2 kc. it is not. At 1.2 kc., log N/N_o for P. aurelia is proportional to V above a certain minimum value of V. Below this value of V, neither P. caudatum nor P. aurelia break down at all.

blood cells. This minimum is a property of the physical equipment; it can be used to measure the maximum pressure at which cell destroying cavitation occurs (Ackerman, '50).

The break in the curve of log N/N_0 against t at the resonant frequency of figures 6 and 7 comes at different times for different sonic outputs. The breaks occur at about the same N/N_0 for a given culture. For cultures in excellent condition this occurred for values of N/N_0 less than 0.1; for cultures in poor condition, e.g. starved, the break occurred at values of N/N_0 about 0.6. Thus cultural conditions altered the curves obtained. The ones illustrated for P. caudatum at 1.2 kc. were chosen because they were not at either extreme. We have however no proof that, even for a completely homogeneous ciliate population, K would be independent of V and t at the resonant frequency. It may be that resonant breakdown obeys different laws from the non-resonant breakdown. Since we have not measured a convenient constant, independent of V and t, we can assign no significance to the shape of the resonance curves or to the height of their peaks. In particular we cannot use them to compute a value of mechanical Q.

Even for long exposures to intense sonic fields, P. caudatum cultures exhibit a significantly increased fragility at 1.2 kc. This optimum of the breakdown rate is not due directly to the sound wave, for the wavelength of sound in water at 1.2 kc. is 1.2 m; i.e. the wavelength is 5×10^3 times the Paramecium length. Even resonant pulsating bubbles would be considerably larger than the Paramecia (Smith, '35). Thus the variation in K appears to to be due to a resonance of the cellular architecture.

Other Paramecium species

To test how this resonance depends on cell size, the experiments were repeated on several distinct strains and species of Paramecium. The results of these experiments were again represented by values of K[5]. The variation of K

[5] The non-resonant values of K indicate the relative mechanical fragilities.

with frequency is shown in figure 8. The relationship between the average size of the animals in the cultures and their resonant frequencies is shown in table 2. Although the resonant frequencies are higher for smaller strains, no simple relationship exists between average cell size and resonant frequency.

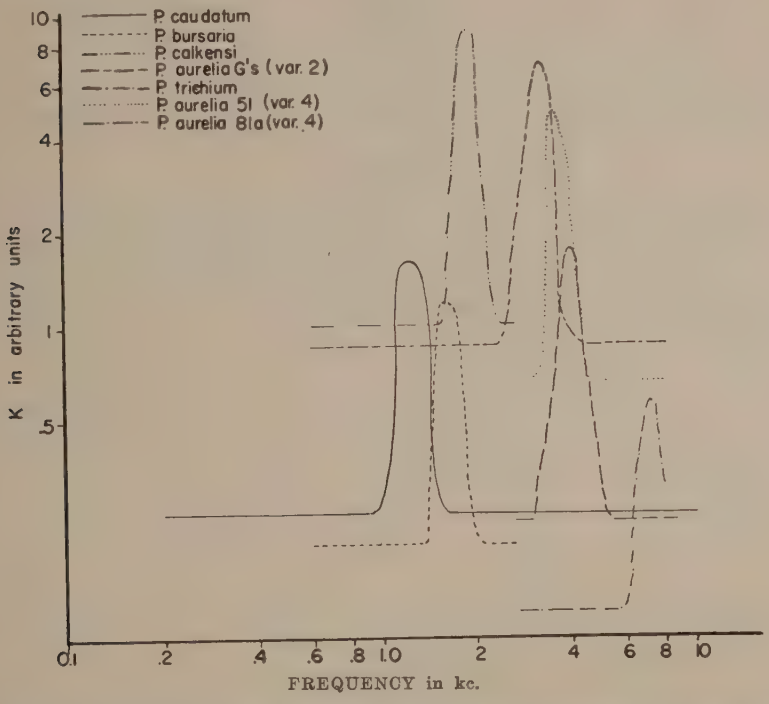

Fig. 8 Variation of K with frequency for various Paramecium cultures. Both K and frequency are plotted on logarithmic coordinates. The non-resonant values of K give the relative mechanical fragilities of the various cultures. Each strain has its own characteristic, resonant frequency.

To eliminate the possibility that the resonance effect could be an artefact due to the physical apparatus we studied the behavior of many mixtures of pairs of species, which were easy to tell apart. Differential counts were made on these mixtures before and after exposure to the sound field. To treat this data we could compute a value of K for each spe-

cies at each frequency. If we divide K_1 for the first species by K_2 for the second species, V and t no longer appear explicitly in the ratio K_1/K_2, since both species have been exposed for the same length of time to the same sonic output. Thus:

$$\frac{K_1}{K_2} = \frac{-\dfrac{\log\,(N/N_o)_1}{Vt}}{-\dfrac{\log\,(N/N_o)_2}{Vt}} = \frac{\log\,(N/N_o)_1}{\log\,(N/N_o)_2}$$

One example of the variation of this type of ratio with frequency is shown in figure 9. Here the subscript 1 refers to

TABLE 2

Average cell sizes of Paramecium in cultures studied and their resonant frequencies. 2a is maximum diameter. 2b is maximum diameter at right angles to $2\bar{a}$. $\bar{a}_{eff} = (2\bar{a} + 2\bar{b})/4$. *h is the average cortical thickness.* $\bar{a}_{eff}/h$ is an important variable in the rigid shell model. *These dimensions were measured on animals in a methocel suspension.*

SPECIES	$2\bar{a}$	2b	$\bar{a}_{eff}$	$\bar{a}_{eff}/h$	RESONANT FREQUENCY
	μ	μ	μ		*kc.*
P. caudatum	222.6	63.0	71.4	8.3	1.2
P. bursaria	117.2	51.4	41.6	9.8	1.7
P. calkensi	125.6	56.2	45.4	6.2	1.9
P. aurelia G's	123.8	29.2	39.8	6.9	3.3
P. aurelia 51	127.8	30.2	38.2	6.8	3.5
P. aurelia 81a	98	38	34.0	5.0	4.1
P. trichium	79.6	37.5	29.2	..	7.2

P. caudatum and 2 to P. bursaria. The ratio K_1/K_2 is plotted on a logarithmic scale against the frequency. The peak corresponds to a P. caudatum resonance, the trough to a P. bursaria resonance. (If V and t were not held constant at the various frequencies, a similar curve would result, although the exact shape would be changed.) Similar experimental results were obtained using other mixtures. Thus these cellular resonances can be demonstrated without the measurement of the peak diaphragm velocities (or time of exposure). They are true properties of the cells involved.

In addition, our experiments show that resonant cellular destruction does not occur, except when cavitation is produced in the suspending medium. Thus the resonant mode must be one which can be excited by cavitation.

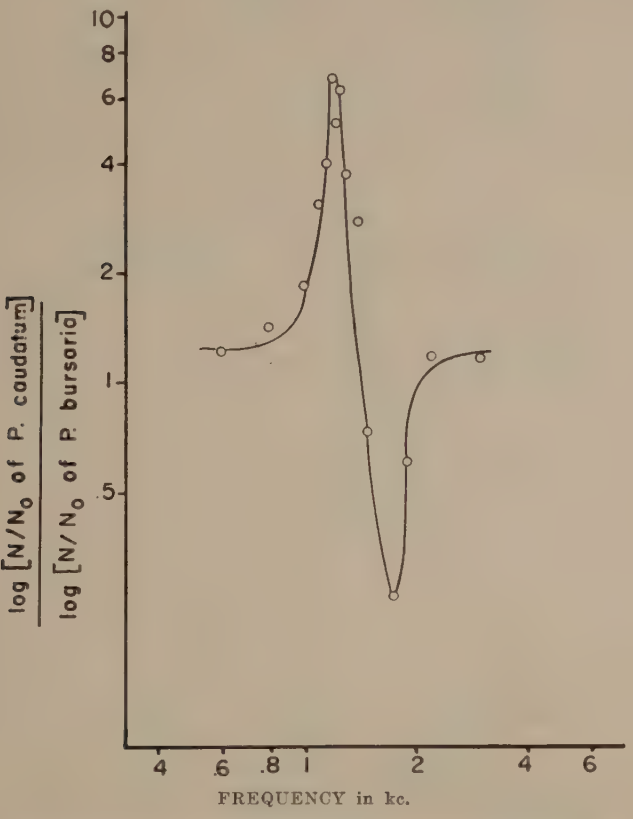

Fig. 9 Graphic summary of results of experiments on mixtures of P. caudatum and P. bursaria. Both the ratio of the logarithms and also the frequency are plotted on logarithmic coordinates. Resonances of P. caudatum (1.2 kc.) and P. bursaria (1.8 kc.) are demonstrated without the use of oscilloscope readings.

Blepharisma pellicles

Since cavitation occurs only outside of living cells (Harvey et al., '46), our first guess was that the resonance depended on the outermost layer of the Paramecium, its pellicle. This could not be checked for Paramecium but could be for

Blepharisma. This ciliate sheds its pink pellicle if the suspending medium contains any of a variety of narcotics (Nadler, '29).

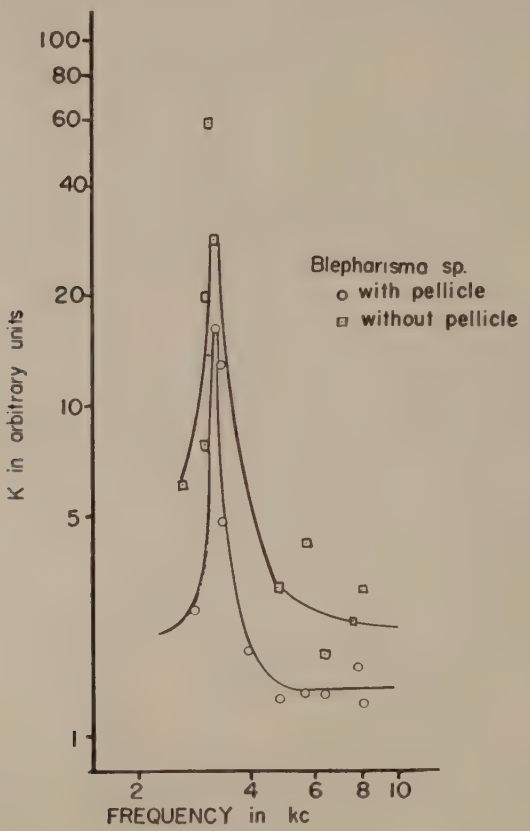

Fig. 10 Relationship of the breakdown constant K for Blepharisma to the frequency of the sonic field. Both K and frequency are plotted on logarithmic coordinates. The pellicle does not alter the resonant frequency but does reduce the mechanical fragility.

A single cell culture of a Blepharisma species was exposed to sonic fields at various frequencies. The experiments were carried out on animals with their pellicles and on animals which had shed their pellicles. Figure 10 shows the variation with frequency of the K values computed from these experiments. It is clear that the pellicle does not have an

appreciable effect on the resonant frequency. Thus other structures must be responsible for the observed resonance.

The pellicle does reduce the mechanical fragility by a factor of two. This confirms the qualitative observations of Nadler (op. cit.) that the animals without pellicles are easier to tear apart. The pellicle seems to have no other function, for it is unnecessary for life, metabolism, or reproduction and does not alter the size, shape or even the resonant frequency of the cells.

Interfacial tension model

Since the pellicle is not the resonant structure, we considered the possibility of resonances of the cell wall. On the basis of either of two cell models, resonances at sonic frequencies are predicted for spherical cells about the size of Paramecia (Ackerman, '51b). The first of these assumes that the cell is surrounded by a membrane of interfacial tension, T, having a negligible rigidity. The vibration of the membrane is similar to the motion of ripples on a water surface.

This model has been used to interpret many quite different experiments including tearing of cells by centrifugation and deforming cells by externally applied pressures (Harvey, '38). These experiments with no alternating force lead to values of T from 0.01 to 3 dynes/cm for a variety of cells including marine eggs, amoebae, and amphibian erythrocytes. (The low values are interpreted to prove that the outermost cell layer is not lipid.)

Our resonance equations lead to values of T from 3 to 10 dynes/cm for different strains of Paramecium. In view of the approximations involved, and the fact that the interfacial tension has never been measured by any other method for Paramecia, our values are in good agreement with the others.

Unfortunately the interpretation in terms of this cell model is not unique. Centrifuge experiments may be really measuring fragilities; deformation experiments and our resonances may be explained in terms of a cell surrounded by a rigid shell.

Rigid shell models

The vibrations of the rigid shell are similar to waves set up in a bowl of gelatin. Using this model, a sheer modulus, μ, is computed for the cell cortex. The values of μ are about 10^4 dynes/cm^2.[6] These are well within the range of 10^3 to 10^5 dynes/cm^2 measured for fibrin gels (Ferry and Morrison, '47). Thus this model is also reasonable. The exact value of μ depends on the thickness of the shell which has been interpreted as the cell cortex; the thickness of the cortex is hard to measure accurately. The ratio of the effective radius a_{eff} to the cortical thickness, h, is given in table 2.

DISCUSSION

Both the rigid shell model and the interfacial tension model predict harmonics none of which have been observed. This might be due to poor coupling to these modes. Thus if the coupling to the first overtone is one-tenth of the coupling to the fundamental, the peak would only be 3 or 4 times the probable error. Even this would be observed only if the frequency were within 1% of the resonant frequency.

Although we cannot choose between the two models, each gives the maximum value of a constant of the cell wall; i.e. T and μ, compatible with a resonance of this structure at the observed frequencies. Thus the interfacial tension of P. caudatum is not more than 3 dynes/cm and its cortical rigidity is at most 10^4 dynes/cm^2.

No resonances were observed for smaller cells such as T. foetus. Cells of this size, resembling either model, would not be expected to have resonances in the audible range.

V. SUMMARY

Vibrating plate transducers have been developed which have sufficient sonic output to produce cellular destruction from 200 cps to 20,000 cps. These are convenient to use be-

[6] By contrast $\mu \cong 10^{11}$ dynes/cm^2 for metals.

cause their frequency can be varied and their sonic output measured.

Using this equipment we find that cellular destruction obeys the equation

$$\log N/N_o = -KVt$$

where:

N_o = the original cell concentration;
N = the cell concentration after exposure to the sonic field;
V = a number proportional to the space average of the peak velocity of the diaphragm;
t = the time of exposure; and
K = the breakdown constant.

It is found for all cells that K is independent of frequency throughout most of the audible range. Although the absolute value of the breakdown constant, K, has no significance, the relative value for various cells is interpreted as a measure of mechanical fragility. Values of K, based on $K = 1$ for human r.b.c., range from 0.01 to 16. The values do not depend on the size alone; they are a quantitative measure of the mechanical fragility.

Paramecium species and Blepharisma have characteristic frequency ranges in which they are much more sensitive to the effects of the sonic field. Differential counts on mixtures of two species show that these are true cellular resonances and not due to errors in measurement of the sonic output. Experiments on a Blepharisma species with and without its pellicle show that the pellicle is not the seat of the resonance. They also show that the pellicle reduces the mechanical fragility by a factor of two.

The cellular resonances can be interpreted in terms of two cell models. One model considers the cell to lack rigidity, but to be surrounded by a membrane with an interfacial tension. This leads to values of 3 to 10 dynes/cm for the interfacial tension. The second model, that of a cell surrounded by a rigid shell, leads to a coefficient of rigidity of about 10^4 dynes/cm^2. Since both the values are plausible the evaluations of these constants are not inclusive. Moreover, overtones predicted by the theories are not yet found.

ACKNOWLEDGMENTS

This work would have been impossible without the help and advice of a large number of people. Special thanks are due to Dr. H. B. Wahlin, who originally suggested the problem to the author, to Dr. W. J. Meek, Dr. B. Chance, and Dr. T. F. Anderson, all of whom encouraged the author to continue these studies. The supply of biological materials from a number of sources is gratefully acknowledged. The author is indebted to Dr. T. F. Anderson for his many valuable criticisms concerning the form and wording of this paper.

LITERATURE CITED

ACKERMAN, E. 1950 The maximum pressure for cavitation in biological suspensions. Phys. Rev., *79:* 231.

———— 1951a Vibrating plate transducers for frequency studies of the breakdown rate of biological cells. Rev. Sci. Inst., *22:* 649.

———— 1951b Resonances of biological cells at audible frequencies. Bull. Math. Biophysics, *13:* 93.

CHAMBERS, L. A. 1936 A study of population growth and survival in cultures of Paramecium caudatum subjected to mechanical vibration. Am. J. Physiol., *116:* 26.

FERRY, J. C., AND P. R. MORRISON 1947 Preparation and properties of serum and plasma proteins. VIII. The conversion of human fibrinogen to fibrin under various conditions. J.A.C.S., *69:* 388.

GREGG, E. C., JR. 1950 Ultrasonics: Biological Effects. Medical Physics, vol. II, ed. O. Glasser, The Year Book Publishers, Inc., Chicago, Illinois, p. 1132.

HARVEY, E. N. 1938 Some physical properties of protoplasm. J. App. Physics, *9:* 68.

HARVEY, E. N., A. H. WHITELEY, K. W. COOPER, D. C. PEASE AND W. D. MCELROY 1946 The effect of mechanical disturbance on bubble formation in single cells and tissues after saturation with extra high gas pressures. J. Cell. and Comp. Physiol., *28:* 325.

NADLER, J. E. 1929 Notes on the loss and regeneration of the pellicle in Blepharisma undulans. Biol. Bull., *56:* 327.

NOLTINGK, B. E., AND E. A. NEPPIRAS 1950 Cavitation produced by ultrasonics. Proc. Phys. Soc., Series B. (London), *63:* 674.

SMITH, F. D. 1935 On the destructive mechanical effects of the gas bubbles liberated by the passages of intense sound through a liquid. Phil. Mag., Series 7, *19:* 1147.

ELECTRICAL CONTROL OF MORPHOGENESIS IN REGENERATING DUGESIA TIGRINA

I. RELATION OF AXIAL POLARITY TO FIELD STRENGTH

GORDON MARSH AND H. W. BEAMS
Zoological Laboratories, State University of Iowa

ONE FIGURE

INTRODUCTION

Externally applied electric fields of appropriate strength have been shown to exert polar control over growth direction, growth rate, and growth quality (differentiation) in developing or regenerating biological systems. The materials have been biologically simple and few in number, being confined to regenerating hydroids (Lund, '21, '24, '25, '47, p. 231; Barth, '34), the first cleavage of the egg of *Fucus* (Lund, '23b), and rhizoid formation in *Griffithsia* (Schechter, '34). Attempts to demonstrate similar phenomena in developing eggs and embryos of higher organisms have met with no success (Gray, '39; Needham, '31, pp. 537–538, 831–833).

Analysis of electrical control of morphogenetic processes offers fundamental contributions, potential and actual, to the nature of organic polarity, to various aspects of growth phenomena, and to the difficult problem of the nature of self-regulation in embryonic systems. There is need therefore for a more extensive body of factual data, with respect to both number of experiments and variety of type of material. It is also desirable to develop the details of control of systems differentiating along more than a single primary axis. These ends are partially served by the present series of experiments on electrical control of regeneration in one of the simpler triploblastic animals, the platyhelminth, *Dugesia tigrina.*

MATERIAL AND METHOD

The material was obtained primarily from commercial sources, secondarily from local habitats. The two populations differed in size and pigmentation, but were indistinguishable on the basis of regeneration and other characteristics, and corresponded to the specific criteria proposed by Kenk ('44) for *D. tigrina*. A limited number of *D. dorotocephala* and *C. foremani* were employed; none survived exposure to current.

The head was severed behind the auricles and the tail cut through the tips of the posterior intestinal branches. Small animals were divided into thirds: anterior, middle (with pharynx) and posterior. Large animals were divided into fourths: anterior, anterior midpiece, posterior midpiece, and posterior, the center cut dividing the pharynx. Piece length varied from 2 to 5 mm. The width never exceeded the length in the resting, relaxed piece and no pieces were small enough to develop two heads spontaneously (Child, '41, and references there). A few heads and tails with one regenerating surface were used; no heads survived. A short longitudinal anterior or posterior slit was made in each piece to assure subsequent recognition of the original polarity. The slit usually healed rapidly, leaving a relatively unpigmented streak and refractile scar. If the scar could not be recognized throughout the regeneration period the piece was omitted from the results. If healing occurred, no effect of this procedure on regeneration could be detected. From 0.5 to 26 hours elapsed between cutting and exposure to the current. In general, mortality was lower for the longer healing times.

Since cut pieces show pronounced cathodal galvanotropism and galvanotaxis, they were imbedded in 3% agar near its setting temperature on tissue paper fragments tied with fine thread to glass slips about $10 \times 5 \times 1$ mm. While this did not produce complete immobilization, it did prevent free turning for pieces with length: width ratios greater than one. Pieces which turned (from the anode) infrequently were reoriented; some which turned freely were reoriented,

others were allowed to remain oriented to the cathode. Movement was often sufficient to turn the axis of the piece at an angle to the current or to produce the equivalent effect through bending. While these were reoriented as observed, many pieces spent only a part of the exposure time parallel to the current. Also, pieces were mounted at, or moved to, small angles from the horizontal. Since the axial component of the current is proportional to the cosine of the angle between the piece axis and the current direction a number of pieces must have been recorded as at current densities higher than that effectively operating. This undoubtedly contributed to the wide range of values and the magnitudes of the standard errors of current density shown in table 1.

The experimental chamber was diamond-shaped, 17.5 cm long, 13.2 cm wide at the center, and 1.5 cm wide at the outlets. Its wall was a continuous glass tube, looped over one outlet, and connected to a cold bath. The outlet tubes were so bent that the fluid level of the outlet vessels was that of the chamber. Thoroughly aerated one-twentieth Ringer's fluid in tap water passed continuously into the chamber from a supply vessel. The outflow was equalized at the two ends by adjustment of constant level siphons discharging from the outlet vessels through funnels into a waste jar. The velocity of outflow was maintained at or above the transference velocity of hydrogen ion at the potential gradient obtaining in the outlet tubes. That this was a more than adequate safeguard against contamination of the chamber by electrode products was shown by absence of toxic effects, following accidental reduction or even cessation of flow for several hours. The specific resistance of the medium at 21°C. was 1031 ohm-cm.

By controlling the rate of flow through the perimeter coil the temperature in the chamber was held at 21 ± 1°C. In a few cases the temperature passed beyond these limits for short intervals without producing detectable effects. Temperature gradients within the chamber were generally small.

Current was supplied from a D.C. power unit with a reversing switch, an adjustable range milliammeter, and a varia-

ble resistance in series. Zinc : zinc sulfate electrodes completed the circuit at the outlet vessels through large area zinc sulfate-agar bridges. Current densities in microamperes per square millimeter were computed from the measured current and the appropriate cross-sectional area of the chamber, deducting the area of the glass slips, and were averaged on a time-weighted basis when these factors varied. Fluid height was measured with an adjustable gauge having a reading error between 2 and 5%. A sheet of millimeter cross-section paper was fixed beneath the base plate of the chamber to facilitate measurements of width and to guide the setting of the pieces.

Through carelessness, a systematic error was introduced into the calculations of current density. The pieces set at any position on a cross-line of the chamber were recorded as at the same current density. Their distance from the chamber center line was not noted. In reality, because of the diamond shape, the isopotential, or constant current density, lines were curved. Although known academically, this point was not appreciated practically until after the experiments were completed. The error along the center line varied from zero at the middle to plus 17% at the ends; the error at the edges varied from zero at the middle to minus 9% at the ends. The errors were thus partially self-compensating, particularly since fewer pieces could be set along the center line than at other positions. They tended to be restricted to the lower values because, as the effect of lower current densities became known, the current was increased for succeeding runs, most of the data thus being obtained in the mid-region of the chamber. It is apparent, however, that the extent of error is unknown, and that this partly accounts for the magnitude of the standard errors in table 1.

The regenerating pieces were placed in known orientation in the electric field and exposed to current 4 to 5.7 days (average 5.1 days), by which time the regeneration axis was determined, although complete symmetry was not yet attained. Approximately one-half the pieces were maintained

at the same position throughout the experiment. About 40% spent from a few hours to approximately one day at low current before being moved to high current for the remainder of the regeneration period, partly in an attempt to reduce mortality and partly to replace pieces dying at the higher current densities. About 10% were exposed to low current densities for 2.8 to 3.6 days or were shifted gradually from low to high density in order to test the limits of effect of duration of exposure. The pieces were examined at frequent, but irregular, intervals through a binocular microscope and a running record kept of their position, orientation, and condition, as well as of the height of the medium, temperature, and chamber current. Adjustments were made at these times; current and temperature were also adjusted at other intervals. At the end of the run regenerated individuals were freed from the agar and examined under binocular and compound microscope for details of polarity, gross structure, and behavior. One bipolar regenerant was fixed in Bouin's fluid and stained with hematoxylin. No animals were sectioned. Three animals were treated with dilute formic acid to bring out the details of the nerve cords.

RESULTS

A. Cathodal orientation. Seventy-four pieces regenerated with their original anterior ends oriented to the cathode at current densities ranging from 1.6 to 24.4 $\mu a/mm^2$. Eleven were tail pieces with a single cut surface. All regenerated in accordance with their original axis, and were similar to control animals at the same temperature. Body symmetry and responses were essentially normal, save in one piece in which the marking slit (posterior) had healed incompletely and in two pieces which developed vesicular swellings about the remnant of the old pharyngeal cavity.

B. Anodal orientation: two regenerating surfaces. Pieces oriented with their original anterior ends to the anode showed morphogenetic responses varying with the current density, as shown in table 1, sections 1 to 6. The first column shows

TABLE 1

Relation of (average final) current density to polarity of regenerated Dugesia oriented to the anode; 5.1 days' average exposure. 1–6, pieces with two regenerating surfaces; 7–8, tails with one regenerating surface

	CURRENT DENSITY IN $\mu A/MM^2$		POTENTIAL GRADIENT	NUMBER OF CASES	MORPHOGENETIC EFFECT
	Average ± S.E.	Range			
			mv/mm		
1	7.92 ± 0.74	1.6 –15.2	81.6	32	Normal regeneration
	(8.49 ± 0.81)	(1.6 –18.99)	(87.5)	(34)	
2	13.28 ± 1.21	8.35–17.21	136.8	10	Normal axis; head behavior in tail
	(14.68 ± 1.42)	(8.35–24.4)	(151.4)	(12)	
3	17.81 ± 0.38	16.43–18.92	183.5	7	Bipolarity with regression to normal
4a	19.45 ± 0.57	17.55–21.62	200.4	7	Bipolarity with anode dominance
b	18.97		195.5	1	Bipolarity without dominance
c	19.14 ± 0.58	16.88–22.67	197.2	13	Bipolarity with cathode dominance
d	19.24 ± 0.39		198.3	21	All permanent bipolars
5	19.92 ± 0.41	18.48–23.03	205.2	11	Bipolarity with progression to reversal
6a	22.09 ± 1.89	18.92–31.05	227.4	6	Reversal of axis; head behavior in tail
	(20.3 ± 0.73)	(18.92–23.03)	(209.2)	(5)	
b	21.28 ± 0.62	18.02–23.03	219.1	8	Reversal of axis
c	21.62 ± 0.85		222.7	14	All reversed animals
	(20.9 ± 0.4)		(215.3)	(13)	
7	13.05 ± 1.54	1.84–21.17	134.5	14	Normal regeneration
8a	18.94 ± 1.94	14.46–24.49	195.1	3	Acephalic
b	22.76 ± 1.58	21.17–24.34	234.3	2	Acephalic; head behavior in tail
c	20.47 ± 1.93		210.1	5	All acephalic animals

the average current density producing the morphogenetic effect noted in the last column. The average is derived from the final current densities, ignoring the lower values applied during initial conditioning or duration test periods. The validity of this procedure will be apparent from section D below. The second column shows the range of final current densities applied to the number of pieces recorded in the 4th column. By Ohm's law, the potential gradient imposed upon the regenerating piece in millivolts per millimeter is 10.31 times the current density. The values of the mean potential gradients are shown in the third column of the table.

At or below 16.5 $\mu a/mm^2$ the pieces regenerated in their original axis. The animal showing temporary bipolarity at 16.43 $\mu a/mm^2$ in section 3 is the single real exception to this generalization. The values in parenthesis in sections 1 and 2 each include two animals exposed for insufficient time to the high current density (section D below). The exception in section 2 was a piece mounted approximately 20° from the horizontal so that the axial component of the current was less than the recorded 17.21 $\mu a/mm^2$.

The regenerants of section 2, while possessing no visible controls. The average current densities calculated for this group, while significanty different from those of sections 2 to 6, have no very useful meaning, since there is no lower limit to the density which will permit normal regeneration.

The regenerants of section 2, while possessing no visible gross structural differences from controls, showed head behavior in the tail. This consisted of any, or all, of the following: (1) locomotor competition, representing attempts of the tail to crawl in the posterior direction, producing accordion-like stretching and contraction of the animal, or adherence of the tail to the substratum, producing checking of the normal forward progress followed by uncoordinated squirming or accordion movements; (2) competition with the head or assumption of the lead, in the righting response; (3) avoiding reaction, wherein the tail withdraws when mechanically stimulated, then extends, often in a new direction; (4) testing move-

ments, in which the tail is elevated with the tip approximately horizontal and moved in various directions as if sampling the environment, generally in response to mechanical stimulation, but sometimes spontaneously following a period of locomotor competition; or extension of the tail and application of its ventral surface to a probe, followed by movement of the tip over and about the probe. Head behavior persisted 2 to 3 days after exposure to the current, followed by resumption of normal tail responses. The range of current densities producing this result was approximately equivalent to the upper half of the range in section 1. The mean current densities for sections 1 and 2 are significantly different, but it is evident that other factors contribute to appearance of head function in the tail, since 18 of the 32 cases in section 1 fall within this range of current densities without appearance of the phenomenon.

Section 3 of the table shows the effect upon 7 regenerants of an average current density of 17.81 $\mu a/mm^2$ from a much narrower range. Animals of this group possessed a typical head on the anode end, and, in addition, an apparent head on the cathode end, so that they resembled the bipolar forms in section 4 a of the table, differing principally in their subsequent development. The "eyes" on the cathode head tended to have pigment spots smaller than normal and frequently multiple, and to lack the clear, vesicular region. The difference from the normal eye was of the same character as the difference between figure 1 E, e_2, and figure 1 A. The cathode head tended to be narrower than the anode head, but broader than a typical tail. The intestine had a single branch into the anode head, and a pair of branches encircling the pharynx, which opened toward the cathode. In two animals the posterior branches remained separate, in two they appeared to join in a closed ring, and in three they were apparently joined with a short single branch extending into the cathode head. The head behavior of the cathode ends was more marked than that of regenerants of section 2, but of the same character; in addition, the responses to light involved both ends

of the animals. The cathode head showed only competition with the anode head, never cooperation as was the case with some regenerants of section 4. Within three days the cathode head reorganized into a tail, the "eyes" disappearing and the intestine separating into two typical posterior branches. The changes were similar to those shown in figure 1, E vs. F, G vs. H. The mean current density for the regressive bipolars is not significanty different from those of sections 4 b, c and d, although it is from all the other means.

At a mean density of 19.24 μa/mm², section 4 d, 21 pieces regenerated a complete head on each end. The intestine in these forms consisted of a single anterior branch into each head joined to a ring surrounding the pharyngeal region (fig. 1 A, B, C, D). Nineteen individuals had a single pharynx (fig. 1 A); two individuals had two pharynges (fig. 1 D). In several animals the alimentary canal contained protozoa, from whose movements it was observed that the lumina of the main branches were continuous. A single pair of nerve cords was present, with a brain in each head (fig. 1 D). These were plainly revealed in two bipolars by treatment with 4% formic acid after about one minute. The cords showed little, if any, change in diameter between the brains; differentiation was sufficiently sharp to show the lateral connections and larger nerve branches. These latter were also observed in treated normal animals as a check upon method.

Unlike the regenerants in sections 3 and 5, the bipolar condition was permanent. No tendency toward division was observed. Fourteen of the regenerants lived two weeks or longer; 7 lived 4 weeks or longer. The longest survival was 41 days. All apparently succumbed to accidental overheating or drying of the medium. Two unsuccessful attempts were made to induce the animal shown in figure 1 D to feed, once on yeast and once on minced liver.

All but one of the regenerants of this section, immediately after removal from the agar, showed dominance of one head in extent of response to mechanical stimulation and to light, and in determination of direction of locomotion. Seven re-

generants (section 4 a) showed dominance of the anode head (fig. 1 A), developing on the original anterior end, at an average current density of 19.45 μa/mm². This was a higher density than the average at which 13 regenerants (section 4 c) showed dominance of the cathode head (fig. 1 B, C), although a lower value might have been anticipated. The difference in the means is not significant. The mean density for all permanent bipolars shown at 4 d is significantly different from the other means in the table except those of sections 3, 4, 5, and 6 a. In general, the dominant head was larger and more symmetrical, had larger eye spots and a longer intestinal branch, and controlled the position of the pharynx, which opened toward the subordinate head.

For 10 of the animals no subsequent record was kept. In 6 the dominance persisted or became more pronounced over a period of 5 to 41 days, as in figure 1 B, C; this includes the animal showing no dominance at the end of the run in which the anode head developed dominance in 13 days. In 5 animals dominance disappeared in 3 to 13 days with the achievement of bipolar symmetry (fig. 1 D). In animals showing dominance locomotion was primarily in the direction of the dominant head, with the subordinate head interfering. Occasionally the subordinate head was drawn about at an angle, but the direction (fig. 1 B) was still that of the dominant head. In animals without head dominance the two heads cooperated smoothly in locomotion, the typical body position being a V of 60 to 80° angle with direction along the bisector. In 9 bipolars a protrusion developed at the midregion, varying from a slight bulge (fig. 1 D) to a tail-like extension rounded at the tip (fig. 1 C), which in one animal achieved a length 50% greater than that of the combined head regions. In all these the pharynx was forced into the protrusion and opened toward its tip. The intestine, however, still formed a closed ring about the pharynx. In animals without head dominance the protrusion was posterior in locomotion. In those showing dominance (4 animals) it was typically carried at right angles to the direction of locomotion (fig. 1 C). That the pro-

trusion was sometimes created by muscular contraction was shown by several animals in which it was occasionally withdrawn; the animal of figure 1 A had such a protrusion equal to about one-sixth the body length three days before the photograph was taken.

Eleven pieces regenerating at a mean density of 19.92 μa/mm² (section 5), emerged as apparent bipolars with strong cathode dominance. Two were actually tripolar, two heads having formed to the anode on either side of the incompletely healed marking slit. In each animal the pharynx opened to the anode. The intestine in one was double at the anode end, in 4 apparently was joined in a closed ring about the anode end of the pharynx, while in 6 was joined and had a single branch extending into the anode head. Head shape, eye condition, behavior and subsequent development were similar to that of animals of section 3, save that the polar axis was reversed. In 3 to 5 days after removal from the chamber the anode head reorganized into a tail and the animals assumed normal symmetry, but with the original axis reversed. One such animal is shown in figure 1 E at the end of 4.6 days exposure to 19.5 μa/mm². The narrower anode head contained a single intestinal branch and two eye spots, marked e_2 in the figure; the left-hand one is partially obscured by superficial pigment. Figure 1 F was taken three days later, at which time the anode end had lost its eye spots and most of its head behavior, and the intestine had separated into two branches. Figure 1 G and H are line drawings from the prints E and F respectively. In figure 1 F the superficial pigment spots may be inventoried against those in 1 E. The mean current density for this group is not significantly different from the means of the permanent bipolars in section 4 of table 1, nor from those of the reversed animals of section 6. It is significantly different from the means of sections 1 to 3.

Fourteen pieces regenerated heads on the original posterior end and tails or potential tails on the original anterior end at an average current density of 21.62 μa/mm² (section 6 c).

The mean, as well as that in parenthesis, is significantly different from those in the upper portion of the table, save for 4 a and 5. The animals were distinguishable into two groups. Six regenerants, section 6 a, upon removal from the chamber showed head behavior in the anode end which disappeared within three days. The average current density for this group was 22.09 μa/mm². One animal was at the extreme density employed, 31.05 μa/mm². As there is no assignable upper limit to the current strength capable of producing reversal, the means in parenthesis were calculated omitting this value. Eight individuals, section 6 b, showed no detectable head function in the tail at 21.28 μa/mm², which is higher than the mean of 6 a if the extreme value is omitted. Neither mean in 6 a is significantly different from that of 6 b and the ranges of values are closely similar. As in the case of the animals of section 2, it is evident that factors other than the applied current are involved in persistence or appearance of head function in the morphological tail. Figure 1 I shows one of the regenerants of section 6 b after 4.6 days exposure to 20. μa/mm²; *s* indicates the scar of the marking slit made in the original anterior end of the piece. The individuals of section 6 were distinguishable from normal regenerants only by the position of the marking slits.

No differences were encountered at any current density which were associated with the size of the pieces or with the body level from which they came.

C. Anodal orientation; one regenerating surface. Nineteen tail pieces having only an anterior cut surface, and oriented to the anode, regenerated as shown in the last two sections of table 1. Fourteen animals, section 7, regenerated normally at a mean density of 13.05 μa/mm². Head behavior was not displayed by the uncut ends. The range of current densities is comparable to that of sections 1 and 2 combined. The mean for section 7 is significantly different from those of sections 1 and 3 to 6, but not from that of section 2; it is also significantly different from those of sections 8 b and 8 c, but not from that of section 8 a.

The 5 animals of section 8 developed no head structures during exposure to the current. One was lost by spilling, one was subsequently overlooked, two died within the first 15 hours, and one of the two in section 8 b died 6 days after removal without further reorganization. Thus no reliable information is at hand as to whether the condition would be permanent.

The two animals of section 8 b, in addition to the acephalic condition, also showed strong head function in the uncut tail. The mean density at which this occurred is significantly different from the means of sections 1 to 5, but not from those of section 6. The mean density of 18.94 $\mu a/mm^2$ for the three animals of section 8 a is significantly different from the means of section 1 only.

D. Duration of exposure. Although the healing times allowed before exposure to the current varied from 0.5 to 26 hours, no differences were produced in the effect of the current upon the subsequent regeneration. Plots of the final current densities producing a given morphological effect against healing time showed in all cases random distribution about the mean. Provided the current is applied 4 or more days the healing time has the character of an indifferent period.

Approximately 40% of the regenerants were exposed to current densities at or below the level of the mean for section 2, table 1 for 2.5 to 25 hours, then moved to a high density position where they remained for 4 to 5.5 days longer. As with healing time, plots of the final current densities producing a given effect against time spent at either low or high current showed random distribution, indicating an additional indifferent period, or that the current produced delay in reorganization.

To test the limits of the exposure time necessary to produce a definitive morphogenetic effect 13 pieces were exposed to low current 2.8 to 3.6 days and to high current 1.8 to 1.86 days. The currents were of the order of the mean for section 2, or less; the animals tested were among those of

sections 4, 5, and 6. In every case the morphogenetic effect was that of the final high current, and the groups at short exposure showed no consistent or reliable differences in the mean final current densities compared to those of longer exposure times.

Four animals were exposed to densities just larger than the mean for section 1, then shifted in 10 steps to final densities of from 16.3 to 24.4 μa/mm². The intermediate exposures were of less than one day duration; the final exposure varied from 0.36 to 1.15 days. All regenerated in the original axis. Two showed head function in the tail. These had spent respectively 1.34 and 1.64 days at densities above the mean for section 2. The two which regenerated normally had spent 1.15 and 1.7 days respectively at densities above this level.

The data appear to define the limits of the necessary exposure time (provided previous exposure to moderate current had obtained) at between 1 and 1.8 days. It may be questioned whether it is sufficiently reliable to place it between 1.7 and 1.8 days. In any case it provides the justification for the use of the final current density rather than a time-weighted average density for those pieces exposed to high current 1.8 days or longer. No inhibition of reorganization was found at any current density, except that described in connection with section 8, table 1, and that implicit in the fact of control of differentiation quality.

E. Mortality. In all, 1053 pieces were mounted and exposed to the current. The over-all mortality was 81.8%. Mortality was least for tail pieces and greatest for midpieces, presumably because of the presence of the old pharynx. Anterior pieces showed a mortality similar to that of the entire population.

The plot of per cent survival of all the pieces against current density descends rapidly to become nearly flat at 6 μa/mm² then drops appreciably at 21 μa/mm² and above. Over the greater part of the current density range mortality is nearly independent of the current. The corresponding curves

for different body regions show considerable variability. Tail pieces and midpieces show a steady decline in per cent survival over the entire range. Posterior pieces give a bell shaped curve with a maximum at about 19.5 μa/mm². Anterior and anterior-midpieces give v-shaped curves with their minima at 6 μa/mm². Lack of uniformity of shape of these curves suggests that the mortality is not due to direct damage by the current. Presumably it is a complex result of adverse conditions of temperature, desiccation, and trauma during the cutting and mounting, extent of healing of cut surfaces, and conditions during exposure to the current. Qualitatively it was noted during the experiments that pieces which failed to heal completely before exposure to the current generally disintegrated from one or both ends, and that mortality was uniformly higher for pieces introduced into the chamber immediately after mounting than for those allowed to heal for several hours. It was also observed that mortality was higher for those pieces which showed active movement during exposure. Upon rare occasions pieces were observed to contract with sufficient violence to rupture a healed surface. Disintegration showed no polar relation to the current, and the latter appeared to act principally as an indifferent stimulus. Occasionally a piece was able to heal and regenerate after degeneration of a considerable portion.

Although abnormalities appeared in the regenerants, such as body asymmetries, abnormal swellings, unequal eye size, their frequency was no greater than that commonly observed in control animals, and they were often attributable to conditions of cutting. They never showed polar relationships, and are believed not due to the current.

DISCUSSION

Electrical control of the polar axis and the differentiated quality of tissues is complete in Dugesia, and more delicately graded with the strength of the electric field than that of any material reported in the literature. This is probably due in part to the strong inherent polarity of the cut pieces, and

in part to the design of experiments on the other forms. For Dugesia the cathode is a head-determining pole and the anode a tail-determining pole, and their respective "potencies" are unequal, head determination being the stronger. This follows from the facts that (1) bipolar individuals are always two-headed, never two-tailed; (2) head behavior and head structure appear in original posterior ends at lower field strengths than those producing tail behavior and tail structure in the original anterior end (table 1, sections 2–6); and (3) that head suppression, but not tail-determination could be produced in the original anterior end of uncut tail pieces (table 1, section 8) while head behavior could be induced in the uncut tail. In the present experiments there is no evidence that head and tail determining forces resident in the piece itself are quantitatively different.

If apicobasal and anteroposterior polarity be considered analogous, the pole determining power of the electric field for regenerating Dugesia is similar to that for Fucus (Lund, '23b) and Griffithsia (Schechter, '34), in which rhizoids regenerate to the anode and thalli to the cathode (in Schecter's experiments the fate of the shoots is not entirely clear). On the other hand in Obelia (Lund, '21, '24) the cathode is clearly a base-determining, the anode an apex-determining pole. This is probably also true for Tubularia (Barth, '34), although no basal structures were reported toward the cathode, whose principal action appeared to be growth inhibition. Barth's ('34) data for Eudendrium and Pennaria do not permit a decision. It is evident that in the action of the electric field as a morphogenetic field the power of a given electrical pole to determine a particular morphological pole is an aspect of tissue competence.

Within the limits of the current densities employed there was observed no tendency toward reorganization of the cells of the end of a piece unless a cut surface was present. This would suggest that the electric field operates upon cellular processes rather than upon cellular states, although the data

presented are not adequate to make this generalization conclusive.

The fact that animals exposed for 3.6 days to moderate current densities insufficient to produce polar structural changes, would develop at suitable high density in 1.8 days to the morphogenetic state attained by other animals exposed to the same high density for 5 days, suggests that the lower current may have produced delay or inhibition of the regeneration process. The maximum healing time plus low current time was 4.17 days. Regeneration delay was found by Lund ('23a, b) for Obelia and Fucus and by Barth ('34) for Tubularia, Eudendrium, and Pennaria. The results of the present experiments do not exclude this since detailed observations necessary to precise determination of this point were not made. The normal variation in regeneration time of controls is sufficient to make a delay of 1 to 2 days difficult to determine with certainty, although a delay of 3 to 4 days should be observable. No obvious differences in developmental state were found in our experiments between cathodally and anodally oriented regenerants and control pieces, except those associated with regressive or progressive bipolarity and the acephalic condition. Head or tail determination under these conditions appear to be very nearly all-or-nothing phenomena, and the first (approximately) 3 to 4 days to be an indifferent period, rather than one of delay or inhibition.

The fact that the morphogenetic state produced by a given field strength is substantially independent of the total time of exposure, provided exposure be longer than a critical time of about 1.8 days, would seem to indicate that electrical control is not effected through the extensive properties of total charge transported or total electrical work performed. Indeed, because of variation in exposure time individual pieces regenerating normally were subjected to the action of slightly greater total charge transported through them than some pieces whose axis was reversed. The control would appear to be established through the attainment of critical

energy levels, which are properly characterized by the potential gradient rather than the current density, as was shown by Lund ('25) for Obelia. In succeeding papers of this series direct proof of dependence upon the potential gradient and substantial independence of the current density will be presented.

In Obelia (Lund, '25) the potential fall across the ectoendoderm necessary to produce cathodal inhibition and reversal of the polar axis, proved to lie between 1.88 and 10 mv, the range of magnitudes of the inherent potential of the tissue. This is obviously not the case in Dugesia, where the controlling potential gradients are about two orders of magnitude greater than the erratic potential differences measurable on either normal or regenerating animals. This discrepancy may possibly be resolved by the following considerations: In Obelia the apicobasal axis is overwhelmingly predominant, differentiation in the other two dimensions being uniform and of minimum complexity. A single external bipolar field corresponds in its properties reasonably well to the prospective organismic polarity and to the presumed character of the inherent morphogenetic field. In a bilaterally symmetrical organism such as Dugesia, while the anteroposterior axis is still predominant, the lateral and dorsoventral axes are relatively complex and are not uniform at different positions along the anteroposterior axis. The morphogenetic field of a regenerating Dugesia piece partakes of Weiss' ('39, p. 293) field property no. 3: "Fields, at least in the most specialized forms, are *heteroaxial*, . . . and *heteropolar* . . ." An external field must control all three axes simultaneously to produce symmetry and viability. The electric field does work upon the dorsoventral and lateral axes under the extreme disadvantages imposed by the cosine law. In order to produce symmetrical control the potential fall along the subordinate axes would presumably have to reach some limiting value, which would inevitably magnify the field strength along the parallel axis. If the average angle of orientation of the subordinate axes to the longitudinal field axis were

89° the potential gradient along them at the field strengths given in table 1, sections 3 to 6, would vary between 3.2 and 4.1 mv/mm. In the absence of further experimental evidence and other clarifying concepts we incline to this explanation.

In this connection it is of some interest that the narrow range of effective field strengths producing recognizable modifications of normal axial regeneration in Dugesia should be nearly identical in extent with the corresponding range in Obelia (Lund, '24, '25). The potential gradient producing regressive bipolars is 82.5% of that producing reversal (table 1, sections 3 and 6 c). In Obelia the potential gradient threshold for cathodal inhibition, above which apical structures were no longer developed on the cathodal ends of internodes regardless of orientation, was 22.4 mv/mm. This is 80.3% of the potential gradient of 27.9 mv/mm above which growth toward the cathode ceased during current flow. Between these values reversal of polarity became more frequent the higher the potential gradient.

SUMMARY

1. Cut pieces of *Dugesia tigrina* of known original polarity were imbedded in 3% agar and exposed to direct current for 5.1 days (average) at 21 ± 1°C. in a continuous flow chamber.

2. Pieces oriented with their original anterior end to the cathode developed normally at all current densities.

3. Pieces oriented to the anode (a) developed in accordance with the original axis below 16.5 μa/mm² current density (7.92 μa/mm² average), but showed temporary development of head behavior in the tail (to cathode) in the higher range (13.28 μa/mm² average); (b) developed temporary head structures and behavior to the cathode at 17.81 μa/mm² (average); (c) developed two permanent heads (bipolarity) at 19.24 μa/mm² (average); and (d) underwent reversal of original polarity at 21.62 μa/mm² (average).

4. Tail pieces with a single cut surface oriented to the anode became acephalic at 20.47 μa/mm² (average), with no

structural alteration, but with occasional head behavior appearing, in the uncut tips.

5. The potential gradient in mv/mm was 10.31 × current density. An explanation of the large magnitude of the potential gradient is offered in terms of the difficulties of triaxial control by a uniaxial external field.

6. The first 3 to 4 days of regeneration have the character of an indifferent period. The minimum effective exposure time to a given current density was about 1.8 days. No regeneration delay or inhibition was observed other than the implicit in control of the polar axis.

7. The morphogenetic effect of the current was not related to piece length or original body position.

LITERATURE CITED

BARTH, L. G. 1934 The effect of constant electric current on the regeneration of certain hydroids. Physiol. Zool., *7:* 340–364.

CHILD, C. M. 1941 Patterns and problems of development. Univ. of Chicago Press.

GRAY, P. 1939 Experiments with direct currents on chick embryos. Arch. f. Entw. mechan., *139:* 732–779.

KENK, R. 1944 The fresh-water triclads of Michigan. Misc. Pub. Mus. Zool., Univ. of Mich., No. 60.

LUND, E. J. 1921 Experimental control of organic polarity by the electric current. I. Effects of the electric current on regenerating internodes of Obelia commissuralis. J. Exp. Zool., *34:* 471–493.

———— 1923a III. Normal and experimental delay in the initiation of polyp formation in Obelia internodes. J. Exp. Zool., *37:* 69–87.

———— 1923b Electrical control of organic polarity in the egg of Fucus. Bot. Gaz., *76:* 288–301.

———— 1924 IV. The quantitative relations between current density, orientation, and inhibition of regeneration. J. Exp. Zool., *39:* 357–379.

———— 1925 V. The nature of the control of organic polarity by the electric current. J. Exp. Zool., *41:* 155–190.

LUND, E. J., ET AL. 1947 Bioelectric fields and growth. Univ. of Texas Press.

NEEDHAM, J. 1931 Chemical embryology. Cambridge Univ. Press.

SCHECHTER, V. 1934 Electrical control of rhizoid formation in the red alga, Griffithsia bornetiana. J. Gen. Physiol., *18:* 1–21.

WEISS, P. 1939 Principles of Development. Henry Holt and Co., New York.

PLATE

PLATE 1

EXPLANATION OF FIGURES

1 Dugesia regenerants after exposure to current. Cathode to left in A, right in B and C, up in D–I. *e*, eye spot; *p*, pharynx; *s*, scar of marking slit. A: permanent bipolar, anode dominance, 16 days old (after cutting); 5 days' exposure, 18.1 μa/mm^2. B: permanent bipolar, cathode dominance, 5.3 days old; 4.7 days' exposure, 17.7 μa/mm^2. C: same animal as B, 10.3 days old; anode eyes present, but indistinct. D: permanent bipolar, cathode dominance (gone at 13 days), 21 days old; 1.86 days' final exposure to 19 μa/mm^2, 3.6 days' exposure to 12.9 μa/mm^2; fixed in Bouin's fluid and stained with Delafield's hematoxylin. E: bipolar with progression to reversal, 5.2 days old; 4.6 days' exposure to 19.5 μa/mm^2; eyes, e_2, and superficial pigment on anode head, intestine joined with single anode extension. F: same animal as in E, 8.2 days old; anode eyes gone, superficial pigment remaining, intestine in two branches. G, H: line drawings from E and F respectively. I: reversed animal, no head function in tail, 5.2 days old; 4.6 days' exposure to 20 μa/mm^2; s shows scar of marking slit in original anterior end.


B
C
E
F
G
H
P
P
P
e_1
e_1
e_2
e_2
e_1
e_1
e_2
e_2
S

A STUDY OF THE VENTRAL HORN CELLS OF THE ADULT CAT BY TWO INDEPENDENT CYTOCHEMICAL MICROABSORPTION TECHNIQUES

JOHN NURNBERGER

Cytochemistry Laboratory, The Institute of Living, Hartford, Connecticut

ARNE ENGSTRÖM AND BO LINDSTRÖM

Department of Cell Research, Karolinska Institutet, Stockholm, Sweden

THREE FIGURES

During the past 15 years several radiant energy microabsorption techniques have been developed which make possible the quantitative or semi-quantitative estimation of some chemical components of the cell. Among these the ultraviolet microabsorption techniques developed by Caspersson ('36, '40, '50) are well known and have been used in a wide variety of problems. Recently a technique has been described for the estimation of the mass of extremely small biological objects allowing, thus, a standard basic value to which may be referred cytochemical analyses made by other microabsorption techniques on the same cells or cell parts. The advantage of stating a given concentration of cell substance in terms of total unit mass is obvious. This technique creates a more satisfactory basis for comparing one group of cells or cell constituents with another than was previously available. This possibility prompted the present study of the ventral horn cells of the adult cat.

An impressive body of information concerning the chemical composition of the immature as well as mature nerve cell of many biological species under a variety of normal and pathological conditions has been obtained using ultra-violet micro-

absorption and ancillary techniques by Landström, Caspersson and Wohlfart ('41), Hydén and co-workers ('43, '47, '48, '50), Gersh and Bodian ('43a, b, '47), to mention but a few of the most outstanding. Cellular protein and nucleic acids have been among components studied by the available techniques. When it is necessary to estimate mean concentrations of either of these substances within a structure as large as the ventral horn cell, particularly within the cytoplasm of such a cell, then it may be questioned whether consistently valid determinations can be made from single or even several measurements within a chosen circumscribed zone of the total structure, as has only been possible with present photoelectric microabsorption techniques. In comparing extinction values at any given wavelength it is imperative, moreover, either to keep the thickness of the absorbing layer constant (a difficult problem with present sectioning techniques), or to correct each extinction value for unit thickness of absorbing layer. Present optical methods for estimating structure thickness at the cellular level are, at best, approximations which become progressively less reliable, the thinner the layer, the greater the focal depth of the optical measuring system. These difficulties have been limiting factors in published studies. Perhaps even more importantly, though the influence of fixation on the magnitude of non-specific light losses has been almost uniformly discussed in such cytochemical studies as noted, specific analyses of comparable neural tissues fixed in different manners have not been reported. The lack of a reliable reference standard, until recently, has made such studies difficult if not impossible.

With a realization of the difficulties noted the immediate goals of the study we are reporting can be stated simply as follows:

1. To establish comparative values for the percentage dry substance (or, by inference, water), protein, and nucleic acids, in the various resolvable components of the adult

ventral horn cell of the cat, viz., the nucleolus, nucleus, cytoplasm, and axon hillock.

2. To examine by two totally independent techniques, the influence of fixation and section manipulations on cytochemical determinations in identical cells and cell parts.

3. To investigate the applicability of Beer's Law for ultra-violet light within the concentration ranges encountered in this type of tissue.

4. To evaluate, as far as possible, the origins and the magnitude of non-specific light loss and orientation effects in the ultra-violet microabsorption technique, by comparing the ultra-violet extinction values, calculated protein and nucleic acid, with mean total mass as measured by soft x-ray microabsorption. The latter is independent of non-specific radiant energy losses and molecular orientation.

5. To define those circumstances, if any, in which agreement may be observed between total dry weight in the nerve cell as estimated by soft x-ray microabsorption and the amount of protein as determined by monochromatic ultra-volet light microabsorption.

6. To evaluate the photographic-integrating ultra-violet microabsorption technique as used in this study and previously developed and described, in every detail, by Caspersson ('36) as a cytochemical tool in the study of nervous tissue, specifically the neuron.

MATERIALS AND METHODS

1. Preparation of tissues for study

A rapid cervico-dorsal laminectomy was performed on an active young adult cat without sterile precautions under ether anesthesia. After full exposure of the dural sac, the animal was rapidly bled by bilateral carotid section. Small segments of cervical spinal cord were removed, sectioned with a razor-blade, at about 1 mm thickness, and placed either in freshly filtered 10% neutral formalin, freshly pre-

pared Carnoy's fluid,[1] or in isopentane cooled below — 150°C. with liquid air. Blocks rapidly frozen in isopentane were transferred to a low vacuum system and dehydrated over the course of one week at — 40°C. These tissues were then transferred to low-melting point paraffin, rapidly infiltrated, and embedded for sectioning.

Material placed in formalin was fixed for 48 hours, then washed, dehydrated in graded alcohols, cleared in benzol, and infiltrated with melted paraffin as above. Carnoy material remained in the fixing solution for one-half to one hour, was then dehydrated in absolute alcohol, cleared as above, and infiltrated with paraffin.

Specimens of lumbar cord were removed from the animal one hour after carotid section, fixed both in Carnoy's fluid and in 10% formalin, and treated as above.

Sections were taken from all of the blocks prepared by the freezing-drying technique, and stained with methylene-blue, eosin. Those blocks showing minimal ice-crystal formation (a relatively few of the total) were used for subsequent microabsorption studies.

2. Microabsorption techniques

(a) The x-ray technique. This technique is described in full detail in a previous publication (Engström and Lindström, '50). Its application to the study of neural tissue poses no special problems nor is it to be anticipated that the concentrations of interfering elements in this tissue exceed the limits established in that publication.

In brief summary, the central element in the x-ray microabsorption apparatus is a demountable x-ray tube in which the section is investigated. X-radiation is generated by bombardment of a water-cooled anode with 3000 v. electrons from a hot filament cathode and is filtered through a 9 μ-thick aluminum foil to give continuous x-rays of wavelength ap-

[1] The Carnoy fluid used contained: Absolute alcohol — 6 parts, chloroform — 3 parts, glacial acetic acid — 1 part by volume.

proximately 8 to 12 Å. The tissue is mounted in the axis of this beam. The actual mounting technique is as follows: A microtome section of appropriate thickness is floated over the 1 mm wide slit in a thin brass disc and is supported by a ca. 0.5 μ collodion membrane. The section is carefully oriented over the slit so that the region to be analyzed is appropriately centered and is then deparaffinized. A step-wedge reference system of superimposed collodion foils of known mass and elementary composition is mounted adjacent to the tissue section over the slit. The x-radiation passes through the section as well as reference system. This takes place in the vacuum of the x-ray tube and produces an image of wedge and tissue on a fine-grained Lippmann emulsion which is clamped in immediate apposition to the tissue and reference. The microradiographic image of the specimen and wedge was enlarged 200–400 × by photomicrography on Gevaert Replica plates. By comparing the optical density in the enlarged image of reference and cell structure, the x-ray absorbing power of the structure under consideration could be expressed in units of the reference system. Since the weight per unit area and the chemical composition of the reference material were known, the relative values so obtained could then be expressed in absolute terms, i.e. milligrams per square centimeter. The resolving power, in this technique, is dependent mainly upon the granularity and homogeneity of the fine-grained emulsion used for recording the microradiogram.[2]

Sections studied in the above manner were, thus, exposed to x-radiation in vacuum for 15 to 30 minutes. After registration of the microradiogram sections were removed immediately from the supporting brass disc together with an adherent fragment of the supporting collodion membrane and

[2] The film used for this study was Lippmann Emulsion on celluloid base, manufactured by Gevaert, Antwerp. The resolving power of this emulsion for qualitative purposes is about 1 μ, but for quantitative purposes about 2–3 μ. The smallest structure studied, the nucleolus, had a minimum diameter of 5 μ and was adequately resolved.

transferred to glass slides which transmitted ultra-violet light. The supporting foil was dissolved with amyl acetate added dropwise over a three minute period. The sections were then passed through absolute alcohol, one minute, immediately placed in doubly distilled glycerin, and studied in monochromatic ultra-violet light after two or more hours. For tissues fixed as indicated and exposed to x-rays in vacuo, the time in the glycerin bath did not appear critical since examination of the same tissues after varying periods up to 18 hours revealed no consistent change in mean absorption value. Tissues variously fixed were likewise extracted with a number of standard lipid solvents before or after x-ray mass estimation as described in the text.

(b) The ultra-violet microabsorption technique. The details of the photographic integrating ultra-violet microabsorption technique used in this study were developed by Caspersson ('36). The reader is referred to pages 71–82 of his classical monograph for a detailed description of the technique.

The ultra-violet light source used was the familiar Köhler type of rotating spark gap activated by approximately 3000 v. 500 cycle current at less than one ampere. The spark generated by this high-intensity source was collimated through a quartz telescope lens, and separated into its monochromatic spectral components by refraction in two water-filled 60° quartz prisms. Appropriate wavelength radiation was then projected on the aperture diaphragm of the microscope condensor after filtration in a Backström filter. The characteristics of this filter are discussed by Thorell ('47). Quantitative photographic densitometric study of the resultant monochromatic beam revealed no measurable visible light in the 257 mμ and 275 mμ cadmium spectral lines used. Pure magnesium electrodes were used to generate the line at 310 mμ, which was unfiltered.

The microscope optics for photographic work were as follows: Zeiss, molten quartz condensor with a maximum N.A. of 0.8 and a focal distance of 6.8 mm, glycerin immersion. The

working aperture of the condensor was chosen to give full and even illumination of the object in the optical system. The objective lens was a quartz monochromat of N.A. 0.85 and focal distance 2.5 mm, glycerin immersion. A quartz 5 × ocular was used and the bellow length of the camera so set to give a linear magnification of exactly 1000 × in the image registration plane with light of wavelength 257 mμ.

The intensity and homogeneity of illumination at the three wavelengths used was checked photometrically. The intensity of incident energy was so regulated by filter and rotating sector that a mean background transmission of approximately 20%, which, for this emulsion was near the top of the "straight-line" portion of the density curve, could be secured repeatedly at a magnification of 1000 with the described optical system, and microscopic preparation in free space. The exposure factors varied, of course, with each wavelength but free space transmissions were found to be relatively constant and reproducible with the light source and optical system used. Careful initial regulation of incident intensity assured that accurate determinations could then be made even of heavily absorbing areas within the image, and that measurements of incident and transmitted intensities would fall well within the straight portion of the density curve, for the emulsion used. Repeated checks for homogeneity of illumination revealed maximal variations of 3–4% from center to extreme periphery of the total field. The central areas of such fields which, in fact, were uniformly used for registering the cell images showed variations of 2% or less. Homogeneous illumination is, of course, a necessity for quantitative photographic densitometry of this type.

One emulsion type and number was used for all the photographic densitometry reported here.[3] All plates were developed at 18.5° ± 0.5° for exactly two minutes, rinsed for a moment, then immediately plunged into a dilute acetic acid

[3] Ilford Ordinary Plates, Ilford Speed Group A, Ilford Limited, Ilford, London.

stop-bath, rinsed and fixed. Because of variations in developmental conditions a calibrating wedge image was registered on one end of every plate with a known constant exposure to visible light. Variations in development were corrected by means of this wedge. Details of this technique are also described by Caspersson ('36). It should be noted that since all readings were adjusted to fall on the straight portion of the density curve these wedge corrections amounted, at most, to a 5% change in the uncorrected mean extinction value. Only in those instances where transmitted intensities were so low as to give readings in the lower curving portion of the density curve did corrections exceed 5% and then rarely so.

Preliminary density curves were obtained at each of the three wavelengths used, under the exact conditions of exposure, calibration, and development used in the later analysis of tissue sections. Curves made prior to the studies were composed of 72 points each by varying bellow length, ocular, and condensor apertures. Repeat curves obtained during the course of the study were found to be precisely superimposable on the original curves.

In the actual analysis of tissue sections it was found unnecessary, as in usual photoelectric microabsorption techniques, to dissect away a free space from one edge of the cell. In both the formalin and Carnoy fixed tissues free spaces were conspicuous because of dehydration-contraction, and, though much less conspicuous in frozen-vacuum-dehydrated, could always be found somewhere about the cell or in the photographic field.

All determinations of optical density were made with a self-registering microphotometer of Siegbahn's construction (Thorell, '47), with a measuring area of about 0.2 by 0.2 mm, corresponding to an area of approximately 0.2 by 0.2 μ in the cell. In the first 20 cells, two complete tracks across the entire extent of the cell (cytoplasm, nucleus, and nucleolus) were run, one at right angles to the other, and the integrated

value for each structural component used for calculating extinctions at that wavelength. Analysis of those readings revealed that the value obtained by using the integrated mean of the track of maximum diameter, did not differ from the integrated value of the two tracks, hence in all subsequent analyses one track across the full maximum axis of the cell was used. Integration was achieved by summing individual values read through a carefully ruled transparent 5 mm lattice grid oriented to the horizontal baseline of the photographed curve, then calculating the simple arithmetic mean of all readings in sequence. Thus each cytoplasmic extinction value in the appendix represents the mean of 60 to 120 individual readings, each of these readings being the visually estimated mean of a 5 mm portion of the recorded transmission curve. The intensities of both incident (likewise a mean value for a free space close to the cell) and transmitted light were read directly in log values from the appropriate density curve. The recorded extinctions are the arithmetic difference between these values.[4] All values are corrected to standard conditions of photographic development by use of the visible wedge image previously described.

No definitive statement can be made concerning the accuracy of this technique for estimating given ratios of protein to nucleic acids in the complex physico-chemical environment of the nerve cell. However the mean reproducibility of extinction values on 14 repeat cytoplasm determinations under most adverse conditions (18 hours between recordings, Carnoy fixation, no visible wedge correction in first run) was 13% for wavelengths 257 and 275 and 20% for wavelength 310 mμ. Corresponding values for maximum nucleolar extinctions in 7 of these cells was 7% and 17%. These represent reproducibility of the technique at its worst. Mean calculated proteins in these two groups were identical and mean calculated nucleic acids varied by 12%.

[4] $E = \text{Log} \frac{I_o}{I_i}$.

A contemporary discussion of the interpretation of these extinction values is found in Caspersson's recent exhaustive report (Caspersson, '50, chapter 3). It is sufficient to state here that the total extinction at wavelength 257 mμ is generally considered to represent the sum of three factors: (a) specific chemical absorption by the purine and pyrimidine rings of nucleic acids which show a maximum at this wavelength; (b) absorption by the amino acid components of tissue protein; (c) a non-specific factor of light loss through reflection and scattering. By the same token the total extinction at 275 mμ is considered to represent a sum of the same three factors except that the heterocyclic amino acid components of tissue protein absorb at or near their collective maximum at this wavelength. Light losses by scattering, at this wavelength, likewise are considered to be less while losses by reflection remain relatively unchanged. The magnitude of the non-specific factor was assessed, in this study, at wavelength 310 mμ where no specific chemical absorption is thought to occur. The validity of these interpretations in terms of the observed data will be discussed later.

The possibility that organically bound iron may complicate the quantitative interpretation of the ultra-violet absorption data is now being investigated.

3. Estimation of mean structure thickness

Since it was necessary to estimate the mean thickness of individual cell components for this study, the interferometric technique could not be applied. Thickness estimates were made by the simple and relatively unreliable optical microscope method. Sections were studied under glycerin immersion, the mounting medium, with and without phase contrast. All measurements were made with a Zeiss H1 objective of N.A. 1.30 at a total linear magnification of 1100 ×. A minimum of 20 separate readings of upper and lower focal limits of each structure were recorded from the fine adjustment set-

tings within the relatively limited range where such readings were mechanically feasible and the mean of these calculated. Fractional readings were rounded off to the nearest $\frac{1}{2}\,\mu$. The focal depth of the measuring system under these circumstances was estimated at about $0.46\,\mu$ (Berek, '27). Thus structures separated by $0.46\,\mu$ in depth are imaged sharply in the microscope and a maximal absolute error of $0.92\,\mu$ in any single observation might be expected. The greater the thickness of the measured structure, the less the relative error, of course.[5]

It is obvious that calculations based on thickness measurements give only a semi-quantitative estimate. Accuracy of thickness measurements was limited not only by the irreducible focal depth of the measuring system but also by the surface characteristics of the studied structure. It was consistently observed, for example, that whereas the surface of cell structures fixed in formalin or Carnoy was readily distinguished, frozen-dried material was extremely difficult to assess, even with the condensor diaphragm sharply cut down. This may, in part, account for the striking lack of correlation between thickness estimates and any measured absorption value in these cells.

In Carnoy-fixed tissues a striking discrepancy was frequently noted between the estimated thickness of nucleolus and cytoplasm within the same cell. This discrepancy was confirmed in a few instances by low-angle metallic shadowing of the cell structures in vacuo. In such shadowed cells the nucleoli appeared like tall steeples casting long shadows over

[5] If d is the mean thickness of n observations the error in thickness is: $d \pm \sqrt{\frac{0.46}{n(n-1)}} \cdot \sqrt{2}$. Where, for example, n is 20 then we have $d \pm 0.033\,\mu$. The probable error in a single determination is $\pm 0.145\,\mu$. For a structure $1\,\mu$ in thickness the error of 20 determinations would be $\pm 3.3\%$, provided all measurements are performed on the same point in the structure. The actual spread of readings at this thickness was observed to be $\pm 25\%$ which is understandable as all readings were rounded off to the nearest $0.5\,\mu$, depending on the difficulty of reading the fine screw with higher accuracy. The observed spread also demonstrates that factors other than focal depth contribute to the over-all error.

a low plain (the cytoplasm). No quantitative inferences were made from these studies.[6]

OBSERVATIONS AND DATA

1. The appearance of ventral horn cells in the x-ray, and in monochromatic ultra-violet light

Photographic reproductions of 5 μ sections of two ventral horn cells fixed in Carnoy's fluid, are shown in figure 1. The contact prints on the left were made from original plate images registered with monochromatic ultra-violet light of wavelength 275 mμ. The prints on the right are comparable enlargements of the same cells made from photomicrographic images of the original contact microradiograms. Heavily absorbing dark areas in the ultra-violet prints correspond to light (heavily absorbing) areas in the microradiographic enlargements. The gross correspondence between heavily absorbing areas as, e.g., the nucleolus and karyosomes, in both techniques, is evident. Likewise it can be seen that the x-ray parameters used reveal far less contrast between the Nissl zones and surrounding cytoplasm than does the ultra-violet technique, even at this wavelength. One reason for this is that x-radiation, so used, demonstrates the distribution of absorbing material present in terms of its contribution to total mass, while the ultra-violet (whether at 257 or 275 mμ) highlights zones of nucleic acid concentration independently of the relative contribution to the total mass of absorbing material. This fact is dependent upon the comparatively high specific extinction of nucleic acids as compared to the markedly lower values for the absorbing amino acid components of tissue proteins. Another reason for the disparity is, of

[6] Evaluation of x-ray mass data indicated that divergences from microtome setting in the Carnoy tissues were the result of structural collapse and cytoplasmic contraction following deparaffinization. For this reason a value of 5 μ, the microtome setting, was substituted for observed thickness measurements in these cells. The mean cytoplasmic thickness of frozen-dried cells, as measured, was 5 μ, while that for formalin-fixed tissues was 5.5 μ. Carnoy-fixed cells, on the other hand, showed a unique contraction to 3 μ at the same microtome setting.

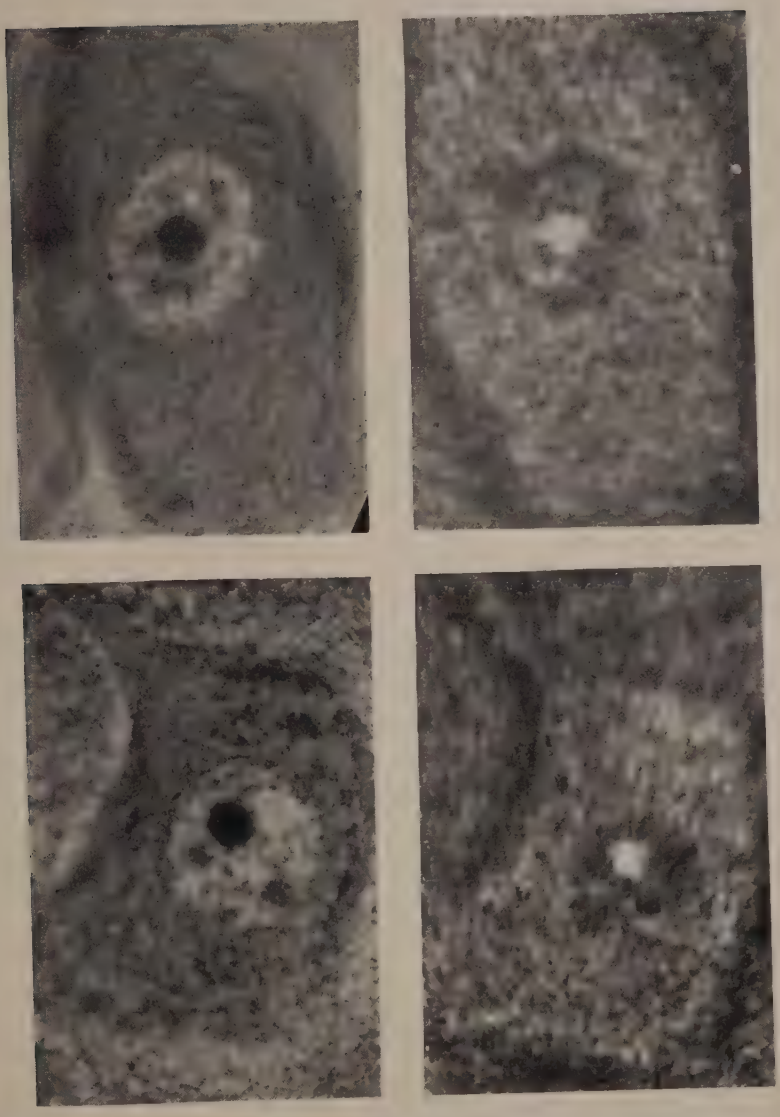

Fig. 1 Ultra-violet (left) and x-ray (right) microabsorption images of two ventral horn cells of the adult cat. Five-micron sections. Carnoy fixation. × 1000. The ultra-violet images registered at 275 mμ, the x-ray images in the range 0.4–1.0 mμ. See text for details.

course, the significant difference between the resolving power of the two techniques used.

2. Mean per cent dry substance of ventral horn cell components as determined by absorption microradiography

The influence of fixation and subsequent tissue manipulation on the quantity and distribution of dry substance in the resolvable components of ventral horn cells was investigated by the x-ray technique. The results of this phase of the study are presented in table 1. Mass values in this table are calculated in terms of the reference standard whose composition approximated that of a standard tissue protein. The heading "mg cm^{-2}" specifies that the stated structure absorbs as much x-radiation as a reference foil of the recorded mass in milligrams per square centimeter. The value "mg cm^{-2}-μ^{-1}" is obtained by dividing milligrams per square centimeter by the observed thickness, in micra, of the absorbing cellular layer. The percentage estimate transforms the latter value into gm $\times 10^{-14}$ per cubic micron of tissue which, in turn, is directly equivalent to grams per cent.[7]

Only the data for mean cytoplasmic mass were statistically analyzed since those for nucleus, nucleolus, and axon hillock were too few for valid treatment. A significant spread of individual observations, as implied in the relatively large sigma values, is clearly evident, particularly in formalin-fixed material deparaffinized with xylol. Data are grouped more closely about the mean in such tissues following chloroform extraction. Sigma values are smaller, and approximately equal in Carnoy and frozen-dried material.

The mean mass of Carnoy-fixed cytoplasm does not differ significantly from values recorded for formalin fixed tis-

[7] Grams per cent is recorded as an estimate because it must be assumed: (1) that the normal specific density of all tissue components is approximately 1 prior to dehydration and that the mass-volume relationship is not altered by this procedure; (2) that the observed structure thicknesses are valid; and (3) that the deviations in elementary composition of the tissue components do not exceed the limits defined by Engström and Lindström ('50).

TABLE 1

The influence of fixation on the mass of the resolvable components of the ventral horn cell of the adult cat, as revealed by x-ray microabsorption

CELL COMPONENT		FORMALIN FIXATION					FREEZING-DRYING	CARNOY FIXATION	
		Overall		Lumbar 1 hour after death: Xylol	Cervical Living: Xylol	Cervical Living: Xylol and $CHCl_3$	Xylol	Xylol	
		(1) Xylol	(2) Xylol and $CHCl_3$						
Cytoplasm	mg cm^{-2}	0.19 ± 0.02 $\gamma = 0.07$	0.25 ± 0.02 $\gamma = 0.07$	0.19 (15)	0.18 (6)	0.25 (16)	0.14 ± 0.02 $\gamma = 0.06$	0.20 ± 0.01 $\gamma = 0.07$	
	mg $cm^{-2}\mu^{-1}$	0.046 ± 0.005 $\gamma = 0.021$	0.034 ± .002 $\gamma = 0.007$	0.047	0.045	0.034	0.031 ± 0.003 $\gamma = 0.010$	0.040 ± .003 $\gamma = 0.013$	(b)
	% (estimate) (a)	46%	34%	47%	45%	34%	31%	40%	
Nucleus	mg cm^{-2}			0.10 (3)			0.07 (1)	0.115 (9)	
	mg $cm^{-2}\mu^{-1}$			0.022			0.020	0.023	(b)
	% (estimate) (a)			22%			20%	23%	
Nucleolus	mg cm^{-2}			0.36 (5)	0.28 (1)	0.31 (2)	0.26 (1)	0.37 (6)	
	mg $cm^{-2}\mu^{-1}$			0.090	0.186	0.050	0.074	0.105	(b)
	% (estimate) (a)			90%	185%	50%	75%	105%	
Axon Hillock	mg cm^{-2}							0.08 (1)	
	mg $cm^{-2}\mu^{-1}$							0.016	(b)
	% (estimate) (a)							16%	

Numbers within parentheses indicate number of individual determinations.

(a) Per cent dry substance recorded as an estimate on the assumption that all tissue components have specific density of 1.0. See footnote 7.

(b) Thickness of all Carnoy fixed structures presumed to be 5.0 μ, the microtome setting. See text for discussion.

sues. Chloroform extraction of formalin fixed cells reduces the estimated per cent dry substance from 46% to 34%, a possibly significant decrease. It is of interest to call attention here to the fact that the mean mass of formalin fixed cytoplasm in cells removed from the living animal is apparently the same as in those removed from a different portion of the spinal cord of the same animal, one hour after death. Frozen-dried xylol-deparaffinized cytoplasm has the lowest estimated per cent dry substance and is possibly significantly lower than the value for formalin material deparaffinized with xylol or Carnoy material similarly deparaffinized.

The mean mass of the nucleus is relatively constant and apparently not influenced conspicuously by the technique of fixation. This is remarkable in view of the fact that the distribution of absorbing material is strikingly inhomogeneous in Carnoy-fixed material (see fig. 1), yet quite homogeneous in formalin and especially frozen-dried material. The estimated value is approximately 25%.

In the small, compact, nucleolus, tremendous variations in mass are evident even in structures similarly fixed and treated. In this structure we might have anticipated the greatest range of alteration due to dehydration and contraction since the largest mass of absorbing material is here confined within the smallest volume.

In general it is justified to conclude that the mean cytoplasmic mass per unit volume, under conditions of most favorable fixation (though far from in-vivo conditions), is somewhat less than 35% and that the ratio of mass for nucleus: cytoplasm: nucleolus: axon hillock is approximately 1 : 1.7 : 3.0 : 0.7, using frozen-dried values, where available, as a control for fixation-dehydration artefact.

Chloroform may remove as much as one-quarter of total absorbing material from the cytoplasm of formalin-fixed nerve cells, though this removal may and probably does reflect mechanical as well as solvent effect. This observation is remarkable when it is recalled that these formalin tissues, be-

fore deparaffinization, have already been exposed to water, graded alcohols, and to benzol for relatively long periods of time.

3. Mean concentrations of protein and nucleic acids as calculated from ultra-violet extinction values

All of the cells investigated by the x-ray technique were subsequently studied in monochromatic ultra-violet light at 257, 275, and 310 mμ. An additional group of cells, frozen-dried but not exposed to x-radiation, were likewise studied to estimate the influence of this treatment on the ultra-violet extinction values. In the calculation of protein and nucleic acid concentrations the equations and extinction values of Caspersson ('42, '50) were used. One might question his hypothetical extinction values for "standard protein." Caspersson assumed ('42) as his standard protein one containing somewhat less than 5% tyrosine and 1% tryptophane. Amino-acid analyses of nerve cell proteins have not been reported to the present though Block's ('37 and '37a) values for mammalian brain protein indicate, on the average, 1–1.3% tryptophane and 3.9–4.2% tyrosine. Until accurate analyses of pure nerve cell protein are available Caspersson's "standard protein" remains as a justified mathematical hypothesis. In this connection it is of interest to mention that Schmitt ('51), in whose laboratory such analyses are now being made, states that protein fraction A of lobster nerve extract, and squid axoplasm, both display an absorption maximum close to 280 mμ, as do so many known animal protein substances. His group has thus far observed no nucleic acid band in this material, nor did we observe any nucleic acid "maximum" in our material, in the region of the axon hillock.

For such calculations as these it is customarily presumed that a certain amount of non-specific light is lost as a result of scattering in the preparation (increasing inversely as the 4th power of the wavelength), that the remaining non-specific light losses are the result of reflection (independent

of wavelength). The fraction of each is usually chosen arbitrarily with the extinction value at 310 mμ as a baseline for corrected calculations. The data recorded here afford a unique opportunity to compare protein and nucleic acid concentrations as calculated from ultra-violet absorption data with total mass (largely protein) in the same cells, as determined by x-ray microabsorption. To make discrepancies clear-cut in terms of non-specific light loss, it is presumed that all such losses are due to reflection alone, hence do not increase with decreasing wavelength.[8] Thus the observed E_{310} is considered to represent total non-specific light losses at all wavelengths. How erroneous this assumption can be becomes more clear from a study of table 2 where these data are tabulated. The sum total of protein plus nucleic acids should be compared with the values in the corresponding categories in table 1 as recorded from the same cells.[9]

The x-ray value for mean cytoplasmic mass in Carnoy-fixed material (40%) agrees rather well with the sum of nucleic acid plus protein (1.7 plus 39 or about 41%) as calculated from the ultra-violet data in the same cells. The fact, however, that one-quarter to one-third of the total recorded extinction at 275 and 257 mμ must be charged to "non-specific" factors to give us this agreement makes one fearful of the quantitative exactness of such calculated estimates.

The sum of cytoplasmic protein plus nucleic acid (89 plus 4.2%) as calculated from the ultra-violet data in frozen-dried material exposed to x-ray in vacuo, is approximately three times higher than the estimated mean cytoplasmic mass of these same cells, i.e. 31%, whereas if similarly treated cells

[8] This assumption may approach a valid estimate since it is probable that the loss of light due to scattering does not vary with 1/lambda^4 but rather with a much lower power of lambda, between 1 and 2. The exponent 4 is applicable for extremely small particles such as molecules in air. When the particles become greater in size, such as in biocolloids, the exponent becomes smaller.

[9] The individual values from which the mean totals recorded in tables 1 and 2 are derived are recorded in Appendix a and Appendix b.

TABLE 2

Mean concentrations of protein and nucleic acids according to technique of tissue manipulation: Calculated from ultra-violet extinction values

(a)

CELL COMP.	CARNOY		FORMALIN							
	Xylol and x-ray vacuum		Xylol and x-ray vacuum							
	Cervical living cord		Overall		Lumbar cord — 1 hour after death		Cervical living cord		Cervical living and lipid extraction	
	% Prot.	% N.A.	% Prot.	% N.A.	% Prot.	% N.A.	% Prot.	% N.A.	% Prot.	% N.A.
Cytoplasm	39 ± 6.0 $\gamma = 29$	1.7 ± 0.3 $\gamma = 1.7$	80 ± 8.0 $\gamma = 45$	2.8 ± 0.2 $\gamma = 1.3$	92 ± 13 $\gamma = 47$	2.8 ± 0.5 $\gamma = 1.8$	95 ± 24 $\gamma = 57$	2.7 ± 0.5 $\gamma = 1.1$	50 ± 3.3 $\gamma = 10$	2.8 ± 0.2 $\gamma = 0.6$
Nucleus	31 (11)	0.9	75 (11)	1.9	90 (5)	1.9	79 (4)	1.9	30 (2)	2
Nucleolus	97 (9)	1.6	153 (11)	3.9	183 (5)	4.4	182 (3)	2.5	77 (3)	4.6
Axon Hillock	25 (3)	0.1			55 (1)	0			11 (1)	0.2

(b)

COMP. CELL	FROZEN-DRIED AND X-RAY VACUUM						FROZEN-DRIED WITHOUT X-RAY VACUUM							
	Overall		Xylol without lipid extraction		Xylol plus addit. lipid extraction		Overall		Xylol		$CHCl_3$		Xylol and lipid extraction	
	% Prot.	% N.A.	% Prot.	% N.A.	% Prot.	% N.A.	% Prot.	% N.A.	% Prot.	% N.A.	% Prot.	% N.A.	% Prot.	% N.A.
Cyto-plasm	56±12 γ=43.4	3.7±1.0 γ=3.7	89±14 γ=36.0	4.2±0.7 γ=1.9	24±6.0 γ=16	3.1±0.7 γ=1.9	28±5.0 γ=20	1.7±0.2 γ=0.7	33±8.0 γ=20	1.7±0.4 γ=0.9	29±11 γ=25	1.7±0.3 γ=0.6	23±8.0 γ=17	1.6±0.4 γ=0.8

Numbers within parentheses indicate the number of individual determination in instances where statistical analysis was not justified.

are extracted with lipid solvents [10] before ultra-violet studies the mean total of protein plus nucleic acid (24 plus 3.1 or 27.1%) is consistent with the x-ray determined mass of frozen-dried cells, though still somewhat high if one includes the probable lipid-solvent effect on total mass. In sharp contrast the ultra-violet calculated value for protein plus nucleic acids in frozen-dried material not exposed to x-ray in vacuo (33 plus 1.7 or 34.7%) is only slightly and not significantly higher than the estimated cytoplasmic mass of similarly fixed cells. Chloroform deparaffinization of such cells gives a similar value (30.7%), likewise, in reasonable agreement with the x-ray data. Here, in contrast to the Carnoy material, "non-specific" losses are so low, as to be scarcely measurable. Lipid extraction of such fresh frozen-dried material produces an apparent decrease in calculated protein from 33 to 23% which is comparable to that estimated by x-ray for formalin tissue extracted with chloroform (there are no directly comparable x-ray data for frozen-dried cells, unfortunately) but the decrease is only suggestive, and not statistically significant.

In formalin-fixed fresh cervical cord material the per cent protein plus nucleic acids as calculated from the ultra-violet data (95 plus 2.7 or approximately 98%) is at least twice as high as the total mean mass of these cells. The same discrepancy is noted for lumbar cord cells formalin fixed one hour after death. Lipid extraction of the former cells produces a decrease in the total calculated protein plus nucleic acids from 98% to about 53%, which change is, of course, statistically significant and reflects, in a distorted way, the influence of chloroform extraction on such cells as revealed by the x-ray technique. However, even after lipid extraction, the calculated per cent cytoplasmic protein plus nucleic acid is still possibly significantly higher that the estimated mean cytoplasmic mass of such formalin-fixed cervical cord cells extracted with chloroform (34%).

[10] The following three solvents were used in sequence routinely: Absolute alcohol (3 parts), plus ethyl ether (1 part), and chloroform.

The x-ray data indicate that the mean cytoplasmic mass of formalin-fixed material may be significantly higher than that for frozen-dried material deparaffinized with Xylol. This difference is clearly not reflected in the data calculated from ultra-violet extinctions in the same cells exposed to x-ray in vacuo. However if one takes the values calculated from extinctions in cells so prepared but not exposed to x-ray in vacuo then the per cent protein plus nucleic acid (approximately 30%) is conspicuously lower than any of the formalin values. The same phenomenon is noted when one compares the Carnoy values with frozen-dried values, with and without exposure to x-ray in vacuo.

X-ray examination reveals no significant difference between the cytoplasmic mass of Carnoy and formalin-fixed material when the latter is deparaffinized with Xylol. In the ultra-violet, on the contrary, the apparent per cent protein plus nucleic acids in both lumbar and cervical formalin-fixed cells (95–98%) is obviously higher by a factor of 2 than the Carnoy values. Moreover, the formalin values are, as previously noted, at least twice the estimated mean mass of the same structures.

Two facts concerning the data calculated from ultra-violet extinctions must be stressed. The first of these is the marked spread of individual observations within the separate categories, clearly implied in the high sigma values of the table. These values are relatively greater even than those for the x-ray data. Secondly the ultra-violet technique as used here does not appear to give even remotely reliable quantitative estimates unless the per cent protein falls somewhere within the limits 20–40% in the presence of a nucleic acid concentration range of 0.5–2.5%. Outside these limits it appears that trends alone are indicated, though the trends are unmistakable. Since a markedly flattened "normal frequency distribution" is characteristic of both the x-ray and ultra-violet data it is probable that large biological variations are playing a part in the observed spread. Such variations are accentuated by fixation and dehydration distortions.

That one cannot interpret the ultra-violet data on a strict quantitative chemical basis seems evident, particularly for formalin-fixed material and for frozen-dried material exposed to x-radiation in vacuo. In Carnoy-fixed cells cautious interpretation is clearly warranted because the non-specific factor remains alarmingly high. Only in the frozen-dried material not exposed to x-radiation in vacuo are the data satisfactory for such interpretation.

It might be urged that had the above calculations been made assuming that all or, at least, a greater part of non-specific light losses were due to scattering the results might be quite different. As a matter of fact all of the data for cytoplasm as recorded in table 2 were recalculated on the assumption that non-specific losses were due entirely to light scattering, increasing inversely as the maximal 4th power of the wavelength. On the basis of this assumption the calculated protein values are, in all instances, close to those recorded in table 2, varying by not more than 5% from the recorded value. The nucleic acid values, on the other hand, are consistently lower in all instances (approximately one-third lower for the frozen-dried cells, one-half lower for formalin-fixed cells, and almost two-thirds lower for the Carnoy-fixed materials). Since non-specific factors are so poorly assessed it is quite clear that materials are most appropriate for such ultra-violet studies when these factors are minimal, as in frozen-dried material not exposed to x-ray in vacuo.

In general the ratio of estimated protein concentration for nucleus: cytoplasm: nucleolus: axon hillock, on the basis of ultra-violet data, is approximately 1:1.3:2.5:0.8. Thus the over-all trends as revealed by x-ray analysis are clearly reflected in the ultra-violet data. Moreover scatter diagrams of ultra-violet calculated protein values plotted against estimated mass in the same structures do indicate a gross correlation between the two, scarcely to be anticipated if one has the temerity to summate the theoretical errors probable in both determinations.

4. The correlations between x-ray and ultra-violet absorption values in ventral horn cell cytoplasm

In table 3 are recorded the "t"-values and correlation coefficients (r) for individual ultra-violet and x-ray microabsorption values on the one hand, and each of these measured values and the observed structure thickness on the other.

TABLE 3

Statistical correlations between ultra-violet and x-ray microabsorption values, for the cytoplasm of the same cells, and between each of these factors and observed structural thickness

Data correlated	STATIST. FACTOR	FREEZE DRYING	CARNOY	FORMALIN LUMBAR — 1 HOUR AFTER DEATH	FORMALIN CERVICAL — LIVING
Degrees of freedom		17	22	15	16
E_{257}/x	t	2.24?	0.14	1.58	3.66*
	r	+ 0.5	— 0.04	+ 0.4	+ 0.70
E_{257}/thickness	t	0.12	...	2.91*?	8.7*
	r	0.04	...	+ 0.63	+ 0.87
E_{275}/x	t	3.79*	0.14	1.58	3.74*
	r	+ 0.7	— 0.04	+ 0.4	+ 0.71
E_{275}/thickness	t	0.4	...	2.65*?	4.80*
	r	— 0.1	...	+ 0.59	+ 0.79
E_{310}/x	t	2.74*?	0.7	1.1	2.37?
	r	+ 0.58	— 0.15	— 0.3	+ 0.55
E_{310}/thickness	t	0.27	...	1.26	0.4
	r	+ 0.06	...	+ 0.33	+ 0.1
x/thickness	t	0.27	...	0.34	3.38*
	r	+ 0.07	...	+ 0.09	+ 0.67

E_{257}/x indicates, for example, individual correlations between ultra-violet extinction at 257 mμ and x-ray microabsorption data in same cell structures. E_{257} and E_{310} denote U. V. extinctions at these wavelengths.

t = calculated "t" value.
r = correlation coefficient.
*: = correlation at better than 1% level.
*?: = correlation at better than 2% level.
?: = correlation at better than 5% level.

The degrees of freedom indicate the number of observations, each individual observation being the mean of a large number of integrated single measurements, as previously mentioned. Correlations between extinctions at 257, 275 and 310 mμ in the ultra-violet and corresponding x-ray measurements were sought. Surprisingly enough most impressive correlation is noted in formalin-fixed cervical cord cytoplasm. At both 257 and 275 mμ there is significant correlation between x-ray estimated mass and ultra-violet extinction values. Likewise ultra-violet values increase linearly with thickness at both wavelengths. X-ray estimated mass is significantly correlated also with estimated structure thickness. Only at the "non-specific" wavelength, 310 mμ, is there no demonstrable correlation of U. V. extinction with thickness, though there may possibly be significant correlation with estimated mass. In striking contrast is the complete lack of correlation between ultra-violet and x-ray microabsorption values in Carnoy-fixed tissues. Thickness correlations were not attempted for Carnoy-fixed tissue because of the previously noted discrepancies between microtome settings and measured structure thickness. The trend in Carnoy-fixed tissue is, if anything, toward the negative side. Frozen-dried and formalin treated lumbar materials are intermediate between these first two groups. The frozen-dried material here evaluated was, of course, exposed to x-ray in vacuo.

These correlations may tentatively be interpreted to suggest that there is some substance or group of substances present in both formalin-fixed and frozen-dried material, but absent in Carnoy-fixed material, which contributes impressively to the total ultra-violet extinction values, particularly at 275 mμ, somewhat less at 257 mμ and least at 310 mμ, and which likewise is correlated to total estimated x-ray mass. It is not justified to presume that this substance is exclusively or even predominantly either of "standard protein" or nucleic acid type as such, particularly on the basis of the

data in tables 1 and 2. As will be recalled calculations based on ultra-violet absorptions indicate that Carnoy-fixed material alone, of the three groups under discussion, gives protein and nucleic acid values consistent with the x-ray data.

It seems clear at this point, that any attempt to assess the applicability of Beer's Law[11] to these ultra-violet microabsorption data, is futile and fruitless since they are compounded of at least three varying "specific" absorptive components plus one or more varying non-specific dispersive components.

5. The distribution of ultra-violet extinction values at 257 mμ with reference to "orientation" effects

Barry Commoner ('49), in a now widely quoted critique on the interpretation of ultra-violet absorption measurements of cellular nucleic acids, suggested that the state of molecular orientation of nucleic acids might influence the amount of monochromatic ultra-violet light (at 257–260 mμ) which could be absorbed by such a layer. He suggested that in the maximally aggregated state a modal E_{260} of 0.3 or thereabout might well be anticipated for nucleic acids, even though the "true concentration in the absorbing layer" could be considerably higher. Among many bits of evidence which he culled from the literature to support this interesting proposition is a series of absorption measurements on rabbit neurones from the work of Hydén and Hartelius ('48) which he presents graphically in a frequency distribution diagram (his fig. 5). One series of extinction values, with a modal value in the vicinity of 0.3 are from normal material and Commoner suggests that in these cells nucleic acid may be

[11] Beer's Law states, in simplest terms, that the attenuation of radiation (monochromatic) on traversing a given path length (thickness) of homogeneously distributed absorbing substance is directly proportional to the concentration of that substance.

oriented. In a second series of cells from animals treated with malononitrile, the modal extinction value is in the neighborhood of 0.6–0.7 and it is proposed that this increase in extinction may be a manifestation of disaggregation of nucleic acid molecules and not, as is inferred by the original workers, of any change in nucleic acid concentration. This criticism is a provocative one but may approach only the fringe of the problem, and even that on the wrong track.

The first and obvious criticism of this interpretation is that the published extinction values here alluded to are only in part attributable to nucleic acids present in the preparation. Cellular proteins likewise contribute their share, perhaps less, at this wavelength. Moreover both a specifically absorbing group of "non-protein" (?) materials as well as a non-specific dispersive factor all contribute to the extinction values so evaluated. As a matter of fact, to substantiate the latter suggestion, recalculation of E_{310} (non-specific) factor in the two groups of data here under consideration suggests that the E_{310} for the "normal" values of Hydén and Hartelius must have been, on the average, in the neighborhood of 0.10 while that for the treated cells must have been in the neighborhood of 0.20; thus double to begin with. But this is not the only criticism of Commoner's interpretation. Another becomes evident if the data obtained by us are plotted in a frequency distribution similar to that used by Commoner. Our data for "corrected" E_{257}, i.e. E_{257}–E_{310}, under 4 different conditions of tissue manipulation, are presented in figure 2. It would appear, from this graph, that Carnoy-fixed cells and frozen-dried cells tend toward a modal Extinction value approximating 0.3 while formalin-fixed tissue and frozen-dried material exposed to x-radiation show a modal displacement far to the right or "disaggregated" side. If, as has been done, these data are used to calculate apparent concentrations of nucleic acids as well as proteins, using either the reflection of scattering hypothesis for adjusting non-

specific light losses, Carnoy- and frozen-dried material yield values consistent with the estimated dry weight of the same cells, while the formalin values are at least twice as high as could be consistent with dry weight estimates while the frozen-dried-x-irradiated values exceed the dry weight estimates by a factor of three. This disproportion in protein estimates also

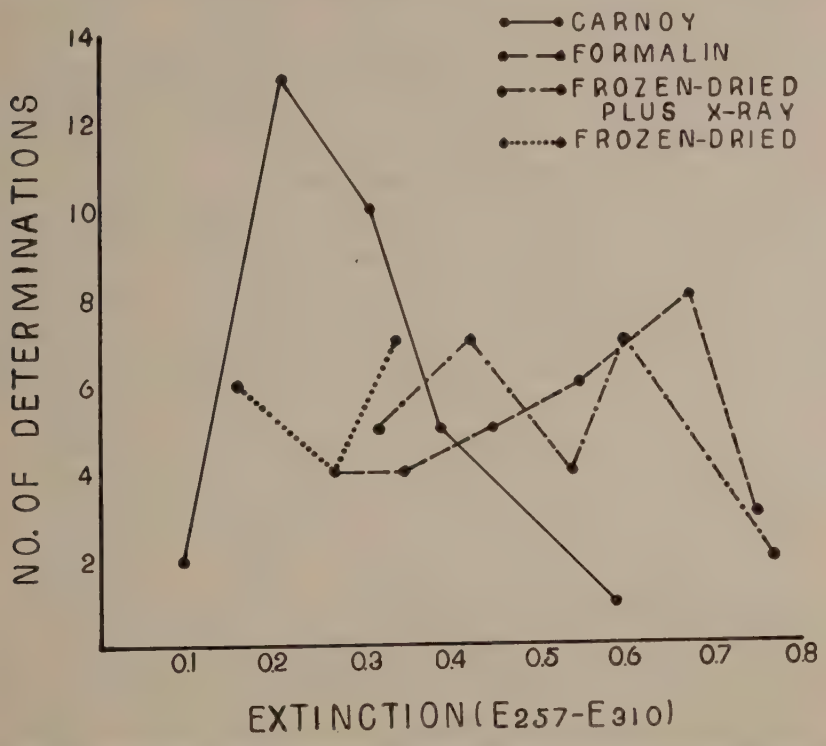

Fig. 2 Frequency distribution of "corrected" ultra-violet extinction values at 257 mμ (E_{257}–E_{310}) for variously fixed spinal cord tissue. Mean cytoplasmic values. Each individual determination on different cell.

manifests itself in the calculated nucleic acid estimates though we cannot check the latter as such by x-ray absorption data. Clearly, factors other than molecular orientation, whether or not it exists under these circumstances, must be considered in interpreting discrepancies noted in our figure 2 or in the reference discussed.

DISCUSSION

A discussion of some sources of error and likewise of frank limitations in the interpretation of the data obtained by these microabsorption techniques is indicated before there is further consideration of the observations themselves.

One source of error in both the x-ray and ultra-violet techniques is inhomogeneity in the distribution of absorbing material. Since the technical resolution of the x-ray method, with the emulsion used, is far below that of the ultra-violet technique it might be expected that inhomogeneities would influence more the data from x-ray than from ultra-violet. Study of these tissues by high resolution ultra-violet photography, in phase contrast, and in visible light both with and without staining aids, leaves little doubt that the absorbing material "measured" was distributed least homogeneously in Carnoy-fixed material, most homogeneously in frozen-dried material, with formalin tissue intermediate between these. Thus, in Carnoy-fixed material there is the strongest possibility that the size of absorbing aggregates might interfere with the aggregation of submicroscope grains in the emulsion and thus giving an apparent absorption value higher than the true value. The facts are, however, that the estimated dry substance in Carnoy cytoplasm is about 40% (intermediate between formalin and frozen-dried), and that the estimated per cent dry substance in Carnoy-fixed nuclei is almost identical to that in formalin-fixed or frozen-dried nuclei.

One important source of error in the ultra-violet technique but not in the x-ray technique, is scattering and reflection of radiation, and this fact makes the combined use of these two techniques of theoretical as well as practical importance.

Concerning the interpretation of x-ray determined mass values it must be emphasized that the mass or per cent dry substance recorded is total mass and not only the protein component. It is impossible to differentiate between proteins and other substances contributing to mass but it can be stated that the major part of the absorption is undoubtedly due to

protein. This is least true, theoretically, for frozen-dried material where all substances in the living cell might be expected to be present except those which volatilize under paraffin infiltrating temperatures, dissolve in liquid paraffin at 56°, and dissolve out during deparaffinization of the sections with Xylol for two to three minutes. Purely mechanical effects, also, might remove some material as is vividly suggested by observing the process of deparaffinization and vaporization of Xylol under the microscope. In formalin-fixed tissue only that material remains which is fixed by 10% neutral formalin and does not thereafter dissolve in water, graded alcohols, benzol, liquid paraffin, and Xylol. Thus, in all probability, all low molecular weight substances whether of carbohydrate, amino acid, lipid or steroid type, and non-organically bound electrolytes, are already removed. Carnoy's fluid might be expected to produce similar effects with probably a much greater influence on chloroform-soluble lipid materials, particularly those ordinarily bound to protein.

In the x-ray technique the nucleic acids present make a minor contribution to mass as already stated while in the ultra-violet they make a major contribution even at the so-called "protein maximum." This fact, however, suggests an additional source of distortion to be considered in interpreting x-ray mass data as "protein mass." Because the concentration of nucleic acids varies considerably in different parts of the nerve cell it is clear that the per cent phosphorus is likewise going to vary being higher in nucleic-acid rich areas. The possibility does exist, therefore, that variations in the per cent of phosphorus may introduce errors in the calculation of "protein" mass, the mass appearing to be higher in phosphorus-rich areas than it might actually be. However in the x-ray region used for measurements, the mass absorption coefficient for phosphorus is actually lower than that of nitrogen. This would indicate that the x-ray pictures show the real distribution of mass (dry weight).

In view of what has already been stated concerning the x-ray data it is of interest to note that the lowest mean cytoplasmic mass is recorded for frozen-dried material which, theoretically, should contain the most substance. The obvious interpretation of this is that in Carnoy, perhaps even more so in formalin-fixed material, there is a local concentration of absorbing substance due to fixation and dehydration contraction. Free spaces are, as a matter of fact, uniformly conspicuous around formalin and Carnoy-fixed cells, yet they are minimal around frozen-dried cells. On the other hand fixation aggregation of absorbing material may be a more important factor since the mean diameter of the neurones studied, whether formalin-, Carnoy-, or frozen-dried, is in the vicinity of 50–55 μ. These estimates were made with close accuracy on the ultra-violet plates registered at 275 mμ at a measured linear magnification of 1000 ×.

It is indeed remarkable that chloroform may remove as much as one-fourth of the total estimated cytoplasmic material contributing to mass in x-ray. The assumption that the substance removed may be of lipoprotein nature is suggested by the fact, first that it has not already been dissolved out in the processes of fixation, washing, dehydration, clearing and embedding; and secondly that it is removed by chloroform. Whether this may be the birefringent liponucleoprotein isolated by Folch-Pi and Uzman ('48) from brain tissue is, of course, purely speculative. The lipids in the substance isolated by them would appear to be more firmly bound than the substance in question though the conditions for solubility here are very different from theirs. There is no evidence that the substance under consideration is related to the neuronal yellow pigment described by Hydén ('50).

Concerning the ultra-violet data a number of pertinent reservations are in order. In the first place it is presently impossible to deduce, with confidence, the amounts of protein in any nerve cell component from microabsorption data because direct amino-acid analysis of neuronal components are

not yet available. Since this is true one can infer concentrations neither of nucleic acids nor proteins with any degree of confidence since both are interdependent in the nerve cell cytoplasm. Nor can ratios between these two components be stated with any greater assurance. It is impossible to establish reliable ratios where the concentration of neither component is known, both being present.

Probably a far greater complicating factor is the difficulty of estimating accurately non-specific light losses in the nerve cell. One must interpret with care so-called quantitative measures based upon extinction values in which non-specific factors may contribute, at times, one-half or more to the total. Present failure of methods to "calculate away" such non-specific factors may explain why estimated proteins exceed total "dry substance" by a factor of two in formalin-fixed cytoplasm, by a factor of three in frozen-dried, x-ray irradiated cytoplasm. On the other hand this distortion may not be totally a non-specific one. Lipid solvents apparently remove a large amount of this so-called "non-specific" component in frozen-dried irradiated cells while the E_{310} of such cells is little if at all reduced. The same is true of formalin cervical cells. In non-irradiated frozen-dried material lipid solvents cause, if anything, a moderate increase in extinctions at 310 mμ. The evidence would point more to the presence of some substance which absorbs at specific wavelengths with, perhaps, a higher specific extinction than the "standard protein" considered in our calculations. The x-ray data would, moreover, suggest the presence of such a substance. Why it should exert such a vastly larger effect in irradiated than non-irradiated tissues is not entirely clear. A recent study of McLean and Giese ('50) may provide a clue. They noted a consistent increase in the absorption values for protein and amino acid solutions below 320 mμ, after increasing irradiation of such solutions with ultra-violet light. A specifically absorbing oxidation product was suggested as the cause and evidence presented to support this thesis. Whether such a

phenomenon could follow irradation with x-ray in vacuo is not demonstrated, but the possibility though small cannot be completely denied.

A third complicating factor, which applies to any microabsorption method utilizing electro-magnetic irradiation, is inhomogeneity of distribution of the absorbing material already partially discussed. In the case of x-rays we are dealing with inhomogeneities in only two dimensions but where magnifying optics with a definite focal depth are used, inhomogeneities in depth likewise introduce an error. This error may be minimized by making measurements in areas as small as possible under conditions of maximal resolution. When the apertures of the illuminating and collecting optical system are different discrepancies will be great. Also depending upon where in the section the objective is focussed differing large errors will arise. These questions are discussed from a mathematical point of view in a paper published by Glick, Engström, and Malmström ('52). A further complicating factor in such an optical system is the biconical form of the rays going through the sample though this will introduce serious errors only when the aperture of condensor and objective are not appropriately adjusted.

The data presented in tables 1 and 2 indicate the impressive influence of the technique of fixation and manipulation of tissue on the resultant absorption values. Particularly is this evident with the ultra-violet microabsorption method.

With the reservations already set forward microabsorption measurements on the ventral horn cell of the adult cat would suggest a distribution of studied materials as represented in figure 3. This figure summarizes in brief the accumulated observations made by both techniques. The mass gradients portrayed in this diagram are undoubtedly distorted and accentuated by tissue manipulation but have, wherever possible, been corrected to data obtained on frozen-dried material. It becomes immediately evident that there

is a striking water gradient from central nucleolar zone to peripheral axis cylinder, within the nerve cell. The values for axis cylinder are appropriated from studies made on the single fresh living amphibian nerve fiber by Engström and Luthy ('50) and may not, in fact, represent the true state

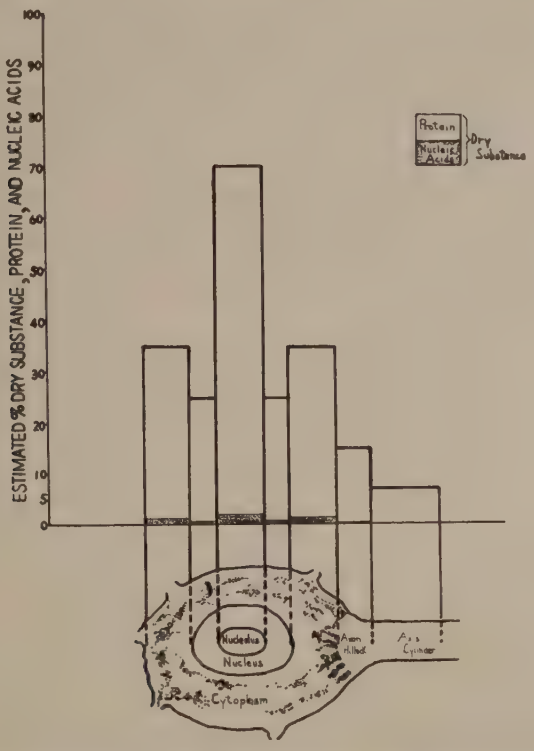

Fig. 3 The distribution of total dry substance, estimated protein and nucleic acids, in the ventral horn cell of the adult cat. The value for axis cylinder derived from x-ray data in fresh amphibian axon (Engström and Lüthy, '50).

in the cat. No microabsorption studies have been performed on cat axoplasm as yet so that the absence of measurable nucleic acid is only inferred from available data. That such a conspicuous gradient in dry substance (or water) as is represented in this figure does actually exist, though probably less in degree, is indicated not only by the x-ray data but

also, in similar ratio, by the calculated protein values from the ultra-violet.

If the "standard protein" we have set up as a prototype is a valid one for nerve cell substance then the nucleic acid gradient indicated in the dotted rectangles in this figure probably reflects reasonably true concentration gradients. Concerning the precise nature of these nucleic acids much has been written. Feulgen and methyl-green pyronin stains of these tissues indicate that the bulk of the nucleic acid found in the nucleus is of pentose type. A rare particle staining positively with Feulgen or methyl-green could occasionally be found in the nucleus, though not consistently oriented around the nucleolus. Almost all of the nucleic acid present in the ventral horn cell of the mature cat is, by these criteria, of the pentose type.

The region of the axon hillock could not be clearly defined in the frozen-dried material or in much of the formalin material. In the few readings possible little or no measurable nucleic acid could be detected. Only in this region did we observe an occasional clear-cut absorption "maximum" at 275 mμ in the ultra-violet, as is found with many animal proteins. The fact that mean extinction values at 257 mμ were, in many instances, clearly lower in this region than that at 275 mμ would also tend to refute the criticism that the usually observed increasing extinction values at shorter wavelengths is a non-specific effect common to many or all tissues. Such a maximum at 275 mμ was observed before any "corrections" for scattering or reflection were applied and are therefore not a mathematically imposed contrivance.

The possible implications of this water, protein, and nucleic acid concentration gradient, particularly in respect to the cytoplasm, axon hillock and, probably, axis cylinder; for intrinsic neuronal metabolic processes, impulse conduction, and synaptic delay, are many and interesting but not within the scope of this paper.

CONCLUSIONS

1. Ventral horn cells of the adult cat have been studied by two quantitative radiant energy microabsorption techniques utilizing "soft x-rays" and monochromatic ultra-violet light.

2. The data indicate that there is a striking water gradient from center to periphery of such ventral horn cells. In fixed preparations the nucleolus contains about 70% dry substance of which 2% is pentose-nucleic acid, the remainder protein. The nucleus contains approximately 25% dry substance of which 0.5% is nucleic acid (almost exclusively of desoxy type), the remainder protein. The cytoplasm contains approximately 35% dry substance of which slightly more than 1% is pentose-nucleic acid, the remainder being protein or lipo-protein. Possibly as much as one-fourth of this cytoplasmic substance is removable by lipid solvents. The axon-hillock region contains about 15% dry substance, almost entirely of protein nature. Previous studies on the amphibian axon indicate that the axon itself contains about 7% dry substance. All of the stated values are, by nature of the experiment, maximum.

3. Formalin and Carnoy fixation are accompanied by an impressive local concentration of absorbing materials as contrasted to frozen-dried tissue.

4. The only material eminently suitable for semi-quantitative chemical study by the ultra-violet technique, of those investigated, is frozen-dried tissue not exposed to x-ray in vacuo. Only restricted and contingent interpretations are valid even for such material.

5. Sources of error and conditions for agreement in both techniques have been observed and discussed.

6. This study would indicate that ultra-violet microabsorption data such as those discussed cannot be assessed for their adherence to Beer's Law. They also indicate, clearly, that the state of molecular orientation and aggregation is a minor, if existent, source of error in such determinations.

LITERATURE CITED

BEREK, M. 1927 Grundlagen die Tiefenwahrnehmung im Mikroskop mit einem Anhang über die Bestimmung der obersten Grenze des unvermeidlichen Fehlers einer Messung aus der Häufigkeitsverteilung der zufälligen Maximalfehler. S. B. ges. Naturw. Marbg., *62:* 189–223.

BLOCK, R. J. 1937a Proteins of the nervous system: considered in the light of prevailing hypotheses on protein structure. Yale J. Biol. and Med., *9:* 445–503.

———— 1937b Chemical studies on the neuroproteins. I. The amino acid composition of various mammalian brain proteins. J. Biol. Chem., *119:* 765–768.

BODIAN, DAVID 1947 Nucleic acid in nerve cell regeneration. Symp. Soc. Exp. Biol., *1:* 163–178.

CASPERSSON, TORBJÖRN 1936 Über den Chemischen Aufbau der Strukturen des Zellkernes. Skand. Arch. f. Physiol., *73:* Suppl. no. 8.

———— 1940 II. Methods for the determination of the absorption spectra of cell structures. J. Roy. Microsc. Soc., *60:* 8–25.

———— 1950 Cell Growth and Cell Function. W. W. Norton and Co., Inc. New York.

CASPERSSON, TORBJÖRN, AND LARS SANTESSON 1942 Studies on Protein Metabolism in the Cells of Epithelial Tumours. Acta Radiol. Suppl., XLVI.

COMMONER, BARRY 1949 On the interpretation of the absorption of ultraviolet light by cellular nucleic acids. Science, *110:* 31–40.

ENGSTRÖM, ARNE, AND BO LINDSTRÖM 1950 A method for the determination of the mass of extremely small biological objects. Biochim. et Biophys. Acta, *4:* 351–373.

ENGSTRÖM, ARNE, AND HERBERT LÜTHY 1950 The distribution of mass and lipids in the single nerve fiber. Exp. Cell Research, *1:* 89–91.

FOLCH-PI, JORDI, AND L. L. UZMAN 1948 Brain Proteins: isolation of a birefringent liponucleoprotein. Federation Proc., *7:* 155.

GERSH, ISADORE, AND DAVID BODIAN 1943a Some chemical mechanisms in chromatolysis. J. Cell. and Comp. Physiol., *21:* 253–279.

———— 1943b Histochemical analysis of changes in rhesus motoneurons after root section. Biol. Symp., *10:* 163–184.

GLICK, DAVID, ARNE ENGSTRÖM AND BO MALMSTRÖM 1952 Errors in microscopical histo- and cytochemical techniques. Science, *114:* 253–258.

HYDÉN, HOLGER 1943 Protein metabolism in the nerve cell during growth and function. Acta Physiol. Scand., *6:* Suppl. XVII.

———— 1947 Protein and nucleotide metabolism in the nerve cell under different functional conditions. Symp. Soc. Exp. Biol., *1:* 152–162.

———— 1950 Spectroscopic Studies on Nerve Cells in Development, Growth, and Function. In: Genetic Neurology edited by Paul Weiss. The Univ. of Chicago Press: 177–193.

HYDÉN, HOLGER, AND H. HARTELIUS 1948 Stimulation of the Nucleoprotein-Production in the Nerve Cells by Malononitrile and its Effects on Psychic Functions in Mental Disorders. Acta Psychiat. et Neurol., Suppl. XLVIII.

LANDSTRÖM, H., T. CASPERSSON AND G. WOHLFART 1941 Über den Nucleotidumsatz der Nervenzelle. Ztschr. f. mikr. anat. Forsch., *49:* 534–548.

MCLEAN, D. J., AND A. C. GIESE 1950 Absorption spectra of proteins and amino acids after ultraviolet irradiation. J. Biol. Chem., *187:* 537–542.

SCHMITT, F. O. 1951 Personal communication to J. I. N.

THORELL, BO 1947 Studies on the Formation of Cellular Substances during Blood Cell Production. Acta Med. Scand., Suppl. CC.

APPENDIX A

Mass and extinction values for cytoplasm

FIXATION	CELL NUMBER	ULTRA-VIOLET			X-RAY
		E_{257}	E_{275}	E_{310}	mg $cm^{-2} \cdot \mu^{-1}$
Carnoy 1 hr. cerv. cord	5	0.67	0.41	0.08	0.036
	6	0.52	0.58	0.16	0.042
	7	0.44	0.42	0.09	0.056
Carnoy ½ hr. cervical cord	19	0.40	0.33	0.14	0.034
	20	0.39	0.33	0.14	0.052
	21	0.50	0.40	0.13	0.046
	22	0.46	0.41	0.15	0.032
	23	0.39	0.47	0.13	0.028
	30	0.33	0.36	0.17	0.046
	31	0.38	0.29	0.18	0.028
	32	0.41	0.38	0.20	0.046
	33	0.29	0.30	0.12	0.028
	34	0.35	0.31	0.14	0.046
	35	0.34	0.30	0.08	0.046
	36	0.37	0.25	0.09	0.062
	37	0.34	0.27	0.00	0.050
	40	0.31	0.28	0.06	0.022
	41	0.36	0.22	0.12	0.014
	42	0.35	0.24	0.17	0.030
Formalin cerv. cord plus lipid solvents	75	0.46	0.38	0.10	0.036
	76	0.49	0.43	0.09	0.032
	77	0.61	0.50	0.10	0.037
	78	0.59	0.49	0.09	0.034
	79	0.54	0.42	0.09	0.029
	80	0.54	0.40	0.05	0.019
	81	0.56	0.42	0.07	0.043
	82	0.49	0.42	0.07	0.043
	84	0.44	0.36	0.05	0.038
Frozen-dried and x-ray	56	0.84	0.66	0.14	0.053
	57	0.60	0.64	0.16	0.023
	58	0.64	0.59	0.15	0.027
	59	0.84	0.63	0.13	0.034
	60	1.28	1.10	0.20	0.043
	62	0.88	0.68	0.17	0.030
	63	1.08	0.84	0.20	0.036
Frozen-dried and	64	0.41	0.31	0.13	0.040
	65	0.36	0.30	0.02	0.016
	67	0.31	0.28	0.06	0.024

	4	0.48	0.48	0.14	0.023	Frozen-dried without x-ray (Xylol)	97	0.22	0.22	0.03	....
	14	1.47	1.03	0.63	0.110		98	0.39	0.25	0.01	....
Formalin lumbar cord	15	0.57	0.62	0.15	0.050		99a	0.33	0.31	0.01	....
	16	0.92	0.85	0.00	0.070		100	0.31	0.27	0.01	....
	17	0.61	0.54	0.16	0.048		101	0.30	0.21	0.01	....
	18	1.06	1.00	0.46	0.48						
	90	0.84	0.74	0.15	0.31						
	91	1.01	0.91	0.19	0.053	Frozen-dried without x-ray (Xylol) plus lipid solvents	97 [2]	0.34	0.22	0.06	....
	92	0.75	0.80	0.14	0.047		98 [2]	0.20	0.16	0.03	....
	93	0.75	0.71	0.10	0.044		99 [2]	0.27	0.22	0.10	....
	94	0.72	0.62	0.14	0.054		99b [2]	0.38	0.38	0.15	....
	95	0.65	0.60	0.08	0.035		100 [2]	0.35	0.26	0.03	....
	8	0.53	0.48	0.08	0.062						
	9	0.53	0.62	0.08	0.040	Frozen-dried without x-ray ($CHCl_3$)	102	0.29	0.24	0.08	....
Formalin cerv. cord	10	0.60	0.50	0.15	0.048		103	0.39	0.35	0.05	....
	11	1.23	1.13	0.23	0.073		104	0.24	0.20	0.08	....
	12	0.74	0.78	0.10	0.032		105	0.45	0.31	0.14	....
	13	0.44	0.31	0.04	0.011		106	0.38	0.34	0.05	....

APPENDIX B

Mass and extinction values for nucleus, nucleolus, axon hillock

FIXATION	CELL	NUCLEUS				NUCLEOLUS				AXON HILLOCK			
		Ultra-violet			X-ray	Ultra-violet			X-ray	Ultra-violet			X-ray
		E_{257}	E_{275}	E_{310}	mg cm^{-2}. μ^{-1}	E_{257}	E_{275}	E_{310}	mg cm^{-2}. μ^{-1}	E_{257}	E_{275}	E_{310}	mg cm^{-2}. μ^{-1}
Carnoy ½ hr.	19				0.032								
	20				0.038								
	21	0.22	0.21	0.04	0.030	0.57	0.53	0.21	0.060	0.26	0.27	0.12	
	22	0.19	0.17	0.07		0.50	0.55	0.26					
	23	0.19	0.27	0.05						0.10	0.15	0.13	
	25	0.19	0.17	0.05	0.020	0.78	0.72	0.26					
	26									0.11	0.16	0.09	0.016
	27	0.14	0.16	0.05		0.55	0.54	0.18					
	37	0.26	0.21	0.00		0.59	0.48	0.07					
	40	0.20	0.20	0.05	0.008	0.70	0.69	0.25	0.130				
	41	0.22	0.12	0.09	0.008				0.022				
	43	0.16	0.25	0.13	0.012	0.66	0.68	0.25	0.072				
	44	0.23	0.18	0.06	0.014	0.79	0.83	0.25	0.108				
Carnoy 1 hr.	5								0.048				
	7				0.024								
	89	0.30	0.25	0.02		0.69	0.74	0.04					
Formalin lumbar	2	0.31	0.26	0.17	0.015	0.63	0.61	0.21	0.035				
	14									0.60	0.67	0.50	
	15	0.51	0.62	0.10	0.040	1.55	1.37	0.25	0.150				
	16	0.83	0.75	0.00		1.63	1.56	0.10	0.170				
	17	0.57	0.49	0.16		1.35	1.39	0.33	0.100				
	92	0.56	0.55	0.07	0.040	1.35	1.05	0.40	0.091				
Formalin cervical	8	0.48	0.46	0.07	0.045								
	11	0.73	0.67	0.17	0.033	1.37	1.43	0.37	0.187				
	12	0.36	0.52	0.10		0.72	0.70	0.10					
	13	0.33	0.17	0.02	0.009	0.86	0.69	0.14					
Formalin cervical after lipid solvents	75	0.32	0.29	0.09		1.00	0.85	0.30					
	80	0.44	0.32	0.06		0.85	0.65	0.10		0.09	0.09	0.04	
	83								0.039				
	84					0.75	0.60	0.05					
Froz.-dried and x-ray	52	0.55	0.69	0.03		0.75	0.65	0.02					
Froz.-dried and x-ray after													

THE ACTION OF THYROXINE ON THE ENDOGENOUS OXYGEN UPTAKE OF MITOTICALLY ACTIVE AND BLOCKED GRASSHOPPER EMBRYOS, THEIR HOMOGENATES AND INTRACELLULAR CONSTITUENTS[1]

JOSEPH H. BODINE AND KIAO-HUNG LU
Zoological Laboratory, State University of Iowa, Iowa City

FOUR FIGURES

The responses following in vitro applications of thyroid preparations to tissues, cells, homogenates and intracellular constituents have recently been catalogued by Barker ('51). Much data seem to have been collected for vertebrates, while a marked scarcity exists for invertebrates. Results for higher organisms, as pointed out by Barker, are both conflicting and confusing since positive as well as negative finding have been reported by different authors for similar sets of experiments. The naked embryo of the common grasshopper, *Melanoplus differentialis*, is readily obtained from the developing egg and is also favorable material for O_2 uptake studies on both intact embryos as well as homogenates and intracellular constituents (Bodine and Lu, '50). Mitotically active and blocked embryos are readily obtained due to an inherent natural block in the animals' development at constant temperature. The present papers deals with the effects of thyroxine upon the endogenous O_2 uptake of mitotically active and blocked intact embryos, homogenates and intracellular constituents.

METHODS

Embryos were dissected in Ringer solution, phosphate buffered (pH 6.8), from eggs of known temperature and de-

[1] Aided by grant from the National Institutes of Health. Grateful acknowledgment is made to Etta Andrews for technical assistance.

velopmental histories. They were freed of yolk and washed several times in Ringer solution which served as the suspension medium for all experiments. One hundred embryos per milliliter of suspension medium were used throughout. Homogenates or intracellular constituents were also made up

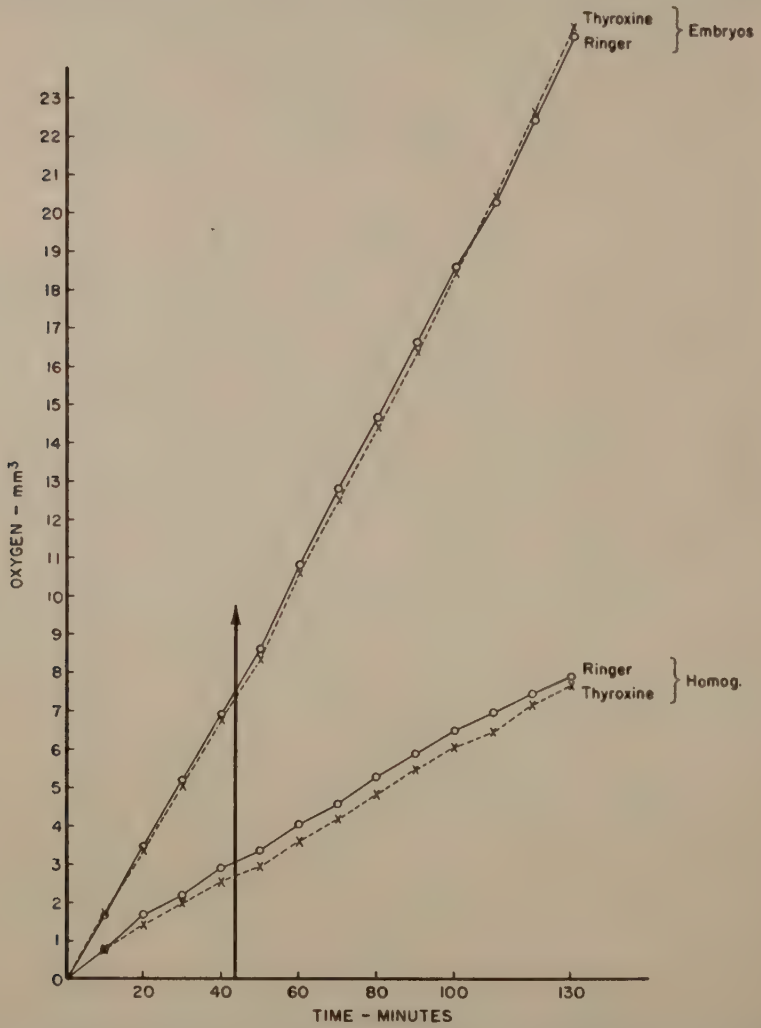

Fig. 1 Shows effect of 0.02 mg/cm³ thyroxine on prediapause embryos and homogenates (16 to 18 day embryos at 25°C.). Arrow indicates time at which reagents were added to respiration flasks.

in the same proportion. A motor driven glass pestle was used for making homogenates and intracellular constituents were thrown down and concentrated by fractional centrifugation as previously pointed out (Bodine and Lu, '50). Oxygen determinations were carried out at 25°C. using Standard Warburg manometers with respiration flasks of 5 ml capacity. Determinations were carried out over periods of two to two

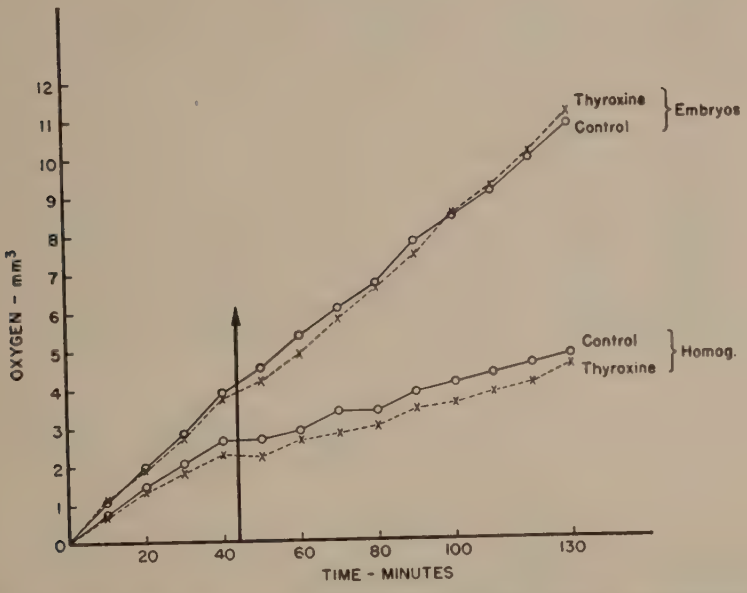

Fig. 2 Same as figure 1 except for 0.2 mg/cm³ thyroxine on diapause embryos and homogenates.

and one-half hours. Thyroxine crystals (Squibb) were employed in concentrations ranging from 0.2 mg/ml to 0.02 mg/ml. Typical results are graphically shown below.

RESULTS

Inasmuch as all concentrations of thyroxine produce similar results only typical experiments will be described. Concentrations ranging from 0.02 mg/ml to 0.2 mg/ml have no effect upon the endogenous O_2 uptake of either mitotically

active or blocked intact embryos, homogenates or nuclei (figs. 1, 2, 3, 4). It would thus seem that such invertebrate materials are quite insensitive to the immediate action of thy-

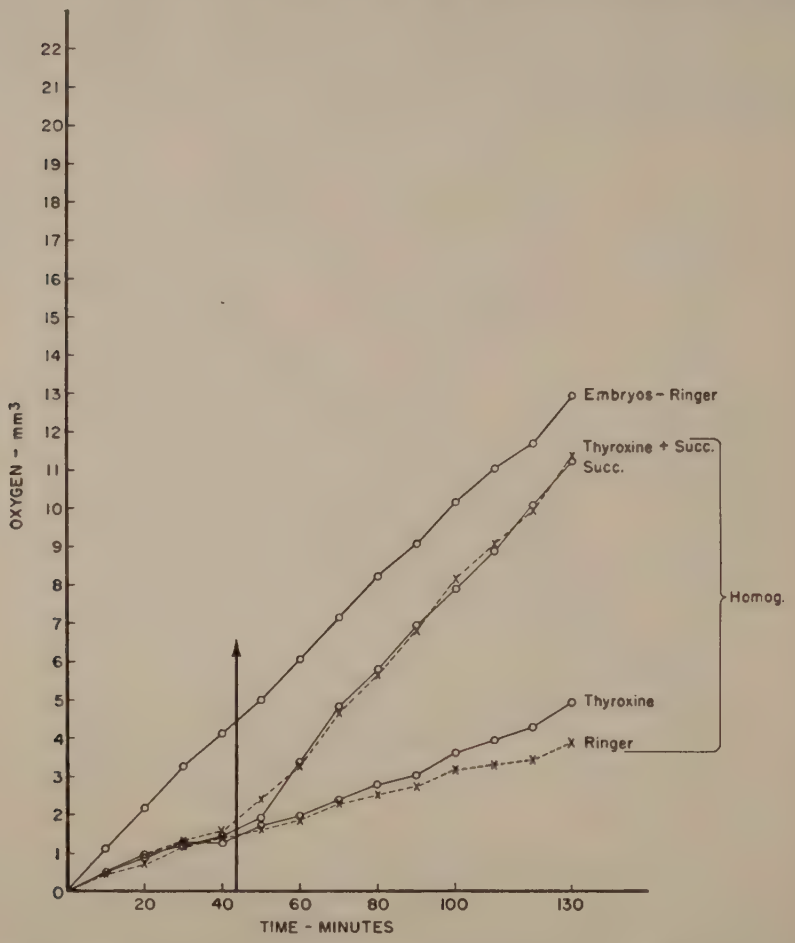

Fig. 3 Shows effect of thyroxine upon succinate treated homogenates of diapause embryos. Arrow indicates addition of reagents.

roxine and there seems no logical reason biologically why they should be affected. Reference is made by Barker ('51) to results obtained on specific enzyme systems of various vertebrate materials and especially to the succinic dehydro-

genase systems. Since it has recently been found (Bodine, Lu and West, '51) that homogenates from grasshopper embryos give rather marked responses to added succinate it was thought desirable to check the possible action of such systems derived from this material. Results from such experiments are graphically indicated in figures 3–4, and show no effect of the reagent upon the succinic dehydrogenase activity either of mitotically active or blocked embryos. It is thus apparent that thyroxine seems to have no effect either upon the endogenous O_2 uptake or the succinic dehydrogenase systems of this form.

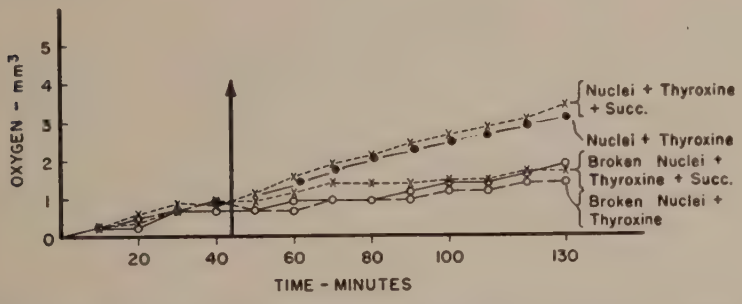

Fig. 4 Shows effect of thyroxine and succinate on O_2 uptake of intact and broken nuclei. Arrow indicates addition of reagents.

CONCLUSION

Thyroxine in concentrations ranging from 0.02 mg/ml to 0.2 mg/ml has no effect upon the endogenous O_2 uptake of either mitotically active or blocked intact embryos, homogenates or intracellular constituents of the embryo of the grasshopper, *Melanoplus differentialis*.

LITERATURE CITED

BARKER, S. B. 1951 Mechanism of action of the thyroid hormone. Physiol. Reviews, *31:* 205–243. (Contains extensive review of pertinent literature.)

BODINE, J. H., AND K. H. LU 1950 Oxygen uptake of intact embryos, their homogenates, and intracellular constituents. Physiol. Zool., *23:* 301–308.

BODINE, J. H., K. H. LU AND W. WEST 1951 Succinic dehydrogenase in mitotically active and blocked embryonic cells. Physiol. Zool., in press.

CHANGES IN INORGANIC SUBSTANCES IN MAMMALIAN NERVE CELLS DUE TO STARVATION

CARRIE C. GILLASPY

Associate Professor of Anatomy. Des Moines Still College of Osteopathy and Surgery, Des Moines, Iowa[1]

INTRODUCTION

The effects of starvation on the various tissues of the body have been of considerable interest for some time. A number of methods of study have been used, such as: fixatives and stains, Peri (1893), Macallum (1897–98), chemical analysis, Macallum (1891), Wiley and Wiley ('33) microincineration, Policard and Pillet ('28), Policard and Okkels ('30), Policard ('33), Scott ('33, '33a, b) and others. Through such methods of study, it has been possible to observe some of the changes which take place in the cells of the body during starvation. The microincineration methods of Policard ('23) and Scott ('33) give a new approach to the recognition of certain fixed salts, such as, calcium, sodium, magnesium, iron, and silica in the tissues. This approach has made it possible, by microscopic observation, to note the changes in the inorganic salts of the cortical layers of the cerebrum during various periods of starvation.

MATERIAL AND METHODS

Twenty-four white mice, 12 white rats, and 3 cats were subjected to starvation for several days, except the cats were

[1] I am greatly indebted to Dr. E. V. Cowdry of the Washington University Medical School for providing me with equipment and working space in his laboratory, to Dr. Gordon H. Scott for his suggestions and guidance during this study and to Dr. H. P. K. Agersborg of the Des Moines Still College of Osteopathy and Surgery for helping prepare this paper for publication.

given 7 cm^3 Pet's milk each day. Eight mice, 4 rats and 1 cat were killed at the end of each period: 2 days, 4 days and 6 days, respectively.

Thin pieces of tissue from the motor and sensory areas of the brain were fixed for 24 hours in a mixture of absolute alcohol, 9 parts, and neutral formaldehyde, 1 part. Dehydration was completed in several changes of absolute alcohol for 6 days, and then passed through 2 changes of xylol during 24 hours. The tissue was then imbedded in paraffin in the usual manner.

Serial sections of 5 μ were cut, with alternate sections mounted for incineration and for staining with hematoxylin and eosin, respectively. The sections for incineration were attached to the slide by pressing the section in contact with the slide at one end and leaving the other end free. As the slide passed through the incinerator, the paraffin melted and spread the section over the slide. This method of flattening the sections on the slides prevented any soluble mineral salts in the tissue from coming in contact with any liquids which might have disarranged the salt granules. After the incineration, the slides were cooled and a coverslip placed over the ash, its edges sealed with a mixture of paraffin, beeswax and balsam.

Two binocular microscopes with cardioid condensers were used for a comparative study of the ash in the various layers of the cortex. Spencer illuminators with 500-watt bulbs were used. The layers of the cortex were studied with low and high power objectives, while the individual cells were studied with oil immersion.

OBSERVATION AND DISCUSSION

Special attention has been given to sodium, potassium, iron, and calcium contents of the motor and sensory areas of mammals during or subsequent to a starvation period. Interpretation of the qualitative and quantitative presence of inorganic salts in these tissues have been based on color spectra in that sodium and potassium appear blue, calcium white,

and iron appears as a reddish yellow brown in incinerated material. A comparative examination of the cortical layers of the motor and sensory areas of animals which have been subjected to various periods of starvation will show the location of inorganic salts in the cells.

The colors of the cortical layers are not sharply defined in the incinerated sections, but by comparing them with

TABLE 1

MICE — MOTOR	CONTROL	2 DAYS	4 DAYS	6 DAYS
Molecular and small pyramidal	*Dark blue* r.y.b.	*Yellow brown*	Dark blue r.b	*Yellow red brown* dark blue
Medium and large pyramidal	*Dark blue* r.b. with more r.b. in large	*Yellow brown* small amount light blue	*Dark blue* r.b.	*Yellow brown* light blue
Stellate, deep pyramidal, fusiform	*Dark blue* y.r.b	*Yellow brown*	*Dark blue* r.y.b	*Yellow brown* some blue
MICE — SENSORY	CONTROL	2 DAYS	4 DAYS	6 DAYS
Molecular and small pyramidal	*Dark blue* r.y.b.	*Red brown blue*	Dark blue r.b.	Dark blue r.b.
Medium and large pyramidal	*Dark blue* y.b.	r.b. *Sky blue*	*Dark blue* r.b.	*Yellow brown* light blue
Stellate, deep pyramidal, fusiform	*Dark blue* y.b.	y.b.r. blue	*Dark blue* y.b.	*r.y.b.* medium blue

stained control sections, it is possible to locate the layers. In general, three distinct colors are noted, with slight variations which also help in the identification of the other layers. In the controls there is a blue reddish yellow brown color combination in the molecular and small pyramidal layers, and dark blue with a small amount of red yellow brown with varying amounts of blue in the stellated, deep pyramidal and fusiform layers.

As starvation progresses, there are notable changes in the amount of the inorganic salts in the different layers (see tables 1, 2, and 3). After two days, there is a decrease in sodium and potassium, with iron predominating in the cortical layers. However, there is a general tendency for the medium and the large pyramidal layers to retain more sodium and potassium after starvation than any of the other layers. Of these two layers, the deeper one shows more iron than the medium.

TABLE 2

RAT — MOTOR	CONTROL	2 DAYS	4 DAYS	6 DAYS
Molecular and small pyramidal	*Dark blue* r.b.y. more r.b. in large	*y.b.* small amount blue	*Dark blue* small amount r.b.	*y.b.* Dark blue
Medium and large pyramidal	Dark blue r.b. more in large	y.r.b. Dark blue	*Dark blue* y.r.b.	*y.b.* Dark blue
Stellate, deep pyramidal, fusiform	*Dark blue* y.r.b.	*r.y.b.* some blue	*Dark blue* y.b.	*y.b.* Dark blue
RAT — SENSORY	**CONTROL**	**2 DAYS**	**4 DAYS**	**6 DAYS**
Molecular and small pyramidal	*Dark blue* r.y.b.	r.y.b. light blue	*Dark blue* r.b.	*y.b.* Dark blue
Medium and large pyramidal	*Dark blue* y.b.	*r.y.b.* Dark blue	*Sky blue* r.y.b.	*r.b.* Dark blue
Stellate, deep pyramidal, fusiform	*Dark blue* y.b.	*y.b.r.* Dark blue	*Dark blue* r.y.b.	*r.b.* Dark blue

When starvation in rats was continued for 4 days, there was a definite let-up of decrease of sodium and potassium in every layer, especially in the medium and large pyramidal layers. Wiley and Wiley ('33) obtained similar results by chemical tests. That is, while at the beginning or first two days of starvation, there is a noticeable decrease in sodium and potassium, but as starvation continues the body begins to conserve these salts, later as starvation is further continued,

these salts are again diminished, as for example, in tissues of cats which had been starved for 6 days. There is a loss of sodium and potassium, with a relative increase in iron in the layers. This again is in accord with the findings of Wiley and Wiley ('33), whose work shows that by decreasing the food-intake of a man, age 23 years, to 1185 gm/day there was a marked loss of sodium and potassium.

TABLE 3

CAT — MOTOR	CONTROL	2 DAYS	4 DAYS	6 DAYS
Molecular and small pyramidal	*Dark blue* r.y.b.	*y.b.*	*Dark blue* r.b.	*y.b.r.* Dark blue
Medium and large pyramidal	*Light blue* r.b.	*Dark blue* r.b.	*Dark blue* y.b.	*r.y.b.* Dark blue
Stellate, deep pyramidal, fusiform	*Medium blue* blue	*r.y.b.* Dark blue	*Dark blue* r.b.	*y.b.* Light blue
CAT — SENSORY	**CONTROL**	**2 DAYS**	**4 DAYS**	**6 DAYS**
Molecular and small pyramidal	*Dark blue* r.b.	*y.b.* Medium blue	*Dark blue* y.b.	*y.b.r.* Dark blue
Medium and large pyramidal	*Dark blue* r.b.	*Light blue* r.b.	*Dark blue* y.b.r.	*r.b.y.* Medium blue
Stellate, deep pyramidal, fusiform	*Medium blue*	*y.b.r.*	*Dark blue*	*r.b.y.* Medium blue

The preceding tables illustrate graphically the findings upon which this paper is based, and emphasize the difficulty encountered in making accurate description of the colors in the cortical layers of the brain. Stratifications that have practically the same color have been grouped together, since the variations in these layers were such as to be of no practial significance. The colors which predominate in the cortical layers have been italicized (r.y.b. — red, yellow, blue; r.b. — red, blue; y.b. — yellow, blue). The letters are arranged in accordance with intensity of the colors.

These tables show that most of the material contained some iron in every layer, but that in almost every case there was a greater amount in the deeper stellate, pyramidal and fusiform layers. In contrast, the medium and large pyramidal layers showed a predominance of sodium and potassium, indicated by the blue color.

Numerous cells were studied. When the cells were viewed with the low power objective the largest percentage of them was very white in contrast to the darker interstitial substance; only a comparatively few cells showed a yellowish tinge. Since the white represents calcium, this seems to indicate that most of the calcium is concentrated in the cells. When these cells were studied with the oil immersion, white, blue and reddish brown were noted. The large brilliant, white granules in the cytoplasm, present in the cells of control animals, were reduced to about half in size in the starved animals. The sodium, potassium and iron granules were medium in size but became smaller and more numerous as starvation continued. The nucleolus was very noticeable in the incinerated sections. The ash in the nucleolus was very brilliant white in the controls, but became dull in the material of starved animals. These observations are closely similar to the findings of Macallum (1896), who noted that in starving animals, iron was present in lesser amount than in the controls. Similarly, Nicholson ('23), who studied the changes in inorganic substances in nerve cells, following injury to their axons by ligation or teasing, found that large masses of iron disappeared, only to be replaced by numerous smaller masses.

SUMMARY

1. Mice, rats, and cats were subjected to starvation for 2, 4 and 6 days.

2. Animals subjected to two days' starvation showed a definite loss of sodium and potassium in the cortical layers of the brain.

3. Animals starved for 4 days exhibited a definite retention of sodium and potassium in the tissues, indicating that as the minerals were no longer supplied from the outside, the cellular activities prevented complete loss of these minerals, or initiated a conservative use of them, at least for the time being.

4. Animals in which the period of starvation was continued to 6 days showed a further loss of sodium and potassium beyond that indicated after the two-day period, while the iron remained relatively constant.

5. In starving animals, the elements sodium, potassium and calcium are decreased in amount in the cytoplasm of the cells.

6. Most of the calcium is found in the cells of the cortical layers rather than in the interstitial tissues.

7. Iron is seemingly diminished to some extent, but apparently relatively less than the other salts.

LITERATURE CITED

BENEDICT, F. G. 1907 The influence of inanition on metabolism. Carnegie Institute Reports, Washington, Pub., *77:* 357–421.

DONAGGI, A. 1907 Effet de l'action combinee du jeune et du froid sur les centres nerveux de mammiferes adults. Arch. ital. de biol., *46:* 407–437.

GAMBLE, J. L., G. S. ROSS AND F. F. TISDALL 1923 The metabolism of fixed base during fasting. J. Biol. Chem., *57:* 633–695.

JACKSON, C. M. 1925 Inanition and Malnutrition. Chapter X: 173–190. The Blakiston Company, Philadelphia.

JACKSON, C. M., AND V. D. E. SMITH 1931 The effects of deficient water-intake on the growth of the rat. Am. J. Physiol., *97:* 146–153.

MACALLUM, A. B. 1896 On the distribution of assimilated iron compounds other than hemoglobin and haematins in animals and vegetable cells. Quart. J. Micro. Sci., *38:* 175–271.

———— 1897a On the demonstration of the presence of iron in chromatin by micro-chemical methods. Proc. Royal. Soc., *50:* 279–286.

———— 1897b A new method of distinguishing between organic and inorganic compounds of iron. J. Physiol., *22:* 92–98.

NICHOLSON, F. M. 1923 The changes in amount of iron-containing proteins of nerve cells following injury to their axons. J. Comp. Neur., *36:* 37–77.

PETERS, JOHN P. 1935 Exchanges Between Tissue Cells and Interstitial Fluids. Body Water. Chapter VI: 128–149.

POLICARD, A. 1923 Detection Histochemique du fer total dans les tissue par la methodes de l'incineration. Compt. rend. acad. Sci., Tome, *176:* 1187–1189.

POLICARD, A., ET H. OKKELS 1930 Method of microincineration. Anat. Rec., *44:* 349–361.

POLICARD, A., ET D. PILLET 1928 Sur la detection par microincineration du potassium et du sodium dans le cytoplasma des globules rouges. Compt. rend. soc. Biol., Tome, *99:* 85–86.

RIVA, E. 1907 Lesion du reseau neurofibrillare de la cellule nerveuse dans l'inanition experimentale etudies avec les methods de Donaggio. Arch. ital. biol., *46:* 437–447.

SCOTT, GORDON H. 1933 A critical study and review of the method of microincineration. Protoplasma, No. 1, *20:* 133–151.

———— 1933a The localization of mineral salts in cells of some mammalian tissue by microincineration. Am. J. Anat., No. 2, *53:* 243–287.

———— 1933b Quantitative estimation of ash after microincineration. Proc. Soc. Exp. Biol. and Med., *30:* 1304–1305.

SUNDWALL, J. 1917 Tissue Alteration in Malnutrition and Pellagra. U. S. Hyg. Lab. Washington, Bull. No. 106: 5–75.

VAN ALYKE, PETER D. 1931 Quantitative Clinical Chemistry, *1:* 1035–1036.

WILEY, FRANK H., AND LEONA L. WILEY 1933 The inorganic salt balance during dehydration and recovery. J. Biol. Chem., *101:* 83–92.

STUDIES ON CELL ENZYME SYSTEMS

VI. COMPETITIVE INHIBITION OF CYPRIDINA LUCIFERASE BY BUTYL ALCOHOL [1]

AURIN M. CHASE AND ELIZABETH H. BRIGHAM

Physiological Laboratories, Princeton University, New Jersey, and The Marine Biological Laboratory, Woods Hole, Massachusetts

THREE FIGURES

INTRODUCTION

The luminescent reaction of luciferin and luciferase from *Cypridina hilgendorfii,* a marine ostracod crustacean, has been under investigation *in vitro* for some 35 years (Harvey, '40). Since 1935 luciferin, the substrate of the reaction, has been available in a relatively pure form, due to the purification procedure published in that year by Anderson. The final product of his purification method is in *n*-butyl alcohol solution and, until relatively recently, such a solution has customarily been used as the stock luciferin solution in luminescence experiments.

Harvey ('17) showed that certain alcohols, including butyl, reversibly inhibit the luminescence (observed by eye) of crude aqueous luciferin and luciferase extracts from *Cypridina.* He found that 8% butanol (about 1 *M*) completely ex-

[1] This work was supported in part by an institutional grant for fundamental research from the New Jersey Section of the American Cancer Society to the Department of Biology of Princeton University, and in part by funds of the Eugene Higgins Trust allocated to Princeton University.

tinguished the light but that subsequent dilution at least partially restored it.[2]

The purpose of the present paper is to present quantitative data obtained in a study of the effects of *n*-butyl alcohol on the reaction of purified luciferin and luciferase from *Cypridina*. As will be shown, *n*-butyl alcohol reversibly inhibits the activity of partially purified luciferase and this inhibition is competitive in nature.[3]

MATERIALS AND METHODS

The luciferin used in these experiments was extracted from dried, powdered *Cypridinae* and carried through one cycle of purification by the method of Anderson ('35). The product from this procedure is in hydrogen-saturated *n*-butyl alcohol solution, stored under an atmosphere of hydrogen. Because the purpose of the present work was to study the inhibitory effect of butyl alcohol upon luciferase, it was necessary to use some other solvent than butyl alcohol. One-tenth *N* hydrochloric acid was chosen.[4]

[2] It has been deduced (Johnson, Eyring and Kearns, '43) that a butyl alcohol inhibition of the purified *Cypridina* luciferin-luciferase reaction was also occurring in certain experiments of Johnson and Chase ('42) on the effects of sulfanilamide and urethane. In the light of the data reported in the present paper, however, it seems doubtful if the butyl alcohol concentration present in their experiments (about 0.034 *M*) could have had more than a very slight effect unless it behaves differently in the presence of sulfanilamide or urethane than when alone.

[3] Competitive inhibition has been thought of as differing from the non-competitive type in that, in the former, the inhibitor and the substrate compete for combination at the same site on the enzyme molecule (implying that they are similar in structure) whereas, in the latter, different sites are involved. Another interpretation which has been advanced for competitive inhibition assumes that the inhibitor, by denaturing (unfolding?) the protein enzyme, alters the normal site of substrate combination. Kinetic data alone do not differentiate between two such mechanisms.

[4] The luciferin stock solution for a day's experiments was prepared as follows. Two milliliters of the butanol-luciferin solution were transferred from the storage vessel to a small vial. By means of a vacuum desiccator, a liquid nitrogen freezing trap and a vacuum pump, the alcohol was removed from the solution, leaving a solid residue. This was dissolved in 5 ml of 0.1 *N* hydrochloric acid and the resulting solution put into a small test tube immersed in an ice water bath. This was necessary in order to retard loss of luciferin by non-luminescent oxidation, which occurs rather rapidly at room temperature.

The luciferase used was an extract of 5 gm of dried powdered *Cypridina* in 100 ml of distilled water. This was filtered and the filtrate subjected to prolonged dialysis; first against running tap water and then, at 6°C., against several changes of distilled water. This treatment removed much dialyzable material and also caused the precipitation of a considerable quantity of inactive protein. The final product of this dialysis, suitably diluted with water, served as the enzyme stock solution.

The luminescent reaction was measured with a photoelectric apparatus slightly modified from that described by Anderson ('33).

The hydrogen ion concentration and that of other ions greatly affect this luminescent reaction (Anderson, '33, '37; Chase, '48) and the reaction mixture used in these experiments therefore consisted of equal volumes of M/15 KH_2PO_4 and M/15 Na_2HPO_4 and was 0.01 *M* for sodium chloride.

Since temperature also affects this reaction (Chase and Lorenz, '45), all measurements were made at 25°C.

EXPERIMENTAL RESULTS

Three distinct types of experiments were performed. In one the relative degree of inactivation of luciferase by various concentrations of *n*-butyl alcohol was studied. The second series was designed to determine whether or not the inactivation was reversible, while the third was concerned with whether the inhibition of luciferase by *n*-butanol was competitive or non-competitive, using the graphical method of Lineweaver and Burk ('34).

Inactivation of luciferase by n-butanol

Having determined the proper concentrations of luciferin and luciferase to use for the uninhibited luminescent reaction to be over in about two minutes, experiments were run in which these concentrations were always present but that of butyl alcohol was varied. A typical procedure was as follows. The standard quantity of luciferase stock solution was measured

into a small beaker and 10 ml of the reaction mixture containing the desired amount of *n*-butyl alcohol added. Next the standard quantity of luciferin stock solution (0.10 ml) was measured into the reaction vessel of the light-measuring

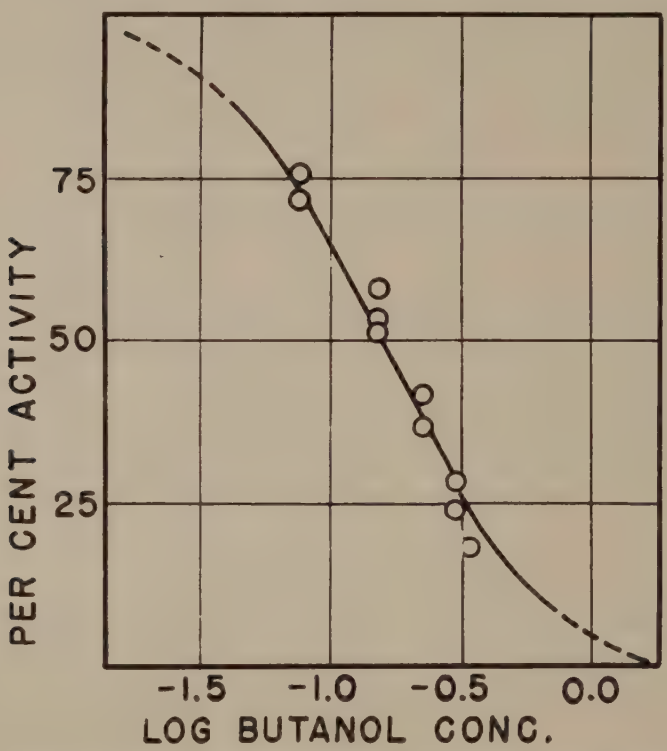

Fig. 1 Relative activity of luciferase in the presence of various concentrations of *n*-butyl alcohol, expressed as $\log_{10}$ butanol concentration. Each experimental point represents the relative first order velocity constant calculated from a complete luminescent reaction. A relatively high concentration, about 0.2 *M*, of butanol is required to reduce the activity of the enzyme by 50%.

apparatus. Ten milliliters of reaction mixture were immediately added and the prepared luciferase solution run in with a fast-flowing pipette. This initiated the luminescent reaction, which was measured until it was over.

The first order velocity constants of the luminescent reactions in presence of various concentrations of *n*-butanol

were calculated as described by Chase ('50). The velocity constant of the reaction in the absence of butyl alcohol represented 100% activity of the luciferase. Velocity constants calculated from luminescence measurements in which butyl

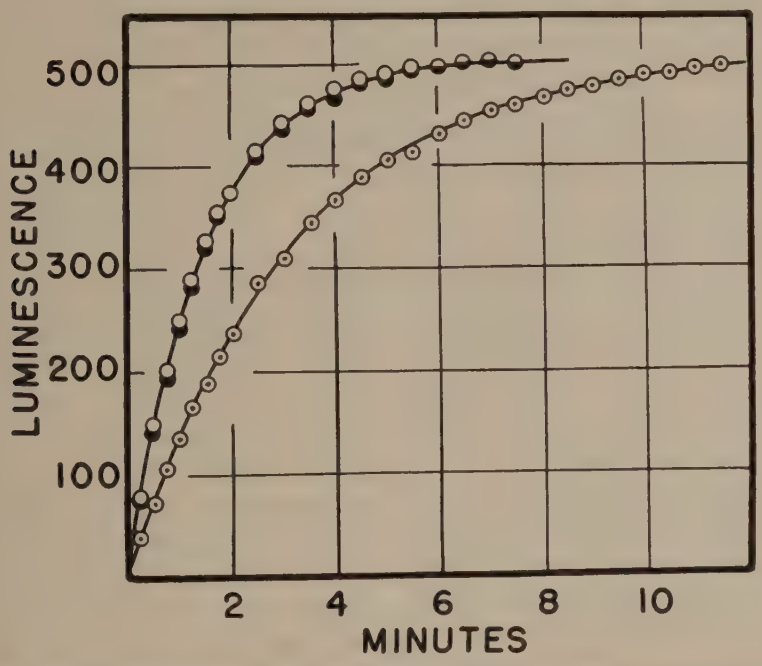

Fig. 2 A demonstration that the inhibition of luciferase by *n*-butyl alcohol is a reversible process. Three luminescent reactions are shown. In one (dotted circles) the luciferase was exposed throughout the experiment to 0.3 *M* butanol. In another (black circles) the luciferase was first exposed to 0.3 *M* butanol but the concentration was subsequently reduced by dilution to 0.15 *M*. In the third experiment (white circles) the luciferase was exposed throughout the experiment to 0.15 *M* butanol. It is evident that the data from the second and third experiments fall on the same curve, indicating that the inhibition is reversible. See text for further discussion.

alcohol was present were expressed as percentages of this value.

Figure 1 shows the per cent luciferase activity plotted against log molar concentration of *n*-butyl alcohol present in the reaction mixture. Three sets of experiments are

represented and it is quite clear that the enzyme, luciferase, is inactivated by the alcohol, although relatively high concentrations are required. Fifty per cent inactivation occurs in the presence of about 0.2 *M* alcohol. The reaction is completely inhibited when 1 *M* alcohol is present, a result which agrees very well with that reported by Harvey ('17).

Reversibility of the inhibition

Whether or not the inhibition of luciferase activity by butyl alcohol is reversible was determined by a dilution method. The procedure was the same as that used by Johnson and Chase ('42).

A luciferase solution was prepared by adding 0.1 ml of luciferase stock solution to reaction mixture, 0.3 *M* for butanol. This was then added to luciferin, prepared either in reaction mixture containing butanol to give 0.3 *M* concentration or in reaction mixture which lacked butanol. In both cases the enzyme was first exposed to the action of 0.3 *M* butanol, which then remained unchanged, or was diluted to 0.15 *M*, depending upon whether or not the luciferin solution to which it was subsequently added contained the alcohol. A third experiment, in which both the luciferin and luciferase solutions contained 0.15 *M* butanol from the start, was carried out in order to determine whether the reversal, by dilution to this concentration, was complete.

The results of a typical experiment of this sort are shown in figure 2, from which it is evident that partial inhibition of luciferase activity by this concentration of butyl alcohol is completely reversible.

Competitive nature of the inhibition

It has been shown (Chase, '49b) that the luminescent reaction of purified *Cypridina* luciferin and luciferase conforms to the Michaelis-Menten ('13) equation for formation of an enzyme-substrate compound. Lineweaver and Burk ('34) have pointed out how suitable modification of the Michaelis-

Menten equation permits a graphical differentiation between competitive and non-competitive inhibition when an inhibitor is acting in an enzyme-substrate system.

Data suitable for analysis by Lineweaver and Burk's method can be obtained in the following way. Two series of experiments are run. In each series the same, constant amount of enzyme is present in all experiments but the concentration of substrate is varied. The two series differ only in that in one a constant concentration of the desired inhibitor is present, while in the other it is absent. The resulting data are analyzed as follows.

When no inhibitor is present the velocity of the reaction studied varies with initial concentration of substrate according to the following modification (Lineweaver and Burk, '34) of the classical Michaelis-Menten equation:

$$\frac{1}{v} = \left(\frac{K_s}{V} \cdot \frac{1}{[S]}\right) + \frac{1}{V} \qquad (1)$$

v is the measured velocity, V the maximum velocity, $[S]$ the concentration of substrate and K_S the Michaelis constant.

In the case of competitive inhibition, Lineweaver and Burk have shown that the following equation should apply:

$$\frac{1}{v} = \frac{K_s}{V}\left(1 + \frac{[I]}{K_I}\right)\frac{1}{[S]} + \frac{1}{V} \qquad (2)$$

where $[I]$ is the concentration of the inhibitor, K_I is the equilibrium constant for the dissociation of the enzyme-inhibitor complex and the other terms have the same meanings as before.

If, on the other hand, non-competitive inhibition is occurring, Lineweaver and Burk's derivation shows that the following equation should describe the data, all terms having the same meanings as above:

$$\frac{1}{v} = \frac{K_s}{V}\left(1 + \frac{[I]}{K_I}\right)\frac{1}{[S]} + \left(1 + \frac{[I]}{K_I}\right)\frac{1}{V} \qquad (3)$$

The data from the first series of experiments (no inhibitor present), are analyzed according to equation (1), above,

plotting the reciprocal of the velocity for each substrate concentration against the reciprocal of the substrate concentration. If the equation is satisfied, a straight line should result, with its slope equal to the Michaelis constant divided by the maximum velocity and its intercept equal to the reciprocal of the maximum velocity.

The velocity data from the series of experiments in which the inhibitor is present are now plotted in the same way; i.e., reciprocal of velocity against reciprocal of substrate concentration. Again, a straight line should describe the data if the equation is satisfied. However, the slope should be greater than in the first case, since it is no longer equal to K_S/V, but, rather, to $\frac{K_s}{V}(1 + \frac{[I]}{K_I})$. The intercept may or may not be the same as for the experimental series in which no inhibitor was present. If the same, then the inhibition is competitive, since equation (2) shows the same value for the intercept, $1/V$, as does equation (1). If the intercepts are different, this analysis shows the inhibition to be non-competitive because, as a comparison of equation (2) with equation (3) shows, the value of the intercept in the case of competitive inhibition is $1/V$ (the same as for no inhibition), while for non-competitive inhibition (equation 3) it is greater, $(1 + \frac{[I]}{K_I})\ \frac{1}{V}$.

Figure 3 shows a plot of the data from two series of experiments of the sort just described. Each point represents the reciprocal of a velocity measurement for a luminescent reaction. Each reaction mixture had the same concentration of luciferase. The concentration of luciferin was varied as shown in table 1. In one series of experiments an 0.188 *M* concentration of *n*-butyl alcohol was always present while in the other series there was no alcohol.

The velocities given in table 1 are initial velocities, measured during the early part of the reaction only, as described in a previous paper (Chase, '49b). The substrate concentrations of table 1 were calculated on the assumption that the luciferin was 100% pure (an unlikely assumption but one

which does not affect the results), and using a molecular weight for luciferin of 300 (Chase, '49a).

The lower set of points of figure 3 is from the series of experiments in which no butanol had been added while the

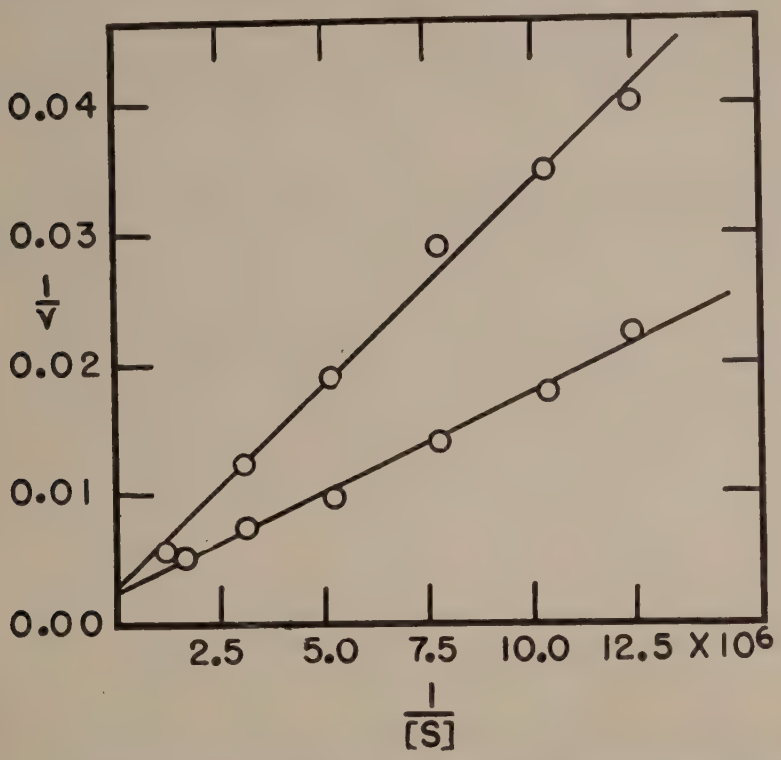

Fig. 3 The data of table 1, plotted as the reciprocals of the velocities against the reciprocals of the luciferin concentrations. The upper set of points is for the experiments in which 0.188 *M* *n*-butyl alcohol was present. No butyl alcohol was used in the experiments represented by the lower set of points. The straight lines were fitted to the two sets of points by the method of least squares. The fact that both straight lines intercept the *1/v* axis at the same place indicates that the inhibition of luciferase by *n*-butyl alcohol is competitive in nature.

upper set represents the measurements made in the presence of *n*-butyl alcohol. The straight lines were fitted by least squares. Inspection of figure 3 shows that, while the slope of the line is increased in the presence of butyl alcohol

(as would be expected since inhibition occurs), the intercept is essentially the same for both series of experiments. This indicates that *n*-butyl alcohol acts here as a competitive inhibitor.

It is interesting to compare the values of K_s (according to the Michaelis-Menten theory, the dissociation constant of the enzyme-substrate compound) and K_I (the dissociation constant of the enzyme-inhibitor compound). These can be cal-

TABLE 1

Initial velocities of the luminescent reaction with a constant luciferase concentration but various concentrations of luciferin, with and without butyl alcohol present (experiment no. 265). The reciprocals of these values appear in figure 3.

LUCIFERIN CONCENTRATION	INITIAL VELOCITIES (MILLIVOLTS/MINUTE)	
	Butanol present	Butanol absent
(moles/liter)		
8.0×10^{-8}	24.8	44.2
9.6	28.4	56.1
12.8	34.3	71.3
19.2	52.8	101.6
31.9	80.5	132.0
61.0	..	190.1
8.0×10^{-7}	171.6	..

culated from equations (1) and (2), above, and from the values of the slopes and intercepts of the two straight lines of figure 3.[5] K_s has a value of 6.4×10^{-7} and K_I a value of 2.6×10^{-1}. If these two constants are regarded as dissociation constants, it would appear that the butyl alcohol tends to dissociate from the luciferase very much more readily than does the luciferin. It must be remembered, of course, that K_s may not actually be a simple dissociation constant, since

[5] In figure 3, the straight line which fits the data for the experiments in which no alcohol was present has a slope of 1.54×10^{-9} and an intercept of 2.4×10^{-3}. The other straight line (0.188 *M* butanol present) has a slope of 3.10×10^{-9} and an intercept of 2.8×10^{-3}.

the simplifications used in the Michaelis-Menten derivation are probably not valid in all cases and certainly not in some.

SUMMARY

The inhibitory effect of *n*-butyl alcohol on *Cypridina* luciferase was studied, using the photoelectric method of Anderson ('33) to obtain the relative first order velocity constant (proportional to luciferase activity) of the luminescent reaction.

It was found that the activity of luciferase was inhibited 50% in the presence of about 0.2 *M* butanol and that this inhibition was reversible.

Suitable experiments, analyzed by a method of Lineweaver and Burk ('34) indicated that the inhibition of luciferase by *n*-butyl alcohol is competitive in nature, K_I having a value of about 2.6×10^{-1} *M*. Since K_s, the Michaelis constant for the luminescent reaction, is about 6×10^{-7} *M*, the luciferase-luciferin complex would appear to be much more tightly bound than the luciferase-butanol complex.

LITERATURE CITED

ANDERSON, R. S. 1933 The chemistry of bioluminescence. I. Quantitative determination of luciferin. J. Cell. and Comp. Physiol., *3:* 45.

———— 1935 Studies in bioluminescence. II. The partial purification of Cypridina luciferin. J. Gen. Physiol., *19:* 301.

———— 1937 Chemical studies on bioluminescence. IV. Salt effects on the total light emitted by a chemiluminescent reaction. J. Am. Chem. Soc., *59:* 2115.

CHASE, A. M. 1948 Effects of hydrogen ion concentration and of buffer systems on the luminescence of the Cypridina luciferin-luciferase reaction. J. Cell. and Comp. Physiol., *31:* 175.

———— 1949a Studies on cell enzyme systems. I. The effect of ferricyanide on the reaction of Cypridina luciferin and luciferase and the combining weight of luciferin. J. Cell. and Comp. Physiol., *33:* 113.

———— 1949b Studies on cell enzyme systems. II. Evidence for enzyme-substrate complex formation in the reaction of Cypridina luciferin and luciferase. Arch. Biochem., *23:* 385.

———— 1950 Studies on cell enzyme systems. IV. The kinetics of heat inactivation of Cypridina luciferase. J. Gen. Physiol., *33:* 535.

CHASE, A. M., AND P. B. LORENZ 1945 Kinetics of the luminescent and non-luminescent reactions of Cypridina luciferin at different temperatures. J. Cell. and Comp. Physiol., *25:* 53.

HARVEY, E. N. 1917 An instance of apparent anesthesia of a solution. Am. J. Physiol., *42:* 606.

———— 1940 Living light. Princeton University Press, Princeton, New Jersey.

JOHNSON, F. H., AND A. M. CHASE 1942 The sulfonamide and urethane inhibition of Cypridina luminescence in vitro. J. Cell. and Comp. Physiol., *19:* 151.

JOHNSON, F. H., H. EYRING AND W. KEARNS 1943 A quantitative theory of synergism and antagonism among diverse inhibitors, with special reference to sulfanilamide and urethane. Arch. Biochem., *3:* 1.

LINEWEAVER, H., AND D. BURK 1934 The determination of enzyme dissociation constants. J. Am. Chem. Soc., *56:* 658.

MICHAELIS, L., AND M. L. MENTEN 1913 Die Kinetik der Invertinwirkung. Biochem. Zeitschr., *49:* 333.

THE ESTIMATION OF POLYTENY IN DROSOPHILA SALIVARY GLAND NUCLEI BASED ON DETERMINATION OF DESOXYRIBONUCLEIC ACID CONTENT [1]

N. B. KURNICK [2] AND IRWIN H. HERSKOWITZ [3]

Laboratory for Cell Research, Tulane University School of Medicine, and Department of Surgery, Louisiana State University School of Medicine, New Orleans

THREE FIGURES

The dipteran salivary gland affords excellent material for the study of chromosome morphology, and provides a frequently used basis for general theories on the physical and chemical structure of genes and chromosomes. The giant chromosomes in these cells are generally regarded as polytene structures (D'Angelo, '50; Metz, '41; Muller, '41; Painter, '41; Slizynski, '50). The degree of this polyteny is thought to be of the order of one to two thousand on the basis of the relative volumes of salivary gland nuclei and diploid nuclei of these species (Metz, '41; Muller, '41; Painter, '41). Since the implication that the chromonema is below the limit of resolution of the light microscope has important bearing on the interpretation of the morphological details of salivary chromosomes, it is desirable to have further evidence on the validity of this hypothesis. Such evidence may be obtained from the determination of the desoxyribonucleic acid (DNA) content of nuclei in view of the abundant evidence for the constancy of DNA per diploid cell in an individual (Boivin et al., '48; Kurnick and Mirsky, '47, unpublished; Mirsky and Ris, '49; Swift, '50).

[1] Presented at the Histochemical Society Meeting, March 19, 1951.

[2] Aided by grants from the National Heart Institute, National Institutes of Health, U.S.P.H.S., and the American Heart Association.

[3] Aided by a grant from the National Cancer Institute, U.S.P.H.S. Present address: Dept. of Zoology, Indiana University, Bloomington, Ind.

It is the purpose of this communication to report observations on the DNA content of *Drosophila* nuclei, as determined by the methyl green method (Kurnick, '50b), in an attempt to determine the degree of polyteny of *Drosophila* salivary chromosomes. These data provide the basis for speculations on the dimensions and molecular composition of the salivary gland chromonema and gene.

MATERIAL AND METHODS

Larvae of the Oregon – R (wild type) stock of *Drosophila melanogaster* were grown at 25°C. on a standard food medium supplemented at intervals with live yeast. For dissection, mature larvae (without regard to sex) were placed in a large drop of 4% formaldehyde adjusted to pH 7.0 (Beckman Model M pH Meter) by the addition of 1 N NaOH. The salivary glands and limb imaginal discs were dissected out and transferred immediately to a fresh bath of 4% neutral formaldehyde, where they were left for at least 10 minutes. The whole tissue was immersed in 0.1 N HCl and stained with purified, buffered methyl green (C.I. 685, Cert. NG-26, National Aniline Corp.) as described by Kurnick ('50b). The uncombined dye was removed by washing in several changes of 0.05 M pH 4.2 acetate buffer over a period of about one hour. The tissues were then immersed in a mixture of 4 parts glycerine to 1 part 0.2 M pH 4.2 acetate buffer for 12–24 hours at 0°C. The tissues were mounted in this medium with and without compression for micro-photometry.

Micro-photometer. The apparatus will be described in some detail insofar as it differs from previously described instruments. A Fish-Schurman 40 watt zirconium arc on a voltage-stabilized 115 V. A.C. line was used to illuminate a Leitz Panphot apparatus, with a double Berek substage condenser of N. A. 1.4. A 2 mm apochromatic oil immersion lens of 1.32 N. A. in a centering collar for a clutch objective changer and a 10 X Ehrlich ocular (with built-in adjustable diaphragm) were used in the monocular vertical tube. An inclined binocular viewing tube was used in conjuction with a movable reflecting prism in the body of the microscope tube. A cross-hair reticule in one of the viewing oculars was centered so as to correspond with the center

of the field in the Ehrlich ocular, and the viewing oculars were adjusted to be parfocal with the Ehrlich ocular. Over the ocular, a right angle totally reflecting prism in an adjustable base was mounted to direct the light to a Farrand Photomultiplier at a distance of approximately 4.6 meters. A 1P 21 photomultiplier tube was used since it provided greatest sensitivity due to its high multiplication factor despite its relatively poor spectral response at the wave-lengths used. The magnification at the phototube was 17,000 $\times$. An iris diaphragm in front of the phototube admitted a circle of light, 1.9 cm in diameter, corresponding to 1.1 μ in the object. Due to the dimensions of the filament (0.8 $\times$ 2.4 cm), the measured area was actually 1.1 $\times$ 0.5 μ. To obtain three nearly monochromatic light bands, two Farrand interference filters and one Corning glass filter were used. The Farrand filters had measured peak transmissions at 540 mμ (half band width 16 mμ, 26% transmission) and 634 mμ (half band width 10 mμ, 25% transmission), and the Corning glass filter (color specification number 5–74) had its peak transmission at 430 mμ. Peak transmissions were confirmed for all filters in the Beckman DU Quartz Spectrophotometer.

The apparatus was used in a dark room and the photomultiplier tube protected from all stray light by a one-half meter length of 3 cm blackened pipe.

The Leitz Panphot apparatus was selected for its massive stability and the ease with which the viewing prism slides in and out without disturbing the other optics. This permits repeated observations of the object in order to focus without disturbing the position of the image at the phototube or the optical axis.

Photometric procedure. The light beam from the zirconium arc, suitably reduced by an iris diaphragm on the arc, was accurately centered to pass through the optical axis of all lenses in the photometric system; and the condensing lenses of the light source and substage were adjusted for critical illumination. The light source diaphragm was then opened fully, and the final adjustment of the substage illuminating system made, using the photomultiplier to check the setting for maximum brightness. The lower diaphragm of the substage condenser was then closed until the numerical aperture was slight smaller than that of the objective as determined by slight but definite reduction (about 5%) in light intensity at the photomultiplier tube.

Using white light, with the Ehrlich diaphragm closed to project a visible 3 cm square on the face of the phototube, the prism over the ocular was adjusted to center the beam on the phototube. The latter was rotated until the galvanometer gave maximal deflection.

Measurements of optical density were made as follows. With the 634 mμ filter on the face of the arc, a blank area of the slide adjacent

to the nucleus to be measured was centered in the field. The corresponding galvanometer deflection was recorded as I_o^{634} and the nucleus then centered and focused. The I^{634} recorded corresponds to the minimum light transmission obtained by altering the fine focus adjustment of the microscope. Changes in focus have no effect on I_o, but do alter I. Without touching the microscope, the 540 mμ and 430 mμ filters were substituted in order and I^{540} and I^{430} recorded. This assured obtaining the transmissions on the identical area and focal plane for all the wave lengths. The slide was then moved to a blank space, I_o^{540}, I_o^{430} determined, and I_o^{634} checked. It was found that the instrument was quite stable throughout the course of measurement. This procedure was repeated three times for each nucleus, using a different portion of the nucleus each time.

The cross-sectional dimensions of the object were measured with an ocular micrometer and the thickness with the scale on the fine adjustment drum.

Calculation of DNA content. DNA content, expressed in mg per nucleus, is obtained in the case of a cylinder (i.e., when the nucleus is flattened so that thickness is much smaller than the cross-sectional axes) from the formula (Kurnick, '50b):

$$\text{DNA} = \text{E} \times \text{area in sq. cm.} \times \frac{310 \times 13}{\varepsilon} \qquad \textit{(Formula 1)}$$

where E is the specific optical density and ε the molar extinction coefficient at the wave length used for E. When the nucleus was not compressed (judged from the fact that the thickness was similar in magnitude to the cross-sectional axes), the formula for an ellipsoid is required, making the expression:

$$\text{DNA} = \text{E} \times \tfrac{2}{3} \text{ area in sq. cm.} \times \frac{310 \times 13}{\varepsilon} \qquad \textit{(Formula 2)}$$

The molar extinction coefficients (ε) used were 82,000 at 634 mμ and 10,300 at 540 mμ (Kurnick and Mirsky, '50). The appropriateness of these molar extinction coefficients when narrow band-pass filters are used in place of a more accurate monochromator was established by comparing the transmission of a methyl green-DNA solution (see Kurnick and Foster, '50, for preparation of this complex) in the Beckman spectrophotometer at 634 and 540 mμ with the transmission determined when the Beckman cuvette was introduced into the light path of the micro-photometer using the corresponding filters (table 1).

The specific absorption at 634 mμ (E_{634}) is obtained as follows:

$$E_{634}^{M} = E_{634} + E_{634}^{N} \qquad \textit{(Formula 3)}$$

where E_{634}^{M} is the measured extinction $\left(\log \frac{I_o^{634}}{I^{634}} \right)$ and E_{634}^{N} is the non-specific

TABLE 1

Comparison of transmission of a methyl green-DNA solution measured in the Beckman spectrophotometer and the microphotometer

λ [1]	% TRANSMISSION	
	Beckman	*Microphotometer*
634	33	34
540	87	90
430	83	82

[1] Measured peak transmission of filter and wave-length setting of Beckman wave-length drum.

absorption at 634 mμ, composed of light lost by refraction (E^R_{634}) and by dispersion (E^D_{634}).

E^N_{634} may be derived from E^N_{540} (see *Formula 5*), which is obtained from

$$E^M_{540} = E_{540} + E^R_{540} + E^D_{540} \qquad \textit{(Formula 4)}.$$

If $E^D_{540} = 0$, $E^M_{540} = E^M_{430}$, since the molar extinction coefficients are approximately equal at these two wave-lengths and light loss by refraction is not thought to be significantly influenced by wave-length (Caspersson, '50).

If $E^R_{540} = 0$, then $\frac{E^N_{540}}{E^N_{430}} = \frac{430^4}{540^4}$ (Rayleigh, 1871) so that $E^M_{430} > E^M_{540}$.

From table 2 it is apparent that $E^D_{540} \neq 0$, since $E^M_{430} > E^M_{540}$ in 29 of 33 determinations. To determine the relative magnitudes of E^D_{540} and E^R_{540}, the mean of $\frac{E^M_{430}}{E^M_{540}}$ for these 33 determinations was calculated (1.41 ± 0.06). Then, substituting in

$$E^M_{430} = E_{430} + E^R_{430} + E^D_{430},$$

the facts that $E_{430} = E_{540}$, $E^R_{430} = E^R_{540}$, $E^D_{430} = \frac{540^4}{430^4} E^D_{540}$

and $E^M_{430} = 1.41\ E^M_{540}$, we obtain:

$$1.41\ E^M_{540} = E_{540} + E^R_{540} + 2.49\ E^D_{540}.$$

Subtracting from this, *Formula 4*, we obtain:

$$0.41\ E^M_{540} = 1.49\ E^D_{540}$$

$$\therefore\ E^D_{540} = 0.28\ E^M_{540}.$$

From *Formula 4*,

$$E^R_{540} = E^M_{540} - E_{540} - 0.28\ E^M_{540} = 0.72\ E^M_{540} - E_{540}.$$

Since $E^N_{634} = E^R_{634} + E^D_{634} = E^R_{540} + \frac{540^4}{634^4} E^D_{540}$ *(Formula 5)*

we obtain $E^N_{634} = 0.72\,E^M_{540} - E_{540} + 0.51\,(0.28\,E^M_{540})$

$$\therefore\ E^N_{634} = 0.86\,E^M_{540} - E_{540}. \qquad \textit{(Formula 6)}$$

Since $E_{540} = \frac{\epsilon_{540}}{\epsilon_{634}} E_{634} = \frac{1}{8} E_{634}$,

Formula 6 becomes $E^N_{634} = 0.86\,E^M_{540} - 0.125\,E_{634}$.

Substituting in *Formula 3*,

$$E^M_{634} = E_{634} + 0.86\,E^M_{540} - 0.125\,E_{634}$$

$$\therefore\ E_{634} = 1.14\ (E^M_{634} - 0.86\ E^M_{540}).$$

Thus E_{634} is obtained from measured values and may be substituted in *Formulae 1* and *2*, which become, in their final form:

$$\text{DNA in mg} = 0.056\ (E^M_{634} - 0.86\ E^M_{540}) \times \text{area in sq. cm.} \qquad \textit{(Formula 1)}$$

$$\text{DNA in mg} = 0.037\ (E^M_{634} - 0.86\ E^M_{540}) \times \text{area in sq. cm.} \qquad \textit{(Formula 2)}$$

Since the nucleolus (which approximates an ellipsoid) contains no DNA, the pertinent area in *Formula 1* is the area of the cylindrical nucleus less $\frac{2}{3}$ the ratio of the nucleolar : nuclear thickness multiplied by the cross-sectional area of the nucleolus. In *Formula 2*, it is the cross-sectional area of the ellipsoidal nucleus less that of the ratio of the nucleolar : nuclear thickness multiplied by the cross-sectional area of the nucleolus (since the factor $\frac{2}{3}$ to convert from a cylinder to an ellipsoid is already included in this formula).

Volumes were calculated for ellipsoids, including nucleoli (cf. *Formula 2)*, from the formula $\frac{\pi}{6}$ abc, where a and b are the axes of the central cross-section and c is the thickness (Micklewright, Kurnick and Hodes, '52), and for cylindrical nuclei from the formula $\frac{\pi}{4}$ abc (Kurnick, '50b).

RESULTS

The data on 15 methyl green stained salivary gland nuclei are presented in table 2. Table 3 contains the data on one unstained and four stained limb anlage cells.

The DNA content of the salivary nuclei, which ranged from 5 to 710×10^{-10} mg, representing approximately a 140-fold difference in DNA, indicated that these cells did not represent a homogeneous population from the aspect of polyteny. It is apparent that the larger basal cells contain more DNA than the smaller neck nuclei. In figure 1, the correlation between

DNA content and nuclear (minus nucleolar) volume is illustrated. The volume calculations, including as they do the measurement of thickness (subject to considerable personal error, although several readings were averaged in each measurement) have an error of about 10% for the larger cells, and even more for the smallest (Micklewright, Kurnick, and Hodes, '52). It should be pointed out that thickness enters into the calculation of DNA content only as a basis for deciding between *Formula 1* (for a cylinder) and *2* (for an ellipsoid), and for the calculation of the nucleolar correction which proves to be negligible in all but the smallest cells. In the former decision, only an approximate dimension is needed.

However, measurements of the cross-sectional axes, which are used for the calculation of area, involve errors that do enter into the calculation of DNA content. These produce errors of about 5% in the calculation of area for large cells, and more for small nuclei (Micklewright, Kurnick, and Hodes, '52). This error is not considered in our calculations of the standard error of DNA content, since this is a constant in the calculations.

The standard error given in the tables does take into consideration variation in homogeneity and errors in the photometric method. The generally good agreement among triplicate (and in some cases more frequent) determinations indicates the reproducibility of the photometric method and the homogeneity of the nuclei, since each determination is made on a different area of 1 μ diameter (near the center for unflattened nuclei — see description of method and apparatus). Homogeneity of the material is essential for the determination of DNA content. When very small areas are analyzed, as here, the integration of heterogeneous areas would become an exceedingly difficult procedure. If larger areas are used on heterogeneous structures, as has been the case in other photometric techniques which have been described (Pollister and Moses, '49; Pollister and Ris, '47), the photo-cell records a mean value rather than an integrated extinction, so that the absorptions (and content) determined are too low. This was

TABLE 2

Salivary nuclei stained with methyl green

CELL NO.[1]	DIMENSIONS OF NUCLEAR AXES, μ			DIMENSIONS OF NUCLEOLAR AXES, μ			E^{M}_{634}	E^{M}_{540}	E^{M}_{430}	FORMULA[2]	VOLUME IN μ^3		DNA CONTENT mg $\times 10^{-10}$	
	Long	Short	Thick	Long	Short	Thick					Nucleus	Nucleolus[3]	Calculated	Mean $\pm$ S.E.
							.179	.102	.113				53	
Ib_1	16.6	13.4	14	8.4	3.7	9.0	.174	.046	.068	2	1630	147	79	63 $\pm$ 4.6
							.170	.063	.095				68	
							.173[4]	.060	.055				67	
							.165	.091	.142				48	
							.152	.050	.071				60	
Ic_1	19.7	18.7	18.5	7.9	7.4	7.0	.180	.060	.068	2	3570	214	129	150 $\pm$ 15
							.187	.052	.091				143	
							.214	.041	.055				180	
Id_1	24.7	23.4	10.5	12.1	4.7	10.5	.152	.027	.055	1	4770	313	307	302 $\pm$ 34
							.207	.065	.097				359	
							.180	.091	.091				242	
Ie_1	20.9	17.0	22.0	7.6	4.5	10.0	.460	.102	.132	2	4100	179	367	342 $\pm$ 19
							.407	.110	.103				305	
							.428	.072	.116				358	
IIa_1	11.6	11.0	9.0	7.9	4.2	(6.1)	.041	.021		2	602	106	7.0	5.6 $\pm$ 1.0
							.040	.023					6.1	
							.040	.033					3.7	
IIa_2	15.3	14.2	9.0	10.5	5.3	(7.9)	.046	.032		2	1025	230	8.8	9.6 $\pm$ 1.3
							.065	.046					12.2	
							.060	.051					7.8	
II...	24.2	21.6	12.0	8.9	5.8	(7.4)	.070	.009		1	4830	206	137	136 $\pm$ 12

							.131	.027				561	
							.120					504	
IIIc$_1$	27.4	22.4	10.5	10.5	5.3	7.0	.148	.067	.065	1	5060	204	233	225 ± 16
							.136	.046	.079				249	
							.133	.067	.086				194	
IVd$_1$	21.3	19.5	27.0	10.5	8.4	(9.5)	.347	.055	.083	2	5880	439	335	318 ± 9
							.363	.097	.105				312	
							.371	.113	.143				306	
IVe$_1$	34.2	31.6	22.5	8.4	5.8	6.3	.305	.067	.091	2	12740	163	765	712 ± 47
							.269	.081	.107				617	
							.314	.083	.118				753	
Vb$_1$	16.8	13.7	9.5	12.6	5.3	5.5	.212	.022	.064	2	1145	193	107	91 ± 9
							.197	.041	.054				90	
							.205	.082	.105				75	
Vb$_2$	17.1	14.2	16.3	7.4	5.3	9.0	.190	.031	.052	2	2070	185	105	101 ± 3
							.162	.027	.032				89	
							.207	.052	.073				104	
							.187 [5]	.029					104	
							.219	.081					96	
							.204	.044					107	
Vc$_1$	15.3	14.5	15.0	6.8	5.8	6.5	.275	.038	.055	2	1744	134	144	163 ± 12
							.323	.058	.086				162	
							.337	.031	.041				184	

[1] Roman numeral identifies the gland; the letter, the relative position therein proceeding from the neck region (a) to the base (e).

[2] *Formula 1* is for a cylinder. *Formula 2* is for an ellipsoid. See text.

[3] Nucleolar volume is always calculated as an ellipsoid. Where its thickness was not measured, the mean of the cross-sectional axes is used (indicated in parentheses).

[4] This and the succeeding two measurements were made 5 days after the first three.

[5] This and the succeeding two measurements were made 24 hours after the first three.

TABLE 3

Anlage cell data

TREATMENT	CELL NO.	DIMENSIONS μ		E^{M}_{634}	E^{M}_{540}	E^{M}_{430}	VOLUME [1] μ^3	DNA CONTENT mg $\times 10^{-10}$	
		Long	Short					Calculated	Mean $\pm$ S.E.
Unstained	A	3.2	3.2	.046	.059	.058	17	— 0.15	0.06 $\pm$ 0.11
				.032	.032	.043		0.12	
				.050	.050	.043		0.21	
	1	3.2	3.2	.073	.057	.064	17	0.71	0.47 $\pm$ 0.12
				.068	.064	.072		0.39	
				.070	.070	.069		0.30	
Methyl green stained	2	4.2	3.7	.209	.144		30	3.8	3.1 $\pm$ 0.6
				.219	.163			3.6	
				.087	.051			1.9	
	3	4.7	3.2	.086	.059		25	1.5	1.7 $\pm$ 0.09
				.094	.060			1.8	
				.090	.059			1.7	
	4	4.2	3.7	.223	.235		30	0.95	

[1] Calculated for prolate spheroid.

previously illustrated in our description of the methyl green method (Kurnick, '50b), wherein the nuclei measured gave values in a heterogeneous state of roughly one-half the values obtained for homogeneous nuclei. Accordingly, in the case of the salivary glands of Diptera, the classic cytologic picture of well outlined, discretely banded chromosomes (fig. 3) should be avoided in a photometric study such as this. Ris and Mirsky have reported ('49) the homogeneous appearance of salivary gland nuclei obtained by dissection of the gland in 10% sucrose. We have observed that dissection of the living larva in accurately neutralized formalin (4% formaldehyde, containing a minimum of electrolyte), which in itself appears to have no deleterious effect on the organism, yielded homogeneous salivary nuclei even more consistently than did dissection of the gland in sucrose. These observations may be compared to the early studies of Doyle and Metz ('35). However, unlike their observations on *Sciara*, isotonic saline produced banding in *Drosophila* salivary chromosomes. This effect appears to be a function of electrolyte concentration rather than tonicity *per se*, since several-fold hypertonic sucrose solution produces no banding and distilled water or markedly hypertonic saline (1 M) tends to reverse the banding produced in 0.14 M saline.

It may be pointed out that photometric measurements made as much as five days apart on the same cells (table 2, cell Ib_1 and Vb_2) revealed no loss of methyl green. Therefore, all the specific absorption determined must have been due to methyl green quantitatively bound to polymerized DNA, in which state it is neither readily removed by prolonged washing nor fades (Kurnick, '50a, '50c).

As illustrated in table 3, the DNA contents for the 4 stained anlage nuclei show considerable variation ($0.47–3.1 \times 10^{-10}$ mg). This may be due, in part, to the difficulty of measuring the dimensions of such small structures. Furthermore, considerable error is inherent in the measurement of very low absorptions, particularly when the non-specific absorption is of the same order of magnitude as the total absorption. In this event, the subtraction of the calculated non-specific ab-

sorption from the measured absorption results in a very small calculated specific absorption, in which the effects of errors of measurement and assumptions as to the nature of the non-specific light loss become greatly exaggerated. In order to determine whether our method was actually detecting such low specific absorptions, an unstained anlage cell was measured (cell A, table 3). Applying the formula for the determination of DNA content to this nucleus, values were obtained in the range -0.15 to 0.21×10^{-10} mg. The mean value does not significantly differ from zero. In every case the values calculated for the stained nuclei exceed the highest value obtained for the unstained control. Furthermore, the measured extinctions at 634 mμ are equal to or less than those at 540 mμ for the unstained nucleus in each determination, while for the stained nuclei they exceed the 540 mμ value in 8 of 10 measurements. It is thus apparent that methyl green staining is, in fact, detectable in the nucleus, but the errors in measurement of absorption and of the area (cross-sectional axes) are so great as to make the absolute value of the DNA content in individual determinations unreliable. A better estimate may be obtained by calculating the mean DNA content from the 10 determinations in table 3. This gives a mean content of $1.7 \pm 0.4 \times 10^{-10}$ mg DNA for the diploid anlage nucleus. The mean volume of the 5 anlage cells (calculated from the cross-sectional axes as a sphere or prolate spheroid) was found to be $24 \pm 3\ \mu^3$.

DISCUSSION

It was our purpose to determine the degree of polyteny of salivary chromosomes from the DNA content of the nucleus. This requires a satisfactory value for the DNA content of diploid nuclei as a basis for comparison. We have selected limb anlage cells as a suitable diploid cell for the determination of this base value. From the value obtained by photometry of $1.7 \pm 0.4 \times 10^{-10}$ mg, one obtains a 420-fold increase in DNA content in the largest salivary gland nucleus measured (712×10^{-10} mg DNA). This represents 840 chromomenata per double salivary chromosome.

Others (Metz, '41; Muller, '41; Painter, '41) have assumed that nuclear volume is a direct measure of polyteny in fly tissues. Our data support this view for *Drosophila* salivary nuclei by the observed correlation between volume and DNA content within the gland (fig. 1, 0.052×10^{-10} mg DNA/μ^3).

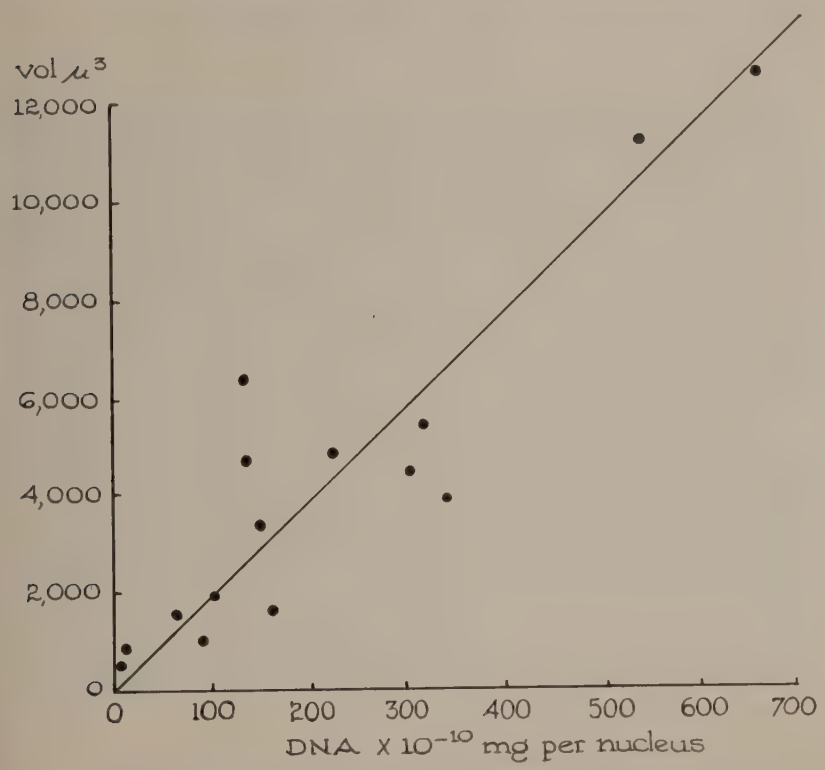

Fig. 1 Relationship between the desoxyribonucleic acid (DNA) contents and nuclear (minus nucleolar) volumes of salivary gland cells.

Accordingly, extending this observation to the anlage nucleus, which has the same dimensions in limb and salivary buds (Sonnenblick, '41), we obtain a DNA content for the average anlage nucleus ($24 \pm 3\ \mu^3$) of $1.2 \pm 0.2 \times 10^{-10}$ mg DNA, which is similar to the value obtained by direct photometry. From this value, we would calculate 1140 chromomenata per double salivary chromosome.

The degree of polyteny thus arrived at by means of the DNA analyses is in the vicinity of 1000. The uncertainty of the exact DNA content for the diploid nucleus makes it impossible for us to give an absolute value for the highest degree of polyteny encountered; nor can it be decided from these data whether or not chromonemal division is synchronous, which would require a polyteny that is a power of 2, such as 1024. In the subsequent

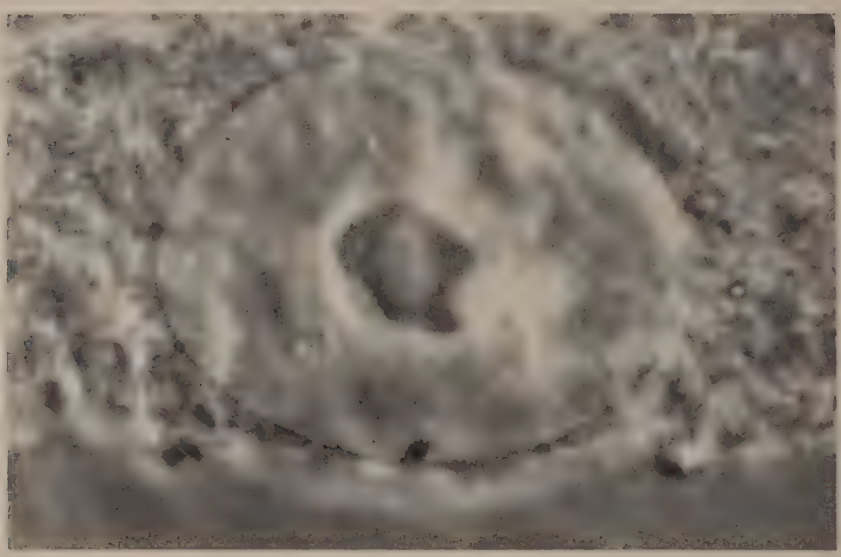

Fig. 2 Salivary gland nucleus dissected in 4% neutral formaldehyde as seen under phase contrast microscopy. Note homogeneity except for the refractile nucleolus. Cytoplasmic structure, which does not stain with methyl green, is visible through the lenticular nucleus. Mag. approx. 2000 ×.

calculations, the mean of the two calculated degrees of polyteny will be applied (990 = 1000 as a suitable approximation).

The salivary nucleus upon which the calculation of polyteny was based had a volume of 12,600 μ^3 (not including the nucleolus) and a DNA content of 712×10^{-10} mg. Both of these values are considered reliable, since measurements of diameters on such large structures have a small percentage error and the small, irregularly shaped nucleolus is of relatively insignificant dimensions. Moreover, the absorption is approxi-

mately 50%, of which the non-specific absorption is less than 20%, permitting accurate photometry and calculations.

Since the *Drosophila* salivary nucleus *in vivo* is optically homogeneous (Buck, '39; and our own observations) and is maintained in this state in our preparations (fig. 2), the entire nuclear volume may be considered to consist of chromosomal material. On this basis, we may calculate that the volume of a haploid set of chromonemata is $\frac{12600}{1000}$ or 12.6 μ^3 in the physio-

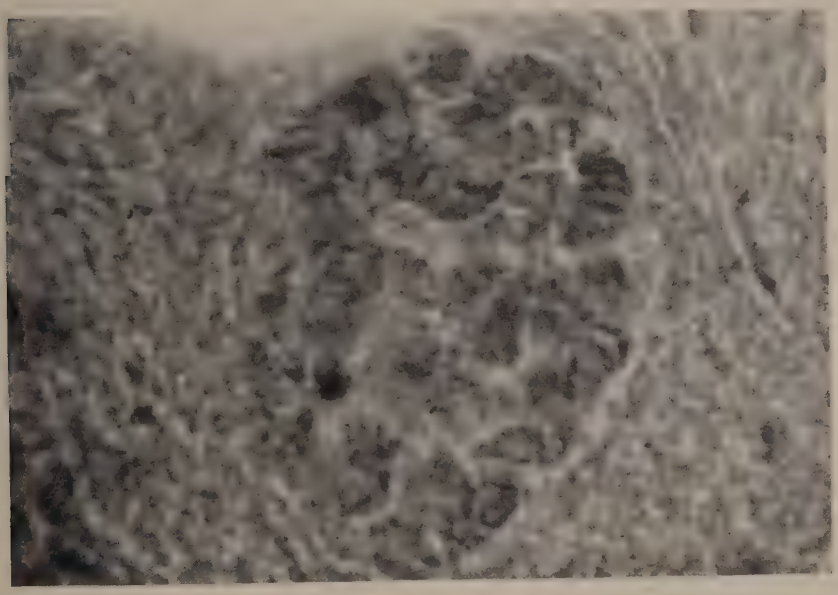

Fig. 3 Salivary gland nucleus dissected in 45% acetic acid, phase contrast microscope. Note shrunken banded chromosomes. Mag. approx. 2000 ×.

logical (swollen) state. On the basis of Bridges' observation ('42) that the relaxed aceto-carmine prepared chromosome complement is about 750 μ long, the mean cross-sectional area of the chromonema is 0.017 μ^2, corresponding to a diameter of 0.14 μ. The entire chromosome, in the physiological state, is then about 17 μ^2 in cross-sectional area and 4.4 μ in diameter. In the contracted, acetic acid preparation, these dimensions are somewhat reduced, since the chromosomes no longer fill the nucleus (fig. 3). Since the chromonemal diameter in the physio-

logical state is already below the limit of resolution of the light microscope, it must be unresolvable in the classical, smear preparation.

The data permit certain further calculations about the dimensions and chemical composition of the salivary nuclear constituents. From the observation (Kurnick and Mirsky, unpublished) that the nuclei of rat and rabbit livers and kidneys prepared by Stoneburg's citric acid method ('39) have dry, fat-free weights of 8% of their original volumes, we would estimate, on the same basis, the dry, fat-free weight of the salivary nucleus under discussion to be about 1×10^{-9} gm. This value is probably too low, since the citric acid isolation of nuclei dissolves some protein. Therefore, the calculated concentration of DNA on a dry weight basis of 7% may be too high. This value may be compared with 45% for calf thymus (Mirsky and Ris, '47) and 20% for rat liver and kidney (Kurnick and Mirsky, unpublished). Since there appears to be a correlation between non-DNA concentration and metabolic activity, it may be inferred that the salivary gland cell stands at a very high level of secretory activity. Since analogous calculations for the anlage nucleus give 6–9% DNA concentration, it also appears to be a very active cell (presumably in synthesis of cell protein).

If we assume a molecular weight of 10^6 grams for polymerized DNA (Mirsky, '43), the mass of a single molecule would be 1.6×10^{-15} mg. Since we have found 710×10^{-10} mg in the 1000-tene nucleus, a haploid set of chromosomes would contain 0.71×10^{-10} mg DNA. Thus, the haploid set of chromosomes contains 44,000 such molecules. Therefore, unless even the largest estimate of 10,000 for the gene number in *D. melanogaster* (Timoféeff-Ressovsky, '40) is much too low, the gene must include several such DNA molecules, or the DNA in the gene must have a molecular weight much greater than the usually applied value of 10^6. It seems unlikely that the gene number approximates 40,000, since so large a number of genes would permit a mean distance between centers of only 17 mμ. It is difficult to conceive of how resolvable bands could

be derived from the unbanded state with units so closely spaced. We cannot decide between the alternatives, but it may be noted that Bunce and Doty (referred to in Blout and Doty, '50) report a molecular weight of 4 million for a sample of DNA.

It would appear that previous estimates of 1000 strands per double salivary chromosome are confirmed by our DNA studies. The data suggest a complex molecular composition of the gene not previously considered.

SUMMARY

The quantitative determination of polymerized DNA in *Drosophila melanogaster* nuclei by the photometric methyl green method reveals a mean DNA content of about 1.7×10^{-10} mg in anlage cells. In salivary gland nuclei, the DNA content varies progressively from 5.6 to 712×10^{-10} mg as one proceeds from the smaller neck cells to the large basal cells. There appears to be a direct correlation between DNA content and nuclear volume. These results imply that the mature double salivary chromosome contains in the vicinity of 1000 strands. The theoretical implications of these findings for the dimensions and composition of the chromonema and gene are discussed.

ACKNOWLEDGMENT

We wish to acknowledge with thanks the collaboration of Dr. Edith Krugelis in some of the early observations on the preparation of homogeneous salivary nuclei.

LITERATURE CITED

Boivin, A., R. Vendreley and C. Vendreley 1948 L'acide désoxyribonucléique du noyau cellulaire, dépositaire des caractères héréditaires: arguments d'order analytique. Acad. Sci. Paris, C. R., *226:* 1061–1063.

Bridges, P. N. 1942 A new map of the salivary gland 2L-chromosome of *Drosophila melanogaster*. J. Hered., *33:* 403–408.

Buck, J. B. 1939 Structure of living salivary gland chromosomes (abstract of paper presented at the 1938 Summer Meeting of the Genetics Society of America, Marine Biological Laboratory). Genetics, *24:* 96.

Bunce, B., and P. M. Doty, referred to in Blout, E. R., and P. M. Doty 1950 Protein and Nucleic Acid Conference. Science, *112:* 639–643.

CASPERSSON, T. O. 1950 Cell Growth and Cell Function, W. W. Norton Co., New York.

D'ANGELO, E. G. 1950 Salivary gland chromosomes. Annals N. Y. Acad. Sci., *50:* 910–919.

DOYLE, W. L., AND C. W. METZ 1935 Structure of the chromosomes in the salivary gland cell in *Sciara* (Diptera). Biol. Bull., *69:* 126–135.

KURNICK, N. B. 1950a The determination of desoxyribonuclease activity by methyl green; application to serum. Arch. Biochem., *29:* 41–53.

———— 1950b The quantitative estimation of desoxyribosenucleic acid based on methyl green staining. Exp. Cell. Res., *1:* 151–158.

———— 1950c Methyl green-pyronin. I. Basis of selective staining of nucleic acids. J. Gen. Physiol., *33:* 243–264.

KURNICK, N. B., AND M. FOSTER 1950 Methyl green. III. Reaction with desoxyribonucleic acid, stoichiometry, and behavior of the reaction product. J. Gen. Physiol., *34:* 147–159.

KURNICK, N. B., AND A. E. MIRSKY 1950 Methyl green-pyronin. II. Stoichiometry of reaction with nucleic acids. J. Gen. Physiol., *33:* 265–274.

METZ, C. W. 1941 Structure of salivary gland chromosomes. Cold Spring Harbor Symposia on Quant. Biol., *9:* 23–39.

MICKLEWRIGHT, H. L., N. B. KURNICK AND R. HODES 1952 The determination of cell volume. Exp. Cell. Res., in press.

MIRSKY, A. E. 1943 Chromosomes and nucleoproteins. Adv. in Enzymology, *3:* 1–34.

MIRSKY, A. E., AND H. RIS 1947 Isolated chromosomes. J. Gen. Physiol., *31:* 1–6.

———— 1949 Variable and constant components of chromosomes. Nature, *163:* 666–667.

MULLER, H. J. 1941 Résumé and perspectives of the Symposium on Genes and Chromosomes. Cold Spring Harbor Symposia on Quant. Biol., *9:* 290–308.

PAINTER, T. S. 1941 An experimental study of salivary chromosomes. Cold Spring Harbor Symposia on Quant. Biol., *9:* 47–54.

POLLISTER, A., AND M. J. MOSES 1949 A simplified apparatus for photometric analysis and photomicrography. J. Gen. Physiol., *32:* 567–577.

POLLISTER, A., AND H. RIS 1947 Nucleoprotein determination in cytological preparations. Cold Spring Harbor Symposia on Quant. Biol., *12:* 147–157.

RAYLEIGH, LORD (J. W. STRUTT) 1871 On the lights of the sky, polarization and color. Phil. Mag., *41:* 274.

RIS, H., AND A. E. MIRSKY 1949 The state of the chromosomes in the interphase nucleus. J. Gen. Physiol., *32:* 489–502.

SLIZYNSKI, B. M. 1950 Partial breakage of salivary gland chromosomes. Genetics, *35:* 279–287.

SONNENBLICK, B. P., DISCUSSION IN PAINTER, T. S. 1941 An experimental study of salivary chromosomes. Cold Spring Harbor Symposia on Quant. Biol., *9:* 53.

STONEBURG, C. A. 1939 Lipids of the cell nuclei. J. Biol. Chem., *129:* 189–196.
SWIFT, H. H. 1950 The desoxyribonucleic acid content of animal nuclei. Physiol. Zool., *23:* 169–198.
TIMOFÉEFF-RESSOVSKY, N. W. 1940 Ueber den Mutationsmechanismus und die Natur der Gene. Nova Acta Leopold, *9:* 209.

PHOTODYNAMIC EFFECTS ON METABOLISM AND REPRODUCTION IN YEAST[1]

PAUL J. FREEMAN AND ARTHUR C. GIESE
Department of Biological Sciences, Stanford University, Stanford, California

SEVEN FIGURES

Photodynamic action occurs when organisms, tissues or cells are exposed to visible light in the presence of certain fluorescent dyes and oxygen. The net effect is one of injury to the biological system involving oxidation of essential cellular constituents. Many workers have attempted to ascertain the nature of the mechanism underlying photodynamic action without complete agreement, some claiming primarily superficial action of the dyes, others indicating action of the dyes deeper in the cell (see Blum, '41, for summary). An effort was made in the experiments reported here to gain further insight into the mechanism of photodynamic action by dyes of the fluorescein series.[2] Specifically the investigation sought to determine the effects of photodynamic action on (1) entry of dye into yeast, (2) some of the metabolic activities of yeast, both during and after irradiation and (3) reproduction of yeast.

MATERIALS AND METHODS

Yeast was chosen as the organism for this investigation because it is easy to obtain in large numbers under fairly well controlled cultural conditions, and because with it endo-

[1] Supported in part by funds from the Rockefeller Foundation.

[2] Penetrating dyes such as neutral red and methylene blue, in fact basic dyes generally, were not studied. It is possible that the mechanism of action of such dyes is different, especially the entry of the dye, and an analysis of their action merits a separate study.

genous metabolism (in absence of substrate) as well as exogenous metabolism may be studied. The strain of *Saccharomyces cerevisiae* used here was originally isolated from Fleischmann's yeast. Cultures were grown at 28°C. in a liquid medium consisting of 2% glucose, 1% yeast extract (Difco), and 1% bactopeptone, made up with M/20 KH_2PO_4 buffer giving a pH of about 5.2. Yeast was transferred from the log phase of a culture and inoculated into 20 cm^3 of the medium placed in a 125 cm^3 Erlenmeyer flask and shaken for 24 hours on a platform oscillator. The yeast was then removed and washed three times by centrifugation and finally suspended in a mono-potassium and di-sodium phosphate buffer adjusted to a pH of 7.0. A densitometer of the type developed by Longsworth ('36) was used to adjust the density of the suspension so that approximately the same number of cells per cm^3 were present in suspensions from experiment to experiment. The number of yeast cells in such a suspension varied from around 3.0 to 3.2×10^7 per cm^3 as obtained by actual cell count. To achieve as nearly the same physiological state in each batch of cells clean, moist air was bubbled through yeast suspensions for 6 hours (Aldous, Fisher, and Stern, '50).

Aluminum foil was used to shield from stray light all vessels involved in storage and transport of samples. Irradiation was carried on in a windowless room which was dimly lighted (under 10 foot candles) and, as preliminary experiments had shown, had no effect in producing photodynamic action. Two milliliter sample aliquots were illuminated in standard Warburg-Barcroft vessels placed in a constant temperature bath. Uniform illumination of the cells was aided through the use of a mirror placed in the tank at such an angle as to reflect the light upwards through the bottom of the vessels. Circulation of the cells throughout the suspension was maintained by shaking the vessels through a small arc described within the spot thrown by the lamp. The source of light was a 100 watt GE CH4 projector spot lamp at a distance of 65 cm from the yeast suspension. Before reaching the yeast

suspension the light was passed through 5 cm of a $CuSO_4$ solution plus 25 cm of water in the bath. These acted as filters to take out the infra-red radiations. Corning filter No. 3389 with a cut-off at about 4100 Å and transmitting about 70% from wavelengths 4400 Å and 86% from 5100 Å on through the visible was also interposed between the source and the vessels. The lamp was turned on at least 20 minutes before use to allow it to reach a fairly constant intensity as determined by photometer readings. The intensity of the light transmitted through a water cell which absorbs out the heat was 48 ergs/mm²/sec. About 60% of this was absorbed by 1:10,000 solution of rose bengal at the distance of the sample from the light source used in all the experiments. Determinations were made by a thermopile calibrated against a standard lamp.

Carbon dioxide production and oxygen consumption were measured by the standard Barcroft-Warburg apparatus (Dixon, '34; Umbriet, Burris and Stauffer, '45). Duplicates were run for each experimental sample of yeast. The figures for the manometric excursions of the two vessels were then averaged for calculation of final gas volumes.

Glucose present in the supernatant from a yeast suspension was determined by the method of Shaffer-Hartmann as recommended by Stiles, Petersen and Fred ('26). Alcohol present in the supernatant from yeast suspensions was determined by the method of Gibson and Blottner ('38), a Klett-Summerson colorimeter being used for the purpose.

Cell counts were made using a Levy hemocytometer and a Thoma leucocyte pipette. Colony counts were made by plating a 1 cm³ sample of yeast suspensions withdrawn directly from Warburg vessels, which was then diluted in 99 cm³ of distilled water and transfers were made from this dilution to give a series ranging from about 10 to 10^5 cells/cm³. These diluted samples were then added to growth medium. Counts were made after 48 hours on the samples of dilutions that proved to be highest in the number that still could be accurately counted.

Radioactive sodium acetate was efficiently metabolized by the yeast, making tracer studies possible. The carbon isotope was located in the carboxyl group of the acetate; it was traced by means of a Müller windowless counter (Calvin *et al.*, '49).

EXPERIMENTAL

The majority of experiments carried out by previous investigators were performed on animal cells or tissues using stored nutrients. Therefore for a comparison, our first experiments on yeast measured the effect of photodynamic action on endogenous metabolism, i.e., in the absence of nutrients in the medium. Yeast under these conditions, continuously illuminated in the presence of rose bengal, showed an oxygen consumption higher than that of the control in the dark (or in the light but in the absence of dye) as seen in figure 1. Evidence that this increase is actually due to photochemical oxidation and not to stimulation of true respiration of the cells was obtained by determining the ratio of CO_2 produced to O_2 consumed, or the respiratory quotients (R.Q.), of such cells during photodynamic action (table 1). The R.Q.[3] of endogenous untreated controls was 1.0 whereas yeast illuminated in presence of rose bengal showed an R.Q. of 0.4, indicating a great excess of oxygen consumed over the carbon dioxide produced. Proof that such oxidations are extraneous to life was demonstrated by boiling yeast and exposing suspensions of sensitized dead cells to light. The data in figure 1 show that the dead cells in rose bengal solution consume oxygen when illuminated, although this consumption stops when illumination ceases. Comparison (fig. 1, table 2) of the oxygen consumption of living and dead yeast illuminated in presence of rose bengal reveals certain differences: (1)

[3] Wohlgemuth and Szorenyi ('33) found R. Q. values as low as 0.04 for erythrocytes undergoing photodynamic oxidation. This represents a much more striking oxygen consumption than that observed in yeast. Analyses of erythrocytes and yeast indicate more protein in the former than in the latter. Since protein is the main material of cells which is photooxidized (Kosman and Lillie, '35; Smetana, '38) this difference is probably accounted for in this manner.

living cells consume more oxygen than the dead, which is to be expected since the normal cell respiration is added to the purely photochemical oxidation; (2) the curves differ initially in that the oxygen consumption of the dead cells rises sharply as soon as irradiation starts, in contrast to the much slower uptake of oxygen by the living cells. The delay in photo-

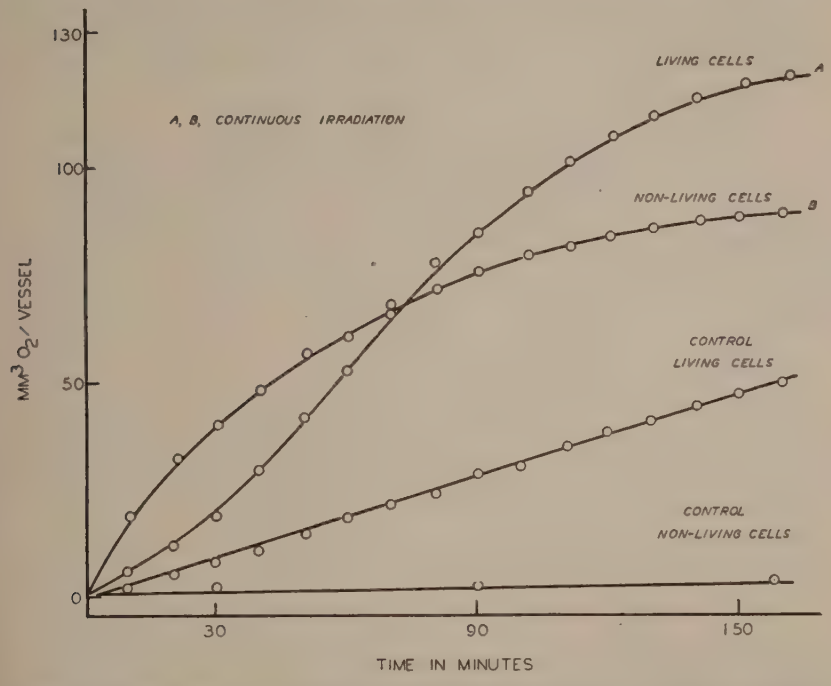

Fig. 1 Comparison of effects of photochemical oxidation between living and boiled cells. Note initial delay of oxygen uptake in the living cells. The cells are under continuous irradiation.

oxidation on the part of the living cells might be due to the existence of a barrier which is not very susceptible to photodynamic action and prevents the dye from getting to the more susceptible materials inside the cell.

Table 2 allows a quantitative comparison to be made between the photochemical oxidation of living and non-living cells. The length of time necessary to accomplish penetration

of the membrane of the intact cells by the dye might possibly be indicated by the time when the difference in oxygen uptake between living and dead cells reaches a maximum; this appears to be about 50 minutes.

To test whether dye penetrates into untreated cells a few yeast suspensions were kept in the dark for periods of 48 hours at the same pH and dye concentration usually used in the experiments. Microscopic examination of such suspensions indicated the absence of dye in the protoplasm of almost

TABLE 1

Respiratory quotients for yeast during and following irradiation

	DURING IRRADIATION (AT 40 MINUTES)		FOLLOWING IRRADIATION (30 MINUTES)	
	Endogenous	Exogenous [1]	Endogenous	Exogenous
Control	1.0	1.8	1.0	2.0
Treated	0.4	0.8	0.9	1.2

Figures reported are averages of two experiments.

[1] The exogenous R.Q. of this strain is usually over 1.0 due to aerobic fermentation which is fairly extensive (see table 5). Such values have been found by others (Swanson and Clifford, '48). Note that photooxidation occurs during illumination in rose bengal solution of yeast supplied with glucose as indicated by the great drop in R.Q. from 1.8 to 0.8.

The failure of such photooxidations to show up in figure 4 exogenous irradiated is thus due to the compensatory decrease in respiration resulting from photodynamic injury.

all the cells.[4] Only the occasional dead cells which occur in any population of cells accumulated dye and were deeply stained. The results indicate that untreated healthy cells are not stained by rose bengal. If the cells were boiled for a few minutes all of them were stained showing that dead cells allow ready penetration and accumulation of dye. After prolonged illumination in rose bengal solution (over 50 minutes) unboiled cells were also all stained, indicating that the barrier to dye penetration and accumulation had also been removed

[4] Possibly dye cannot be seen within the cell because it changes color. Since the fluorescein dyes are not redox dyes nor do they change color wih pH, this seems unlikely.

in the cells killed by photodynamic action. It is possible that dye penetrates gradually when the cells are illuminated. To test this, yeast suspensions were illuminated for consecutively increasing time periods and examined microscopically; the oxygen consumption was measured at the same times. Table 3 correlates rate of oxygen uptake with the visibility of dye within the yeast, readings being taken at 10-minute intervals for 60 minutes of irradiation.

TABLE 2

Comparison of photochemical oxygen uptakes between living and non-living sensitized cells during 160 minutes of continuous irradiation. Figures reported are mm³ O_2/vessel

MIN. OF IRRAD.	LIVING CELLS	NON-LIVING CELLS	DIFFERENCE BETWEEN LIVING AND NON-LIVING CELLS
	Irrad. minus control [1]	Irrad. (control zero)	
20	6.0	33.0	27.0
30	11.2	40.0	28.8
40	18.8	48.0	29.2
50	24.2	57.0	32.8
60	33.4	60.0	26.6
70	45.0	66.0	21.0
80	54.0	72.0	18.0
90	58.0	76.0	18.0
120	68.0	87.0	17.4
160	80.0	97.0	17.2

[1] To rule out normal respiration of living cells.
Average of data from two experiments.

The number of visibly stained cells present during the first 30 minutes of irradiation is approximately the same as that found in unirradiated samples. One of the points demonstrated in table 3 is the fact that although the number of stained cells does not increase significantly in 30 minutes, the rate of oxygen consumption of the irradiated sample is nearly twice that of the controls. This could mean that (1) photodynamic action during the first 30 minutes is confined to the surface or near the surface of the cell or (2) it could mean that the dye has entered the cells but cannot be seen

because it is present in too low an overall concentration.[5] Since most of the photooxidizable material present in the cell is oxidized by this time (table 2), the second possibility is the more likely one. The progressive oxidation of cell substances might conceivably provide the very means for such movement of the dye into the cell. If this is so, dye uptake by cells that have been irradiated in the presence of dye should be demonstrable even if the dye is not visible in the cells by microscopic examination. This was tested by meas-

TABLE 3

Correlation of rate of photochemical oxygen consumption of sensitized living cells during irradiation with the presence of the dye, rose bengal, diffused throughout the cytoplasm. Counts are number of cells/cm³. Oxygen consumption is mm³/vessel

MIN. OF IRRAD.	DYE NOT VISIBLE		DYE VISIBLE		RATE OF O_2 CONSUMPTION	
	Control	Irrad.	Control	Irrad.	Control	Irrad.
0	3.2×10^7	..	6.2×10^5	..	0	..
10		2.6×10^7		6.0×10^6	3.3	7.5
20		2.7×10^7		6.6×10^6	3.2	5.5
30		2.6×10^7		6.8×10^6	3.5	6.3
40		2.6×10^7		7.0×10^6	3.7	10.4
50		1.5×10^7		1.7×10^7	3.3	12.0
60	3.1×10^7	0	5.8×10^5	2.9×10^7	3.4	11.0

Average of 3 counts.

uring the loss of dye from a dye solution in contact with yeast in one case kept in the dark, in the other illuminated for 10 minutes. The cells were then centrifuged off and the absorption spectrum of the supernatant dye solution was determined with a Beckman spectrophotometer. The decrease in density of the dye solution shown in figure 2 indicates that dye has been removed from the solution.

To determine whether the dye so taken up by yeast was firmly bound in the cells or only weakly held, yeast cells in contact with dye which had been illuminated in one case and

[5] See footnote 4, page 306.

kept in the dark in the other were centrifuged and washed in fresh buffer several times in succession until the supernatant was entirely free of the color of the dye. The cells were now resuspended in dye-free buffer solution and illuminated continuously for 90 minutes. The results in figure 3 show that photooxidation occurred in cells which had previ-

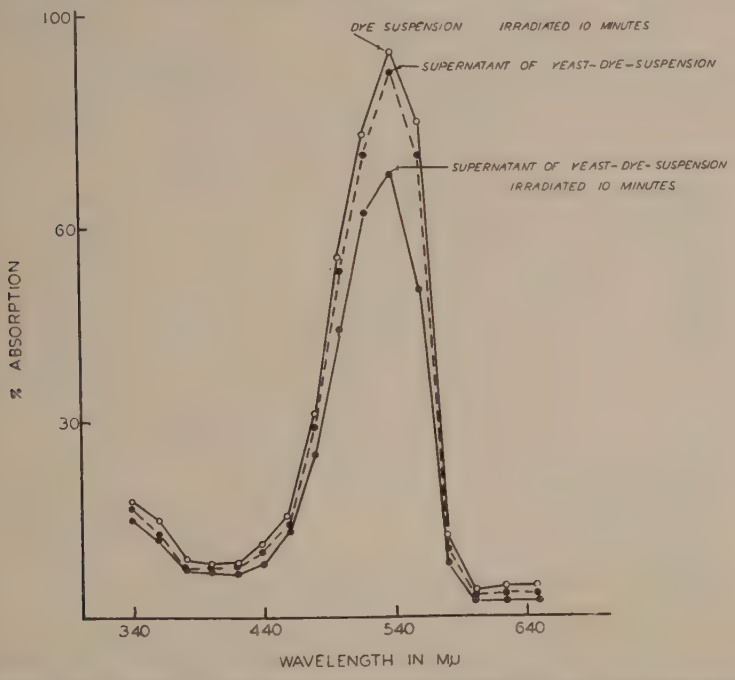

Fig. 2 The effect of a 10-minute irradiation period on the absorption spectrum of a yeast-dye suspension compared to a similar suspension kept in the dark. Only the supernatants have been tested. The dye is a 1/5000 dilution of rose bengal.

ously been in contact with dye in the light, even though they had been thoroughly washed. No photooxidation occurred in cells which had been in contact with dye in the dark and washed. It is evident that the dye had been bound in the yeast as a result of illumination in presence of dye and that the degree of binding depended on the extent of such illumination, those exposed to light for 5 minutes showing much less photo-

oxidation and so presumably having much less dye than those exposed for 20 minutes.

The experiments performed thus far tell us only that the dye has been taken up but do not tell us where the dye is located and where it acts — whether at the surface or deeper in the cell — since the dye cannot be seen in the cells. We

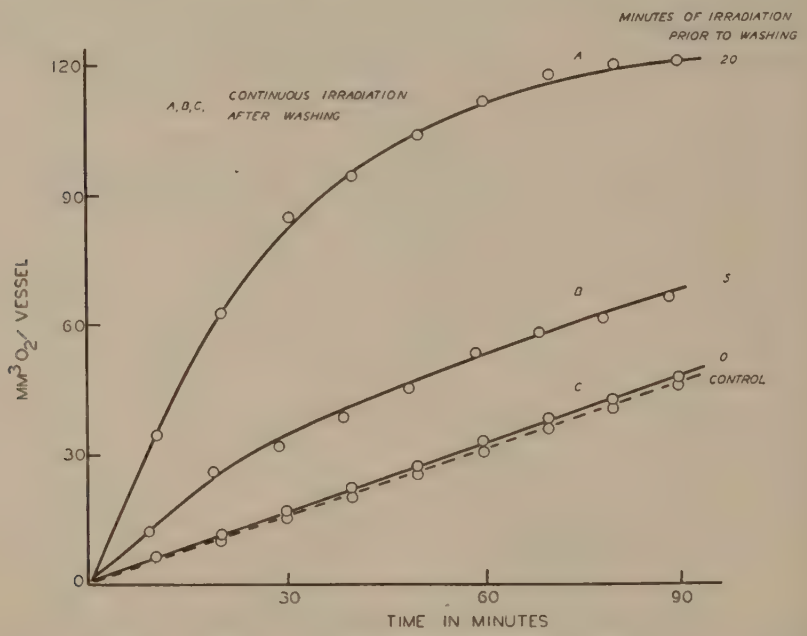

Fig. 3 Effect of light in producing an irreversible uptake of dye by cells. The cells were first irradiated in rose bengal suspension, then washed until the supernatant was clear. Finally, they were resuspended in a dye-free buffer and re-irradiated continuously.

must therefore locate the dye by its action on the cell. If the dye penetrates into the cell and reaches enzymes within the cytoplasm, illumination should reduce the respiration of yeast so exposed. Thirty minutes' exposure to light of yeast in a solution of rose bengal did not significantly affect the endogenous respiration of yeast, 60 mm^3 of oxygen being consumed per hour per vessel in both experimental and control. However this does not constitute a fair test of our

hypothesis since the "idling" respiration of endogenous metabolism requires only a small fraction of the battery of enzymes present in the yeast cell. It is necessary to saturate the enzymes with substrate to determine whether the photosensitized cells possess fewer active enzyme molecules than the controls. The data in figures 4 and 5 bear this out and show that the reduction in oxygen consumption is proportional

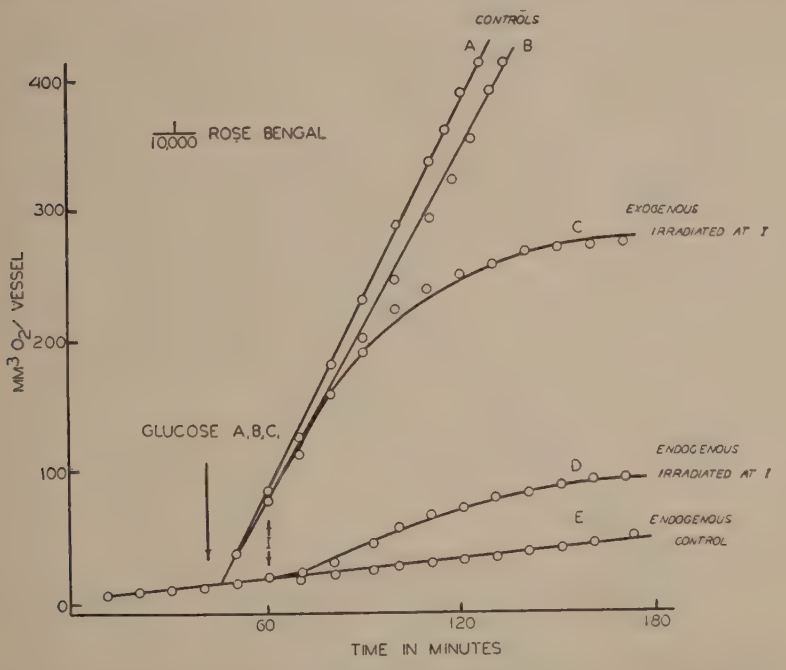

Fig. 4 Comparison of the effects of photodynamic action on exogenous and endogenous respiration of cells while they are being continuously irradiated.

to exposure of the yeast to light in presence of rose bengal. A 50-minute dosage reduced respiration to zero; this correlates well with the visible presence of dye in the cytoplasm (table 2). Such an exposure appears to have destroyed all labile materials in the cell including the enzymes.

To extend the information on the change in metabolism of yeast following photodynamic sensitization, the utilization of ethyl alcohol and acetate after illumination in presence of

rose bengal was compared to controls and the data are given in figure 6. It is evident that the respiration is decreased to the same extent for all three substrates by a given photodynamic exposure.

Not merely the respiration but also the uptake of sugar is affected by photodynamic action as shown by determinations

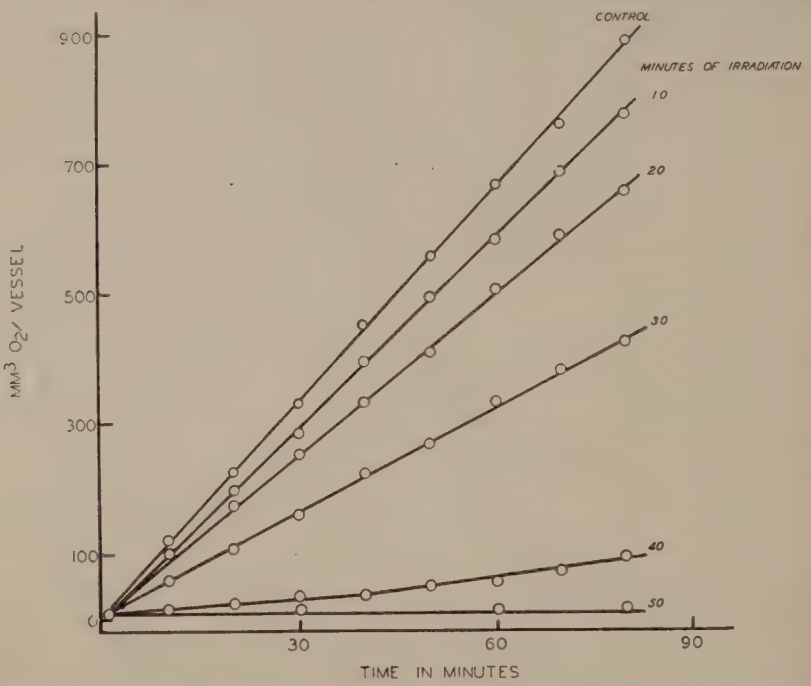

Fig. 5 Effect of photodynamic action on cells carrying on endogenous respiration. The sensitized cells were irradiated previous to the respiration determinations.

of the glucose present in the medium after the treated cells had been centrifuged off (table 4). The aerobic fermentation is similarly decreased in the exposed cells as shown by analyses for alcohol of the supernatant medium from exposed cells. The data are given in table 5. The data in tables 4 and 5 show that a proportionality exists between glucose taken up and alcohol produced. Since uptake of glucose, fermentation and respiration are all affected by photodynamic action, one

might predict that reproduction would be similarly affected. Counts from a series of 4 plates given in table 6 show that reproduction was considerably reduced.

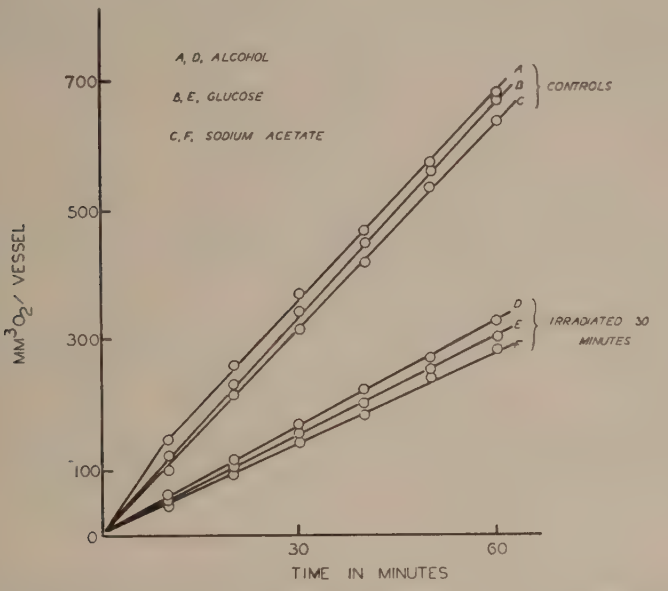

Fig. 6 Effect of photodynamic action on the use of various metabolites. The sensitized cells were irradiated previous to the respiration determination. The concentration of each metabolite is 2%.

TABLE 4

Photodynamic effects on the ability of yeast to remove carbohydrate from the medium. Yeast irradiated and shaken for 30 minutes. Two milligrams of glucose added per cubic centimeter of yeast suspension. Figures reported are milligrams of glucose remaining in 1 cm³ of supernatant

EXPERIMENT	CONTROL	IRRADIATED
1	0.75	1.71
2	0.84	1.80
3	0.41	1.01

By the use of radioactive acetate[6] an attempt was next made to determine the amount of acetate which enters photodynamically sensitized cells as compared to controls. The

[6] The authors are indebted to Drs. E. L. Tatum and R. Ottke for making available their equipment for tracer studies and for help in its operation.

TABLE 5

Photodynamic effects on the ability of yeast to produce alcohol. Samples used are those remaining from the determinations for carbohydrate. All figures reported are in milligrams of alcohol contained in 1 cm³ of supernatant

EXPERIMENT	CONTROL	IRRADIATED
1	0.53	0.03
2	0.56	0.03
3	0.81	0.01

TABLE 6

Four-plate dilution counts on yeast given glucose before and following a 30-minute irradiation period. Plates examined for colonies at end of 48 hours. Figures reported are cells/cm³

YEAST GIVEN GLUCOSE BEFORE IRRADIATION [1]		YEAST GIVEN GLUCOSE FOLLOWING IRRADIATION	
Control	Irradiated	Control	Irradiated
2.5×10^7	1.6×10^7	2.8×10^7	8×10^6

[1] Yeast allowed one hour in 6% glucose then removed, washed free of original medium, and resuspended in a glucose-free buffer solution. Each count is the average of two plates per dilution.

TABLE 7

The uptake of 1% radioactive sodium acetate by cells subjected to photodynamic action compared with the uptake by cells poisoned with sodium azide. Figures reported are disintegrations $\times 10^3$/16 mg yeast/min.

EXP.	SAMPLE	CONTROL	IRRAD. (30 MIN.)	CONTROL	NaN_3 (0.015 M.)
I					
	1a	8.1	2.9	6.8	3.7
	1b	7.0	2.4	6.6	3.3
II					
	2a	6.9	2.7	6.8	3.8
	2b	7.3	2.8	7.5	4.2
Average of both exp.		7.3	2.8	6.6	3.6

All figures reported are the average of two counts per sample. Each sample was first placed in a Warburg vessel and respiration determined for 60 minutes (see fig. 7 for example). The average weight per sample was 16 mg of yeast (dry weight) per vessel. Two-tenths cubic centimeter of 1% sodium acetate containing 2.1×10^4d/min. radioactivity was added per vessel.

results gven in table 7 show that the sensitized cells possessed much less of the labelled acetate than the controls. This could be due to failure to enter or to the lesser utilization of the acetate because of injury to the enzymes of the photosensitized cell. Circumstantial evidence that the latter is

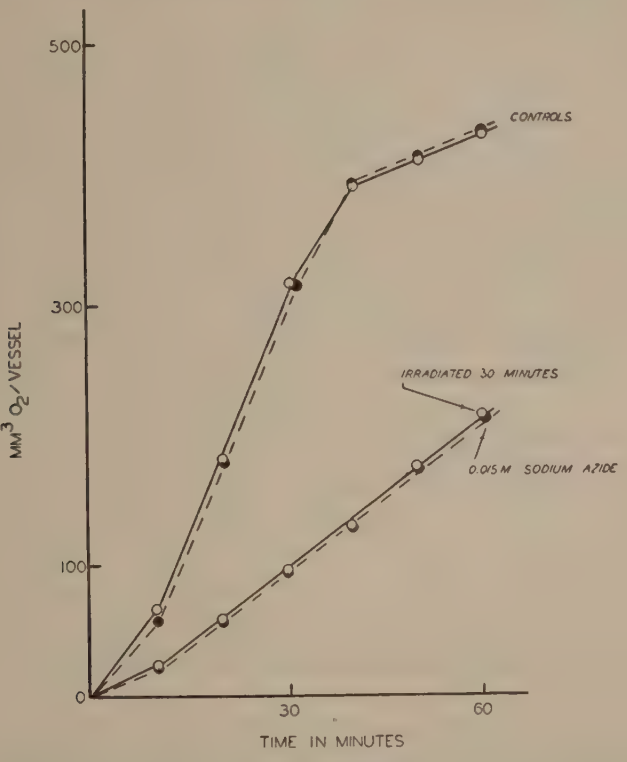

Fig. 7 Comparison of the effects of photodynamic action with poisoning by sodium azide on exogenous respiration of cells. The metabolite is 1% radioactive sodium acetate. Irradiation and poison added prior to respiration determinations.

the more likely possibility was obtained by studying the effect of sodium azide on the presence of acetate within the cells. Azide affects cytochrome oxidase activity, along with that of other enzymes, but it is not known to affect the permeability of cells. Uptake of radioactive acetate was followed to see if it was reduced in correspondence to the reduction in the

respiration. A concentration of 0.015 M azide was found to reduce the respiration of the yeast suspension to a degree comparable to the reduction produced by a 30-minute exposure to light in the presence of dye. Ten minutes after the addition of azide the radioactive sodium acetate was added. Figure 7 shows that the inhibition of acetate respiration by sodium azide parallels that brought about by photodynamic action.

DISCUSSION

Some investigators working with fluorescein dyes have reported results which could be adequately explained by photodynamic action confined to the cell's surface, e.g., the activation of marine eggs (Lillie and Hinrichs, '23) and the progressive leakage of potassium ions through the membrane of red blood cells (Davson and Ponder, '40). On the other hand a number of experiments previously reported suggest action deep within the cell, e.g., the breakdown of the germinal vesicle in *Nereis* (Alsup, '41); the alteration of the viscosity of *Ameba* (Alsup, '42); the sensitization of paramecia to heat (Giese and Crossman, '46); the effects on mitosis in tissue culture (Lewis, '45); the production of mutations in *Neurospora* (Doring, '49) and *Bacillus prodigiosum* (Kaplan, '50).

For the sake of argument let us assume that photodynamic action is confined to the cell membrane. What difficulties do we encounter in interpreting our results and those of others? We might say that the decreased respiration of yeast on glucose, alcohol and acetate reported here is due to blockage of entry of these materials by photodynamic injury at the cell membrane. Entry of glucose into the yeast cell is thought to require the action of surface phosphorylases (LeFevre, '47, '48; Barron *et al.*, '48; Rothstein, '48, '51), but no enzymes have been postulated for acetate or alcohol entry. Alcohol enters most cells readily (Collander and Bärlund, '33), certainly more rapidly than glucose in general. It is therefore difficult to see how photodynamic alteration of the membrane would decrease to the same degree the entry of all three materials. Furthermore it is difficult to postulate

decreased permeability resulting from photodynamic action when data to the contrary are available for red blood cells (Davson and Ponder, '40) and for yeast (preliminary studies with the flame photometer performed here), indicating increased permeability to salts after photodynamic action. It strains the imagination to develop a theory to explain photodynamic effects on viscosity, heat sensitivity, nuclear and mitotic changes, decreased rate of cell division and mutations on the basis of a change in cellular permeability by the photosensitized reactions at the surface of the cell only.

However, it is probable that a photodynamic dye such as rose bengal begins its action at the surface forming a reversible union with the cell as shown by spectrophotometric measurements on red blood cells (Gilbert and Blum, '42). Similar results were obtained here with yeast. This union is independent of the time of immersion in the dye since the yeast can be washed completely free of the dye after several hours. However illumination of the yeast in dye solution changes the relationship between the yeast and dye. When cells so illuminated are centrifuged down they contain a small amount of dye which will not come out even in several washes of fresh buffer solutions. Illumination of such washed yeast cells suspended in fresh buffer solutions resulted in photodynamic oxidation as if all the dye necessary to produce a photochemical effect had been taken up in the previous 20 minutes of illumination in dye solution.

The experiments on yeast further suggest that the dye is not permanently fixed but migrates into the protoplasm with continued illumination. The most direct evidence for this is the fact that the amount of photooxidation of the cells under continued illumination is the same whether the cells are killed by boiling (allowing the dye to penetrate freely as shown by deep staining), whether they are disrupted by passage through a needle valve under high pressure,[7] or whether they are intact. The oxidation occurs immediately in the boiled or

[7] The authors are indebted to Drs. S. French and H. Milner of the Carnegie Laboratory for permitting the use of equipment and helping in its operation.

disrupted cells and only after a lag in intact cells, but to about the same degree in all three cases. The delay in appearance of the photooxidation in intact cells suggests that a barrier has to be passed before the oxidizable materials can be reached; this delay may represent the time required for the dye to pass through the cell membrane. This barrier may be the lipid in the cell membrane (Parpart and Dziemian, '39) since lipids are not very susceptible to photodynamic action (Kosman and Lillie, '35; Smetana, '38). Oxygen consumption would then be expected to rise only after the dye penetrates and comes in contact with a larger amount of photodynamically oxidizable substrate deeper in the cell. The main oxidizable materials in the cell are probably proteins since the other cellular constituents are not photooxidized to a significant extent.

It seems exceedingly unlikely that the same amount of photooxidation could occur in the dead or disrupted cells as in intact cells if in the latter the reaction were confined to the surface of the cell only. Yet even when the photooxidation is pretty well completed (30 minutes) the dye is still not visible inside the cells under the microscope (even under a fluorescence microscope). We are forced to conclude that some dye is present inside the cell but in quantities too small to be seen. This fits in with the calculations of the minimal amounts of dye necessary to cause photodynamic effects. The minimal amount is less than enough to form a monomolecular layer on the surface of the cell (Blum and Hyman, '39; Ponder, '39). Such a small amount of dye moving inwards during illumination would hardly be visible. Previous calculations indicate that the same dye molecule oxidizes many molecules of substrate (Blum, '32), in other words it has a definite turnover value which is different for the various dyes, but large for rose bengal. The final deep staining of the protoplasm of the intact cell exposed to photodynamic action for a long time is therefore an after-effect on a moribund protoplasm and of no particular significance to photodynamic action.

If the above interpretation of the facts is correct, we have the clue to interpreting both surface and deep effects of photodynamic action. The first effect of a dye such as rose bengal (or any other of the fluorescein series) to which cells are relatively impermeable under the conditions of testing, would be at the surface of the cell. Therefore surface effects would be observed such as activation of a marine egg (Lillie and Hinrichs, '23) or changes in the permeability of the cell (Davson and Ponder, '40). However, while surface changes are occurring, the dye is also penetrating and affecting other parts of the cell. It may alter the cytoplasmic proteins changing the viscosity (Alsup, '42) and the heat sensitivity (Giese and Crossman, '46) or the nuclear constituents directly or indirectly leading to mitotic effects (Lewis, '45) or genetic effects (Doring, '49; Kaplan, '50). Enzymes inside the cell are affected by the entering dye and respiration of various substrates such as glucose, alcohol and acetate herein tested is decreased after irradiation. Fermentation is also decreased and sugar is less readily taken up and stored in the cells. Yeast might also reproduce less readily when affected by photodynamic action because of destruction of enzymes necessary for growth and division.

In summary, photodynamic action of rose bengal [8] on yeast appears to begin at the surface and to work inwards, affecting in apparently non-selective fashion, the various functions of the cell. Since the material in cells photooxidized seems to be primarily protein (Kosman and Lillie, '35; Smetana, '38), the non-selective nature of the effect is hardly surprising, since all of the vital activities of the cell probably involve proteins.

SUMMARY

1. The effects of photodynamic action on yeast both during and following irradiation were studied. The major features investigated were the photochemical oxidation, effects on endogenous and exogenous respiration, mechanism of dye uptake,

[8] See footnote 2, page 301.

site of dye action within the cell, and effects of photodynamic action on use of various metabolites.

2. Living and non-living cells show similar photooxidation except for less oxygen consumption by the living cells during the first 20 minutes of irradiation.

3. Light is instrumental in producing an irreversible binding between cell and dye. The amount of dye taken up by the cell is proportional to the light exposure.

4. Following 30 minutes of irradiation of yeast in dye, the dye is not visible within the cell, yet oxygen consumption at the time is nearly twice that of the control.

5. Photodynamic action on cells during irradiation reduces their exogenous respiration below that of the controls.

6. The endogenous and exogenous respiratory quotients ($\frac{CO_2}{O_2}$)of cells undergoing irradiation are significantly below those of the controls, indicating photooxidations using oxygen but not liberating carbon dioxide.

7. The endogenous respiratory quotient of cells following irradiation approaches that of the controls but the exogenous respiratory quotient is significantly below that of the controls, indicating a change in metabolism, possibly a reduction in aerobic fermentation.

8. Uptake of glucose is hampered by photodynamic action, resulting in a proportional decrease in alcohol formation.

9. Photodynamic effects on cells following irradiation reduce their exogenous respiration in proportion to the dosage of light to which they were exposed.

10. Starved cells demonstrate a greater degree of sensitivity to photodynamic action in ability to form colonies than cells with stored reserves.

11. The use of glucose, ethyl alcohol, and sodium acetate in respiration is similarly decreased by photodynamic action.

12. The uptake of radioactive acetate by cells affected by photodynamic action is reduced as it is also by addition of sodium azide.

13. The results are discussed especially with reference to possible mechanisms of action for the phenomena observed.

LITERATURE CITED

ALDOUS, J. G., J. FISHER AND J. STERN 1950 The respiration of yeast at different concentrations of glucose. J. Cell. and Comp. Physiol., *35:* 303.

ALSUP, F. W. 1941 Photodynamic action in the eggs of *Nereis limbata.* J. Cell. and Comp. Physiol., *17:* 117.

———— 1942 The effect of light alone and photodynamic action on the relative viscosity of amoeba protoplasm. Physiol. Zool., *15:* 168.

BARRON, E. S., J. A. MUNTZ AND B. GASVODA 1948 Regulatory mechanisms of cellular respiration. I. The role of cell membranes: uranium inhibition of cellular respiration. J. Gen. Physiol., *32:* 163.

BECK, L. W., AND A. C. NICHOLS 1937 Action of fluorescent dyes on *Paramecium* as affected by pH. J. Cell. and Comp. Physiol., *10:* 123.

BLUM, H. F. 1932 Photodynamic action. Physiol. Rev., *12:* 23.

———— 1941 Photodynamic action and diseases caused by light. Reinhold Publishing Corp., New York.

BLUM, H. F., AND C. HYMAN 1939 Photodynamic hemolysis. V. The effect of concentration of dye on hemolysis time. J. Cell. and Comp. Physiol., *13:* 287.

CALVIN, M., C. HEIDELBERGER, J. REID, B. TOLBERT AND P. YANKWICH 1949 Isotopic carbon. J. Wiley and Sons, Inc., New York.

CELLANDER, R., AND H. BÄRLUND 1933 Permeabilitätsstudien an Chara ceratophylla. II. Die Permeabilität für Nichtelektrolyte. Acta. Bot. Fennica, *11:* 1.

DAVSON, H., AND E. PONDER 1940 Photodynamically induced cation permeability and its relation to hemolysis. J. Cell. and Comp. Physiol., *15:* 67.

DIXON, M. 1934 Manometric methods. Cambridge University Press.

DORING, H. 1938 Photosensibilisurung der Gene? Die Naturwissenschaften, *26:* 819.

GIBSON, J. G., AND H. BLOTNER 1938 The determination of ethyl alcohol in blood and urine with a photoelectric colorimeter. J. Biol. Chem., *126:* 551.

GIESE, A. C., AND E. CROSSMAN 1946 Sensitization of cells to heat by visible light in presence of photodynamic dyes. J. Gen. Physiol., *29:* 193.

GILBERT, H., AND H. F. BLUM 1942 The mechanism of uptake of the dye, rose bengal, by the red cell. J. Cell. and Comp. Physiol., *19:* 257.

KAPLAN, V. 1950 Mutationsforschung an Bakterien. Die Naturwissenschaften, *11:* 249.

KOSMAN, A. J., AND R. S. LILLIE 1935 Photodynamically induced oxygen consumption in muscle and nerve. J. Cell. and Comp. Physiol., *6:* 505.

LEFEVRE, P. G. 1947 Evidence of active transfer across the human erythrocyte membrane. Biol. Bull., *93:* 224.

———— 1948 Evidence of active transfer of certain non-electrolytes across the human red cell. J. Gen. Physiol., *31:* 505.

LEWIS, M. R. 1945 The injurious effect of light on dividing cells in tissue cultures containing fluorescent substances. Anat. Rec., *91:* 191.

LILLIE, R. S., AND M. A. HINRICHS 1923 Activation of starfish and sea urchin eggs by photodynamic action. Anat. Rec. Suppl., *26:* 370.

LONGSWORTH, L. 1936 The estimation of bacterial populations with the aid of a photometric densitometer. J. Bact., *32:* 307.

PARPART, A. K., AND A. J. DZIEMIAN 1940 The chemical composition of the red cell membrane. Symp. on Quant. Biol., *8:* 17.

PONDER, E. 1936 On the spherical form of the mammalian erythrocyte. J. Exp. Biol., *13:* 298.

ROTHSTEIN, A., AND C. LARRABEE 1948 The relationship of the cell surface to metabolism. II. The cell surface of yeast as the site of inhibition of glucose metabolism by uranium. J. Cell. and Comp. Physiol., *32:* 247.

ROTHSTEIN, A., R. MEIER AND L. HURWITZ 1951 The relationship of the cell surface to metabolism. V. The role of uranium complexing loci of yeast in metabolism. J. Cell. and Comp. Physiol., *37:* 57.

SMETANA, H. 1938 Studies on photodynamic action. J. Biol. Chem., *124:* 667.

STILES, H. R., W. H. PETERSEN AND E. B. FRED 1926 A rapid method for the determination of sugar in bacterial cultures. J. Bact., *12:* 427.

SWANSON, W. H., AND C. E. CLIFTON 1948 Growth and assimilation in cultures of *Saccharomyces cereviseae.* J. Bact., *56:* 115.

UMBREIT, W. W., R. H. BURNS AND J. F. STAUFFER 1945 Manometric techniques and related methods for the study of tissue. Burgess Publishing Co., Minneapolis.

WOHLGEMUTH, J., AND E. SZORENYI 1933 Über die Wirkung des Lichts auf den Chemismus der Zelle. Z. Biochem., *264:* 371.

DIRECT MEMBRANE RESTING AND ACTION POTENTIALS FROM SINGLE MYELINATED NERVE FIBERS[1, 2]

J. WALTER WOODBURY[3]

Department of Physiology, University of Utah College of Medicine, Salt Lake City

SEVEN FIGURES

INTRODUCTION

The development and perfection of the glass capillary microelectrode for the recording of inside-outside potentials of single muscle cells by Gerard and coworkers (Graham and Gerard, '46; Ling and Gerard, '49) has proved a powerful tool for studying excitable tissues. A microelectrode of tip diameter 0.5 μ or less is inserted transversely across the membrane of a single tissue cell achieving functional isolation without the difficulties of microdissection. Gerard's group made measurements only of the resting potentials of single frog sartorius muscle fibers. Nastuk and Hodgkin ('50) improved the frequency response of the recording apparatus sufficiently to permit the accurate recording of muscle action potentials. More recently recordings of single fiber resting and action potentials have been obtained from frog ventricle by L. A. Woodbury et al. ('50, '51), from dog

[1] This paper is based on material contained in a thesis submitted to the faculty of the University of Utah in partial fulfillment of the requirements for the degree of Doctor of Philosophy. Two copies of the thesis are on file at the University of Utah Library.

[2] The research reported in this paper was supported in part by a grant-in-aid from the U. S. Public Health Service. Preliminary report, 1950, Federation Proceedings, *9:* 139–140.

[3] U. S. Public Health Service Junior Research Fellow, 1947–1950. Present address: Department of Physiology and Biophysics, School of Medicine, University of Washington, Seattle 5.

Purkinje tissue by Coraboeuf and Weidmann ('49), from embryonic chick heart by Fingl et al. ('51), from cat auricle by Burgen and Terroux ('51) and from the endplate region of frog muscle by Nastuk ('50) and by Fatt and Katz ('50).

In the present experiments inside-outside resting and action potentials were recorded from single myelinated fibers of frog sciatic nerve. Considerable difficulty was met in obtaining satisfactory records for the following reasons. Firstly, the largest fibers have an axoplasm diameter of only 10 μ. Thus the fiber is likely to be damaged when impaled with a CME (capillary microelectrode). Secondly, the high resistance of the CME (20–100 megohms even when filled with 3 M KCl, Hodgkin and Nastuk, '49) combined with the shunt capacity of the CME to the surrounding medium reduces the frequency response of the circuit below that necessary for the accurate recording of the nerve action potential. Nerve has one advantage over muscle in that the contraction of muscle dislodges the electrode.

A new method for improving the high-frequency response is described. Membrane damage continued to be troublesome but satisfactory records of membrane resting and action potentials were obtained. Also, records from fibers undergoing block by electrode damage gave evidence of saltatory conduction.

METHODS AND MATERIALS

Glass capillary microelectrodes having a tip diameter of about 0.5 μ were drawn according to the method of Ling and Gerard ('49) and filled by immersing them in a solution of 3 M KCl, boiling for one hour and cooling. The use of 3 M KCl was suggested by Hodgkin and Nastuk ('49) to reduce both electrode resistance and junction potential. In use the CME is immersed in about 2 mm of the Ringer's solution in which the nerve trunk is bathed (fig. 1). The resistance of the electrode and the capacity between the internal and external conducting media make the CME, electrically, a continuous resistance-capacitance transmission line

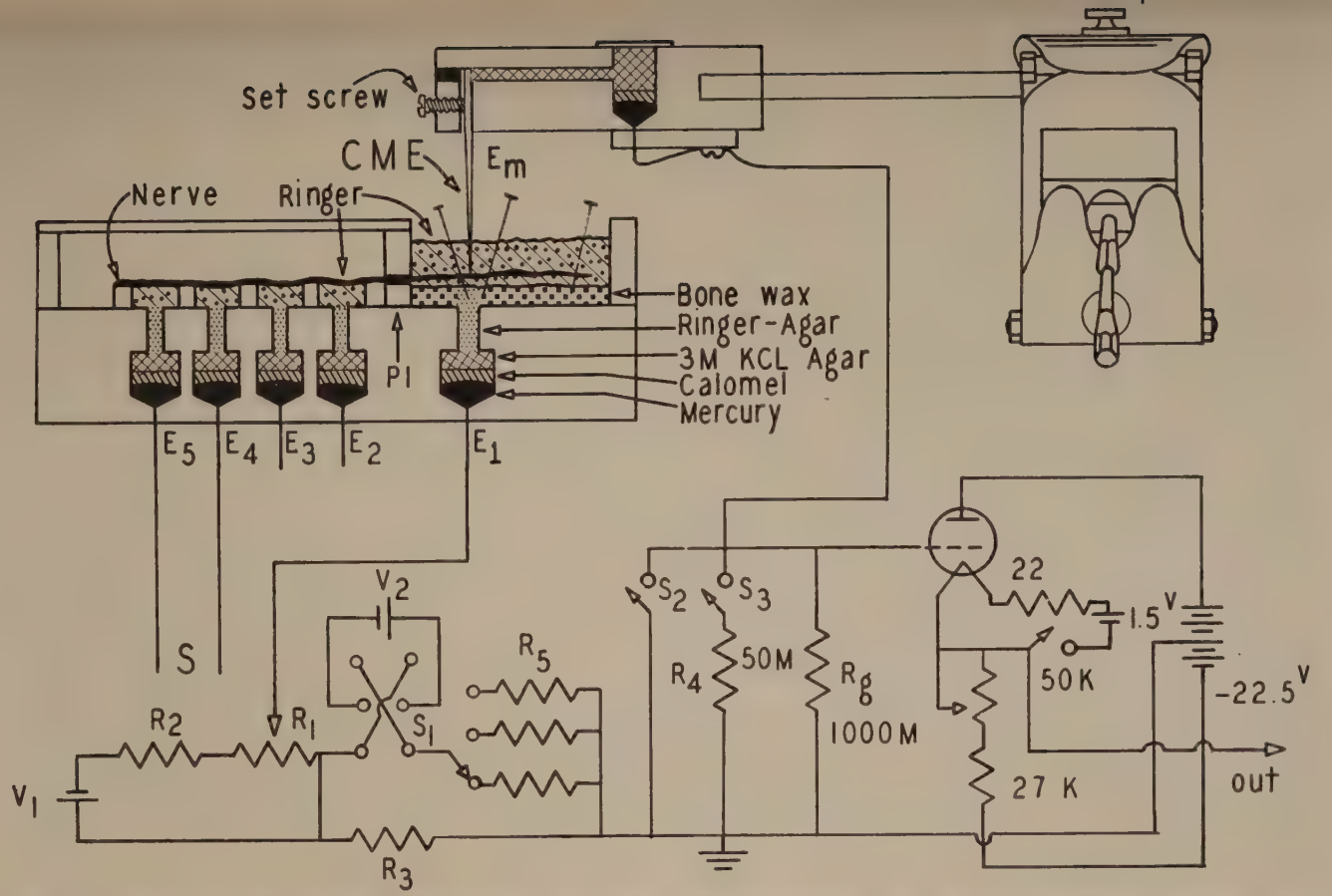

Fig. 1 Diagram of nerve chamber, microelectrode and holder, micromanipulator, and input and calibrating circuits. CME, capillary microelectrode; Pl, plastic separator; E, electrode.

which will distort in a definite way any applied potential. Electrode resistance varies from 20 to 100 megohms and is usually about 50 megohms. The capacitance per unit length is about 1 μμf per millimeter.

Figure 2 shows the electrical properties of the CME. The top section (a) represents the terminal 0.5 mm of the electrode immersed in a conducting medium. The taper is drawn approximately to scale. The approximate equivalent electrical circuit of the electrode shown in 2b was obtained by arbitrarily dividing the electrode into 0.1 mm segments and calculating the resistance and capacitance for each segment. The resistances were calculated on the assumptions that the total resistance of the CME is 50 megohms and that the electrode is conical in shape with a slope of 1/66. For the frequencies present in a nerve action potential rising in 0.1 milliseconds or longer the circuit of figure 2b can be closely approximated by the circuit of 2c obtained by combining all the resistances and all the capacitances of 2b. The resultant approximate equivalent circuit can be easily analyzed and the distortion of any applied signal, V_a, calculated. The current produced by V_a through R_e is $(V_a - V_o)/R_e$, where V_o is the measured potential. The current through C_e is $C_e dV_o/dt$. Equating these two currents and rearranging terms:

$$V_a = R_e C_e dV_o/dt + V_o. \qquad (1)$$

Thus the applied voltage is found by adding to the measured voltage the product of the time constant of the input circuit and the time derivative of the measured voltage. In practice, R_e is the total series resistance of the input circuit and C_e is the total shunt capacitance to ground. R_e is generally 25–100 megohms and C_e amounted to 8–10 μμf making the input time constant, T_e, 0.2–1.0 msec.

To the approximations involved in equation (1), within the limitations set by noise and the accuracy with which the operations of the equation can be carried out, the actual potential appearing at the tip of a CME can be found. Rosenblueth et al. ('48) point out that random noise limits the extent of this type of correction and indeed noise was at a

noticeable level in some of these experiments. They give a general expression for correcting the distortion of any amplifier.

Figure 1 shows the arrangement of the nerve chamber, nerve, recording and stimulating electrodes and the input circuit. The shunt resistance of the input stage was 1000 megohms. For $R_c = 50$ megohms, 95% of the d-c signal

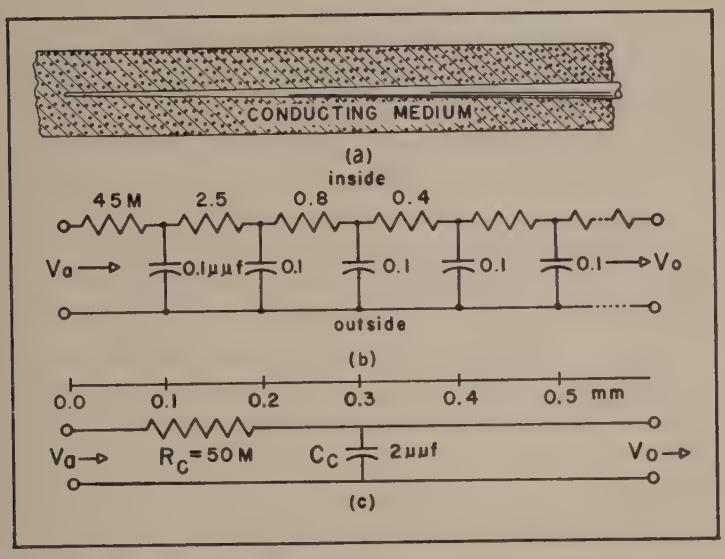

Fig. 2 Electrical properties of the CME: (a) Scale drawing of microelectrode tip in a conducting medium. (b) Approximate equilavent electrical circuit of the CME drawn to the same scale. (c) Above, scale for (a) and (b), below, simple equivalent circuit obtained by lumping resistances and capacitances of (b). See text for explanation.

appears at the grid of the input vacuum tube, an electrometer triode operated as a cathode follower. The circuit V_1, R_1, R_2 is used to balance electrode potential variations. Circuit V_2, S_1, R_3, R_5 is used to apply a known potential across R_3 giving a measure of the sensitivity. Since the calibrating potential is divided between the microelectrode resistance and the grid resistance in the same manner as the input signal, variations in electrode resistance are compensated for when calibrating. Rectangular pulses can also be applied across R_3 to obtain

an estimate of the high frequency response of the amplifier (see below). Switch S_2 can be closed momentarily to give the baseline or zero reading while the electrode is impaled. Closing it briefly had no detectable effect on the measured potential. Switch S_3 and resistance R_4 in conjunction with the calibrating voltage can be used to estimate the resistance of the CME.

The output from the input electrometer was fed to a direct-coupled amplifier and amplified to a level of about one volt. After a mixer, the signal was directly coupled to the Y-axis amplifier of a cathode ray oscilloscope.

In their work on frog muscle resting and action potentials, Nastuk and Hodgkin ('50) used a unity gain cathode follower input stage with a microelectrode lead shield connected to the cathode. This maneuver reduces the input capacity to about 1.5 μμf which with the capacity of 2 μμf between the electrode and the medium gives an input time constant of about 75 microseconds. This time constant is too great to permit the distortionless recording of an action potential rising in 0.15 to 0.2 msec. Since a time constant of 75 microseconds is too long and since there is little possibility of improving the performance of the unity gain cathode follower type of circuit it becomes necessary to resort to other methods to obtain an adequate high-frequency response. Equation (1) indicates the way in which this can be done. While a combination of the cathode follower and direct correction techniques would probably be best, in the experiments described here no attempt was made to reduce input capacitance except by the exercise of due care in the placing of components.

Since all the operations that occur on the right hand side of equation (1), differentiation, multiplication by a constant and addition can easily be performed electronically, it appeared feasible to make the corrections in this manner and thus present a true picture of the action potential on the screen of the cathode ray oscilloscope. This proved possible and this technique was used throughout these experiments. It is both more rapid and more accurate than any graphical

means of making the required corrections. The output from the d-c amplifier was differentiated, amplified and added to the direct amplifier output in a mixer stage. Differentiation was approximated by the voltage across the resistor of a resistance-capacitance circuit of time constant, $T_d = 35$ microseconds. Analysis of the overall compensating circuit shows that the half-power frequency after compensation, f_c, is related to the time constant of the differentiator by the equation $f_c = 1/2\ T_d$ providing that the input time constant, $T_c = R_cC_c$ = 200–1000 microseconds, is much larger than T_d which is the case here.

The gain of the differentiation circuit amplifier determines the value of the parameter T_c in the electrical correction circuit. Since electrode resistance is subject to large variations, a simple rapid and accurate method of determining T_c is necessary. That is, a visual indication of T_c on the CRO is needed which can be used to adjust the differentiator gain control to the proper value. An indication of the value of T_c was obtained by applying a square wave across the resistance R_3 of figure 1. The output voltage of the circuit in response to a square wave applied in this manner consists of a jump followed by an exponential rise and a downward jump followed by an exponential decay the time constants of which are the same as the input time constant. If the gain control is adjusted to change the exponential decay into a horizontal line, ignoring the pip caused by differentiating the downward jump, then the proper amount of compensation has been obtained. A square wave applied in this manner and showing the pips caused by differentiating the jump components is shown at the left hand edge of the sweep in figure 4. In this case the gain of the differentiator was about 10% too high as shown by the negative slope of the top of the square wave.

The accuracy of this method of compensation was established in two ways: If a square wave is applied to a circuit equivalent to that of the CME, an exponentially rising and falling curve is obtained with a rise and fall time constant

of 200–1000 microseconds. However, in accordance with expectation, when the amplifier is compensated by the means described above the rise and fall have a time constant of 35 microseconds and the response shows neither overshoot nor undershoot. The validity and accuracy of this method was established in another way by comparing the electronically restored action potential with one restored by graphical computation. This is shown for one action potential in figure 3. Curve c is the action potential obtained without compen-

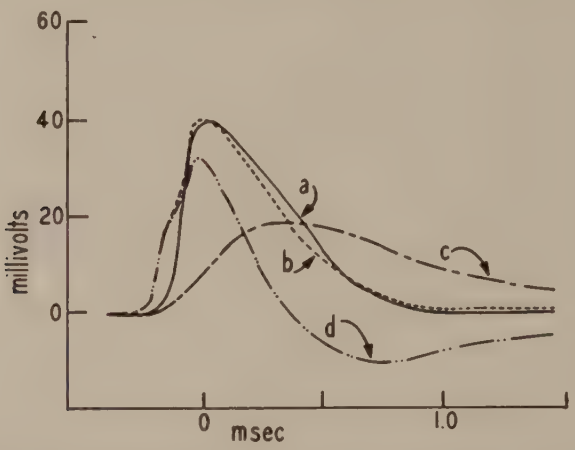

Fig. 3 Comparison of graphical and electrical restorations of the AP distorted by input time constant of 1 msec. Curve c, tracing of uncorrected action potential; d, derivative of c obtained by graphical methods; b, graphically corrected AP obtained by summing curves c and d; a, electrically corrected AP.

sation and curve d the graphical derivative of c. In this case the time constant, T_c, was about 1 msec so the graphically corrected action potential, b, was obtained by adding c and d directly. The electronically corrected potential, a, agrees well with b considering the errors involved in graphical differentiation.

Frog sciatic nerves were dissected out and kept in Ringer's solution for 30 to 60 minutes. The nerve was placed in the chamber and the plastic separator, Pl, figure 1, sealed into place with vaseline. The nerve in the region of E_1 was covered

with Ringer's solution to a depth of about 2 mm to keep it from drying out and to make electrical connection to the CME. The nerve sheath was then split for about 3 mm directly above E_1 and the edges of the split carefully spread apart about 2 mm and fastened down with small pins. The microelectrode was then lowered into the split and the nerve probed until a single fiber was hit. The dissection had no observable effect on the gross action potential. The criterion for impalement was a sudden negative voltage change and the appearance of a positive action potential if the nerve was being stimulated. This sequence of events is good evidence that a single fiber has been impaled. This conclusion is also supported by the following observations. The action potential obtained had a definite threshold, showing alternation when the stimulus strength was just threshold. No action potential was observed at the gain used when the tip of the CME was in the immediate vicinity of the nerve. This is what would be expected when both recording electrodes are at the same region of the nerve.

RESULTS AND DISCUSSION

Measurements of the resting potentials of single nerve fibers varied greatly. Values from 20 to 80 millivolts (mv) were obtained in impalements that met the sudden jump criterion of penetration. Since there was evidence of damage to the fiber in many cases, averaging of all measurements is unwarranted. Moreover, the average value increased as the technique improved. The average of 49 measurements made from January to April, 1950 was 44 mv while the average of 17 measurements made from April to July was 56 mv. The only criteria used in selecting these data were that the jump occur on impalement and that the observed value be greater than 30 mv. The largest value observed, 80 mv, was obtained twice, once from an excitable fiber. All of the values contributing to the 56 mv average were obtained from excitable fibers, as compared with 19 of the 49 observations which gave the 44 mv average. The higher average, 56 mv, agrees well

with Lorente de Nó's ('47) estimate of 52 to 64 mv for the bullfrog sciatic made from measurements of the injury potential. It is considerably lower than the averages given by Huxley and Stämpfli ('50, '51) of 67 and 71 mv measured potentiometrically on isolated motor fibers of the frog.

Measured values of the membrane action potential were somewhat more variable than those of the resting potential. However, there is a statistically significant correlation coefficient (p less than 0.001) of 0.48 between the resting and the action potentials of single fibers. The average value of the action potentials from the 17 fibers that had an average resting potential of 56 mv is 73 mv. Both averages are probably too low, but their ratio, 1.3, is the same as those found for heart muscle by L. A. Woodbury et al. ('50) and striated muscle by Hodgkin and Nastuk ('49). However, in three instances action potentials of 120 mv or greater were observed. One of these, the largest recorded, is shown in figure 4. The resting potential is 63 mv and the action potential is 170 mv. As recorded, the action potential is about 10% too great because the gain of the differentiator circuit was set too high.

Because many factors such as injury can lower the values, it is felt that the highest values are more nearly correct than the obtained average of 73. On the basis of the three observations in which the action potential was 120 mv or greater it is not unreasonable to assume that the "actual" average is 100 to 130 mv. On the same basis the average resting potential is 60 to 80 mv. These maximal values are in good agreement with the averages given by Huxley and Stämpfli ('50, '51). Figure 5 shows two typical resting and action potential records.

In many cases impalement so damages the fiber that conduction past the electrode fails, sometimes immediately, sometimes after many minutes. This failure characteristically occurred in the manner illustrated in figure 6. The successive tracings were taken from photographs made at 5- to 10-second intervals. The first action potential (1) was recorded immediately after impalement with the microelectrode and appears

to be a nearly normal spike. However, in (2) an inflection has appeared in the record about half way up the rising phase with the falling phase only slightly prolonged. In succeeding records the inflection is seen to widen and develop into a

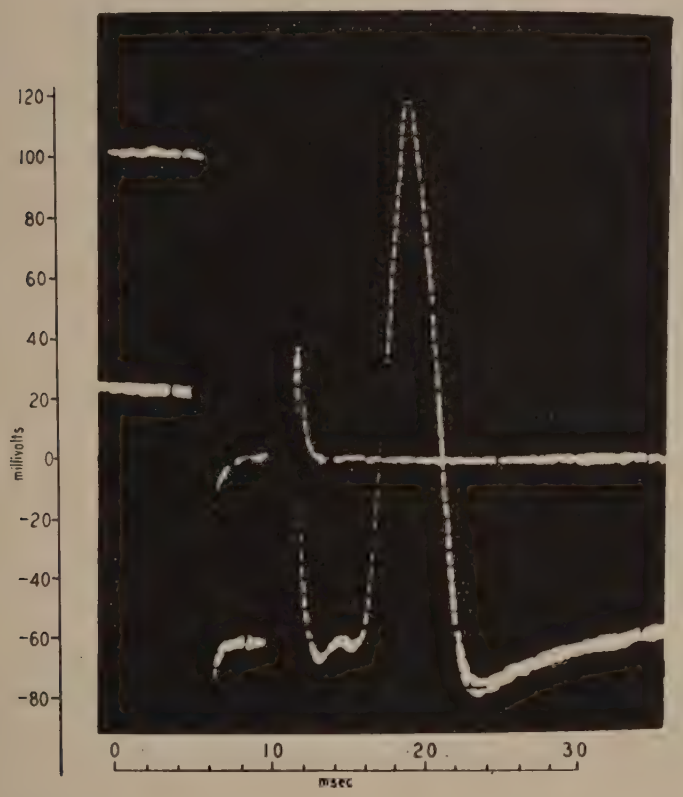

Fig. 4 Largest AP recorded. AP as shown is about 10% too high because of over-correction as shown by negative slope of top of square wave at the left hand edge. Upper 40 mv of AP retouched to increase contrast in light fogged region. RP, 63 and AP, 155 mv.

distinct notch (3, 4). This potential is apparently the sum of two separate similarly shaped spikes and in (5) it is seen that the later one has completely disappeared. All gradations between (1) and (5) were observed and there was considerable variation in the latency of the second spike from

sweep to sweep at the time of (3) and (4) and considerable intermittency was seen before conformation (5) was exclusively obtained.

This behavior is very similar to the behavior of single myelinated nerve fibers blocked by anodal polarization as reported by Erlanger and Gasser but dissimilar to the spontaneous failure at a single node observed by Pfaffmann ('40). The simplest interpretation of the behavior illustrated in figure 6 is that the electrode damaged the fiber sufficiently to block conduction past it. The records interpreted in this way suggest that conduction in noded nerve fibers is saltatory. Three arguments support this conclusion: Firstly, analysis

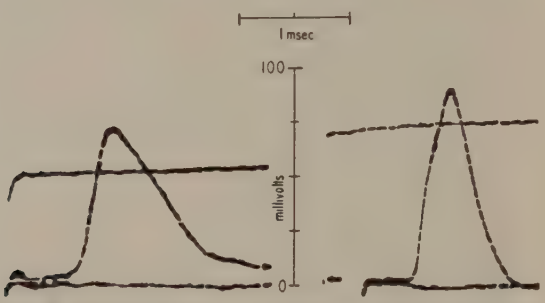

Fig. 5 Typical resting and action potential records.

of figure 6 shows that the amplitudes of the two portions of the action potential remain nearly constant during the course of block. If the region around the electrode were initially excitable and progressively failed over a wider area the amplitudes of both should continuously decrease. On the other hand, if only discrete regions along the fiber were excitable and an injury between two such regions progressively shunted more and more of the exciting current flowing from the distal to the proximal node then the recorded action potential would be expected to behave exactly as shown in figure 6. Secondly, if conduction were continuous, both portions of the failing potential would always be about equal in amplitude, whereas if conduction were saltatory then a wide range of ratios of the amplitudes of the first and second por-

tions would be found depending on the position of the CME relative to the nodes. In these experiments, this ratio varied between one-third and one. Thirdly, since the time course of failure is similar to that recorded externally by Erlanger and Gasser it appears that the axoplasmic and extramedullary currents have the same characteristics — at least during conduction failure.

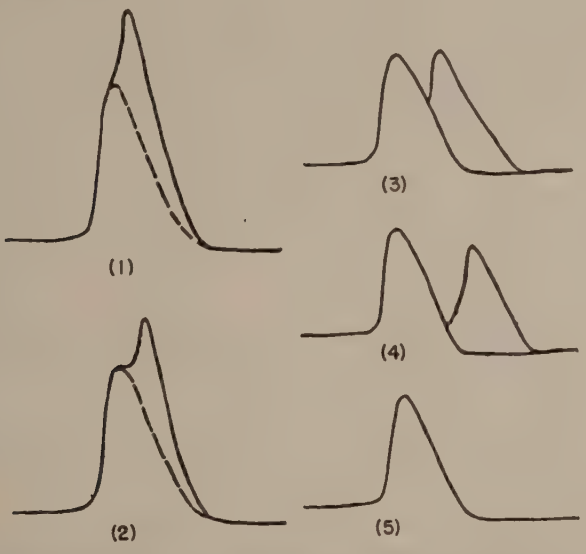

Fig. 6 Tracings showing the progressive loss of excitability at the point of impalement. Five- to 10-second intervals separate successive tracings. See text for explanation.

This indirect evidence sheds some doubt on the belief that the myelin sheath is merely protective and that conduction is a continuous process taking place within the sheath. However, it can be argued that the injury depolarization in the region of the electrode can draw current only from nodes of Ranvier and, therefore, that conduction is saltatory only when injury is present. This evidence affords some confirmation of the results of Huxley and Stämpfli ('49) who have demonstrated saltation in single, isolated myelinated nerve fibers.

Bullock and Turner ('50) have described a similar type of block in giant invertebrate nerve fibers. In their experiments, as expected, the size of the first potential ("a" in their figure 3) decreases and the time delay of the second potential ("b") increases as the region of inexcitability spreads. It would be expected that the size of the "b" potential would also decrease but it does not in their records.

The long time interval (ca. 1 msec) between the two spikes of figures 6 (3) and (4) requires explanation. There are probably two causes of this delay: (1) the long, variable latencies following barely threshold stimulation when the current from the last active proximal node is just sufficient to stimulate the first excitable distal node; and (2) the time necessary for the action current to excite and for the new activity to reach the CME.

The behavior shown in figure 6 suggests a possible explanation of a frequent observation that the recorded action potential is smaller than the measured resting potential. The act of impalement could so damage the fiber that conduction past the CME would be immediately blocked and the final state (5) of figure would be the first condition observed at the stimulation rate of 6 times per second.

Figure 7 shows the response of a single fiber to test shocks given at different intervals after a suprathreshold conditioning shock. As the time interval decreased the action potential showed the characteristic splitting described above, but in this case it was completely reversible by increasing the time delay. The action potential of figure 7 was recorded without change for about one hour despite the damage. However, its small size, about 25 mv, the absence of any resting potential and the greatly increased electrode resistance during the recording period lead to the belief that the CME was in the myelin sheath but had not penetrated into the axoplasm. Similar results were obtained by Huxley and Tasaki ('51) in experiments with the CME on single fibers of the frog.

Conduction velocities were estimated from data obtained by moving the stimulating electrodes. Velocities of 14 to 43

meters per second were observed which is just the range of frog A fibers (Erlanger and Gasser, '37). This velocity range corresponds to fiber diameters of 7 to 22 μ using the results of Tasaki et al. ('43) on frog nerve showing that conduction velocity in m/sec is about twice the fiber diameter in microns. Most of the recordings were made from fibers having velocities of 30 to 40 m/sec.

Combining the data of this experiment with that of many other workers it was found that for the velocity range of 10 to 40 m/sec the equation relating the rise time, t (time in msec to rise from 10 to 90% of peak), to the conduction velocity, v, is $vt = 6.7$.

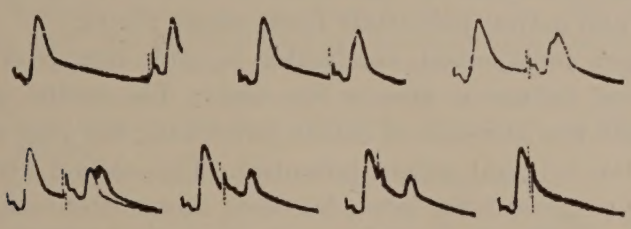

Fig. 7 AP records illustrating recovery of excitability in an impaled nerve fiber. Upper portion of second AP shows notching, alternation and finally failure as time interval between conditioning and testing shocks is decreased.

Strength duration curves were obtained on 10 fibers having velocities of 20–40 m/sec by stimulating the nerve trunk 2 to 3 cm from the recording CME. The individual curves were indistinguishable from each other or from that of the whole bundle. The average time constant of excitation was $k = 0.18$ msec.

SUMMARY

1. The capillary microelectrode (CME) technique has been applied to the measurement of membrane resting and action potentials of single myelinated frog nerve fibers.

2. In a conducting medium the CME behaves electrically as a resistance-capacitance transmission line which distorts any applied potential. A new method of correcting the distortion is described. For the frequencies occurring in the

NOTICE TO CONTRIBUTORS

THE JOURNAL OF CELLULAR AND COMPARATIVE PHYSIOLOGY, appearing bimonthly, is intended as a medium for the publication of papers which embody the results of original research of a quantitative or analytical nature in general and comparative physiology, including both their physical and chemical aspects. Short preliminary notices are not desired and papers will not be accepted for simultaneous publication or which have been previously published elsewhere. While not specifically excluding any particular branch of physiology, contributors should recognize that excellent journals already exist for publication in the field of experimental and physiological zoology, dealing particularly with genetics, growth, behavior, developmental mechanics, sex determination, and hormonal interrelationships, and also for pure mammalian functional physiology and the physical chemistry of non-living systems. Preference will be given to analyses of fundamental physiological phenomena whether the material is vertebrate or invertebrate, plant or animal. Since the journal is restricted, it is not possible to publish more than a limited number of papers which must be short and concise.

It is recognized that prompt publication is essential, and the aim will be to issue papers within three months of acceptance.

Manuscripts and drawings should be sent to the Managing Editor, DETLEV W. BRONK, Office of the President, The Johns Hopkins University, Baltimore 18, Maryland.

The paper must be accompanied by an author's abstract not to exceed 225 words in length, which will appear on the advance abstract cards of the Bibliographic Service of The Wistar Institute in advance of complete publication. Nothing can be done with the manuscript until the abstract is received.

Manuscripts should be typewritten in double spacing on one side of paper $8\frac{1}{2} \times 11$ inches, and should be packed flat — not rolled or folded. The original, not carbon, copy should be sent. The original drawings, not photographs of drawings, should accompany the manuscript. Authors should indicate on the manuscript the approximate position of text figures.

Manuscripts and drawings should be submitted in complete and finished form with the author's complete address. All drawings should be marked with the author's name. The Wistar Institute reserves the privilege of returning to the author for revision approved manuscript and illustrations which are not in proper finished form for the printer. When the amount of tabular and illustrative material is judged to be excessive, or unusually expensive, authors may be requested to pay the excess cost.

The tables, quotations (extracts of over five lines), and all other subsidiary matter usually set in type smaller than the text, should be typewritten on separate sheets and placed with the text in correct sequence. Footnotes should not be in with the text (reference numbers only), but typewritten continuously on separate sheets, and numbered consecutively. Explanations of figures should be treated in the same manner, and, like footnotes, should be put at the end of the text copy. A condensed title for running page headlines, not to exceed thirty-five letters and spaces, should be given.

Figures should be drawn for reproduction as line or halftone engravings, unless the author is prepared to defray the additional cost of a more expensive form of illustration. All colored plates are printed separately and cost extra. In grouping the drawings it should be borne in mind that, after the reduction has been made, text figures are not to exceed the dimensions of the printed matter on the page, $4\frac{1}{4} \times 6\frac{3}{4}$ inches. Single plates may be $5 \times 7\frac{1}{2}$ inches, or less, and double plates (folded in the middle), $11\frac{1}{2} \times 7\frac{1}{2}$ inches. Avoid placing figures across the fold, if possible.

Figures should be numbered from 1 up, beginning with the text figures and continuing through the plates. The reduction desired should be clearly indicated on the margin of the drawing.

All drawings intended for photographic reproduction either as line engravings (black-ink pen lines and dots) or halftone plates (wash and brush work) should be made on white or blue-white paper or bristol board — not on cream-white or yellow-tone. Photographs intended for halftone reproduction should be securely mounted with colorless paste — never with glue, which discolors the photograph.

Galley proofs and engraver's proofs of figures are sent to the author. All corrections should be clearly marked thereon.

The journal furnishes the author fifty reprints, with covers, of the paper gratis. Additional copies may be obtained according to rates which will be sent the author as soon as the manuscript has been examined at The Wistar Institute, after acceptance.

JOURNAL OF
CELLULAR AND COMPARATIVE
PHYSIOLOGY

VOL. 39 APRIL 1952 No. 2

CONTENTS

PRESS OF
THE WISTAR INSTITUTE
OF ANATOMY AND BIOLOGY
PHILADELPHIA

Printed in the United States of America